INVESTIGATING THE BIOSYNTHESIS OF THIO-QUINOLOBACTIN AND THE DEVELOPMENT OF A PROTEOMICS PROBE FOR THIAMIN UTILIZING ENZYMES

A Dissertation

Presented to the Faculty of the Graduate School

of Cornell University

In Partial Fulfillment of the Requirements for the Degree of

Doctor of Philosophy

by

Amy Marie Godert

August 2006

INVESTIGATING THE BIOSYNTHESIS OF THIO-QUINOLOBACTIN AND THE DEVELOPMENT OF A PROTEOMICS PROBE FOR THIAMIN UTILIZING ENZYMES

Amy Marie Godert, Ph. D.

Cornell University 2006

Quinolobactin, 8-hydroxy-4-methoxy-quinaldic acid, is a siderophore produced by *P. fluorescens* ATCC 17400. A tryptophan catabolite, quinolobactin is isolated as the thio-carboxylate, referred to as thio-quinolobactin. The biosynthesis of thio-quinolobactin appears to combine two pathways that have been studied previously in the Begley laboratory. The first half of the pathway catabolizes tryptophan to 3-hydroxykynurenine and appears to require similar enzymes to those found in the biosynthesis of nicotinamide. The latter half of the pathway incorporates sulfur into the quinolobactin molecule as a thio-carboxylate. The enzymes responsible for the sulfur transfer are highly similar to those found in sulfur transfer in thiamin in *B. subtilis* and cysteine in *M. tuberculosis*.

We have identified activities for the proteins in the pathway that are responsible for the transformation of 3-hydroxykynurenine, the point at which this pathway diverges from that of nicotinamide biosynthesis, to quinolobactin. QbsB, a hydroxykynurenine aminotransferase, is responsible for the deamination and cyclization of 3-hydroxykynurenine to xanthurenic acid.

QbsL then methylates the 4-hydroxy position of xanthurenic acid, and also activates the carboxylate as the acyl adenylate. Although we have not characterized sulfur transfer to quinolobactin to form thio-quinolobactin, we have identified roles for the putative sulfur transfer proteins QbsC, QbsD, and QbsE. QbsE is a small sulfur carrier protein that likely delivers sulfur to quinolobactin. Before the C-terminus of QbsE is activated as the thiocarboxylate, the two amino acids at the C-terminus following the diglycine are hydrolyzed by QbsD. This diglycine C-terminus can be adenylated and sulfurylated by QbsC, forming the thio-carboxylate.

In another project, we have synthesized and tested thiamin analogs incorporating a photo-labile substituent as proteomics probes. Thiamin pyrophosphate is an essential cofactor utilized by proteins in key prokaryotic and eukaryotic metabolic pathways. The ability to observe and compare relative amounts of these proteins when cells are grown under different conditions gives valuable insight into how cells respond to stressors. A promising probe was successfully synthesized and did exhibit the desirable properties of photo-lability and inhibition of thiamin pyrophosphate utilizing enzymes. Unfortunately, a high amount of non-specific labeling prevented it from being a useful proteome probe.

BIOGRAPHICAL SKETCH

Amy Marie Godert was born to Tom and Sandra Augustine as the oldest of three daughters in Buffalo, NY, where she grew up. She can still remember her early enthusiasm for chemistry, sitting on the floor of her grandparents' basement playing with her first chemistry kit given to her by her grandfather. Amy is sure that her mother remembers all the 'concoctions' that were made in the kitchen by mixing anything and everything that wasn't too high to reach. In 1997, Amy graduated from Hamburg Senior High School and went to Canisius College in Buffalo, NY to major in computer science and chemistry. Amy's primary interest in chemistry began in college while taking organic chemistry with Prof. Joseph Bieron. While at Canisius, Amy was able to work in the Erie County Forensics Lab under the direction of Michael Dujanovich and Mike Krajewski. In May 2001, Amy graduated *summa cum laude* with a B.S. in chemistry and computer science. It was also at Canisius that she met her future husband, Aaron B Godert while he was working in the computer science lab. The following August she began her graduate studies at Cornell University and joined the lab of Professor Tadhg Begley. Amy received her Masters degree in chemistry in May 2004 and was awarded the Chemistry and Biology Interface Training Grant from May 2003 to May 2005. While on the Training Grant, she had the opportunity to work with Dr. Janice Sufrin at Roswell Park Cancer Institute in Buffalo, NY. Amy will begin her post-graduate school life as an assistant professor of chemistry at Wells College in Aurora, NY.

To Mom, Dad, Mindy, Melissa, and Granny for all of your support and understanding,
to my grandfather who will always be an inspiration to me,
and most especially to my husband, Aaron, for your support, patience, and all the countless things you have helped me with.
Without all of you, none of this would have been possible.

ACKNOWLEDGMENTS

I would like to thank Prof. Tadhg Begley for being my scientific advisor, he has helped me to learn how to think critically and independently about research. I hope to have fruitful collaborations with him in the future. Tadhg has a never-ending amount of enthusiasm for anything related to science, whether it is how a camel's blood pumps when it runs, or why the water is shrinking in Cayuga Lake. He also has a high tolerance for loud noise that cannot be overlooked. I would like to thank Professors Tyler McQuade and Dostevi Sogah for serving on my special committee, and Prof. Roald Hoffmann for writing me a letter of recommendation. I would also like to thank Dr. Ronald Hines for reading portions of my dissertation.

One of the best experiences I had was a result of an internship with Dr. Janice Sufrin at Roswell Park Cancer Institute while on the NIH Chemistry and Biology Interface Training Grant. I will always be grateful to Dr. Sufrin for all of the great conversations about how women can and do succeed in chemistry while having a family life. I appreciated her allowing me to work in her laboratory. Another memorable internship I had was while I was in college at the Erie County Forensics Lab, and I would like to thank everyone there for their patience and willingness to show me around and let me see how things really go during a forensic investigation. I would also like to thank my college professors for encouraging me to pursue a graduate degree and for inspiring me to become a college professor.

The support and friendship of all of the Begley laboratory group members,

both past and present, has made my time here much more enjoyable. I would like to thank Kristin for all of our conversations about science and life in general, and for letting me come into “her” lab. To Amy H (soon to be J) and Colleen for all the wonderful lunches that we had, and for our great discussions – you two were willing to listen to and say anything, and our lunches will be among the more memorable events during my time here. To Jennie for always looking on the bright side and maintaining a positive spin on things, I will certainly try to do that more in the future. Thanks also to Abhishek for all of his advice on synthesis, named reactions, and various other tid-bits. To Kalyan and Tots, between the broken shoes and grandpa-fisherman outfit, you made the Chicago trip much more entertaining. To all the younger people (Jackie, Amrita, Sean), it was fun to help you start off on your careers and I truly hope that you succeed in all of your scientific endeavors. Also to Jeremiah and Dave (Go Sabres and Bills!), thank you for all of your helpful advice. I would like to thank all of the people in the Chemistry Department, for having answers to all of my questions.

Most importantly are my family members, I always knew that no matter what happened or how things turned out, I would always have their support. Aaron, without your seemingly endless patience and encouragement, I would never have made it. Somehow you wanted to be around me even when I know I was impossible to be around. Thank you.

TABLE OF CONTENTS

LIST OF FIGURES

LIST OF ABBREVIATIONS

α-KG	α-ketoglutarate
ATCC	American type culture collection
Amp	Ampicillin
AMP	Adenosine monophosphate
ATP	Adenosine triphosphate
β-ME	β-mercaptoethanol
BLAST	Basic Local Alignment Search Tool
BSA	Bovine serum albumin
ce	Crude extracts
CysDe	Cysteine desulfurase
Chlr	Chloramphenicol
CoA	Coenzyme A
Cont	Control
DMSO	Dimethylsulfoxide
dNTPs	Deoxyribonucleotide triphosphates
DNA	Deoxyribonucleic acid
DTT	Dithiothreitol
DXP	Deoxy-D-xylulose-5-phosphate
DXS	Deoxy-D-xylulose-5-phosphate synthase
EDTA	Ethylenediaminetetraacetic acide
ESI-FTMS	Electrospray ionization – Fourier transform mass spectrometry
FAD	Flavin adenine dinucleotide
$FADH_2$	Flavin adenine dinucleotide, reduced form
HO-Kyn	3-hydroxykynurenine
HPLC	High perfomance liquid chromatography

IPTG	Isopropyl β-D-1-thiogalactopyranoside
IROMP	Iron-repressed outer membrane protein
Kan	Kanamycin
KAT	Kynurenine aminotransferase
kDa	Kilodalton
KFA	N-formyl kynurenine formamidase
KMO	Kynurenine-3-monooxygenase
KYN	Kynureninase
LB	Luria-Bertani broth
LR	Lambda recombination
mRNA	Messenger ribonucleic acid
MS	Mass spectrometry
MWCO	molecular weight cut off
NAD	β-nicotinamide adenine dinucleotide
NADH	β-nicotinamide adenine dinucleotide, reduced form
NADP	β-nicotinamide adenine dinucleotide phosphate
NADPH	β-nicotinamide adenine dinucleotide phosphate, reduced form
Ni-NTA	Nickel-nitrolotriacetic acid
NMR	Nuclear magnetic resonance
OD_{xxx}	Optical density at xxx nm
Ox/red	Oxido-reductase
Pi	Phosphate
PCR	Polymerase chain reaction
PDTC	Pyridine-2,6-(bis)monothiocarboxylic acid
PLP	Pyridoxal-5'-phosphate
PMP	Pyridoxamine-5'-phosphate

PMSF	Phenylmethyl sulfonyl fluoride
PPi	Pyrophosphate
QB	Quinolobactin
RNA	Ribonucleic acid
SAM	S-adenosyl methionine
SDS-PAGE	Sodium dodecyl sulfate-polyacrylamide gel electrophoresis
TCEP	Tris(2-carboxyethyl)phosphine
TDO	Tryptophan dioxygenase
Thio-QB	Thio-quinolobactin
TLC	Thin-layer chromatography
TPK	Thiamin pyrophosphokinase
TPP	Thiamin pyrophosphate
XA	Xanthurenic acid

CHAPTER 1:

THE BIOSYNTHESIS OF THIO-QUINOLOBACTIN – A SIDEROPHORE PRODUCED BY *PSUEDOMONAS FLUORESCENS*

1.1 Overview of siderophores

Siderophores (from the Greek “iron carriers”) are typically defined as low molecular weight, ferric ion specific chelators. These molecules are made by bacteria growing under iron-deprived conditions. Iron is required in a number of essential reactions occurring in microorganisms such as in the reduction of oxygen for synthesis of ATP, for the formation of heme, reduction of nitrogen gas to ammonia, and the reduction of ribotide precursors of DNA. Hundreds of different siderophores have been identified and are generally grouped into various classes based on their iron complexing functionalities. The two most common classes being phenol-catechols and hydroxyamates.[1] Even within a particular genus, a wide-range of different siderophores are produced.

Although iron is abundant in the earth’s crust, it is essentially unavailable to microorganisms living there. Since we live in a highly oxidizing environment, most of the iron exists as the ferric ion. Iron in this oxidation state has a very low solubility at physiologically relevant pH’s, around 10^{-9}M.[2] Under low-iron conditions, the genes encoding proteins involved in the formation of siderophores are de-repressed. The microorganisms biosynthesize their siderophores inside the cell, but they must be transported to the outside environment where they can encounter and bind to the insoluble ferric

hydroxides. The siderophore-ferric ion complexes are recognized by specific outer membrane proteins that are responsible for their internalization so the iron can be utilized by the cell.

Interest in siderophores has risen as their importance in virulence, agriculture and clinical applications became apparent. Since iron is essential for survival in the pathogenic organism, they must have some way to acquire it from the host. The human pathogen, *Yersinia pestis,* produces the siderophore yersiniabactin, which is capable of extracting the ferric ion from human iron-carrying proteins.[3] Agricultural interest stems from the symbiotic relationship between leguminous plants and their nitrogen-fixing symbiotic bacteria. The bacterium must have mechanisms to acquire iron from its host in order to construct the nitrogenase complex, essential for reduction of nitrogen gas to ammonia.[4] In the treatment of transfusion-induced siderosis, iron deposition in tissues, a siderophore from *Streptomyces pilosus*, desferrioxamine B, is prescribed.[5] Other potential therapeutic uses of siderophores are being investigated, such as specific targeting of antibiotics.[6]

1.2 Quinolobactin

Quinolobactin, 8-hydroxy-4-methoxy-quinaldic acid, is a siderophore produced by the fluorescent pseudomonad, *P. fluorescens* ATCC 17400 (figure 1.1). The molecule is isolated as the thio-carboxylate, referred to as thio-quinolobactin, and it hydrolyzes to generate the carboxylate.[7] The primary siderophore of *Pseudomonas fluorescens* is pyoverdine, which is responsible for its fluorescence. Although the wild type organisms produce thio-quinolobactin, mutants that were unable to produce pyoverdine (pvd-) were

shown to have an increased production of thio-quinolobactin and were still able to grow under iron-limiting conditions. In addition, the production of an iron-repressed outer-membrane protein, IROMP, was observed in pvd- strains, indicating that a quinolobactin-ferric ion complex could be transported into the cell.[8]

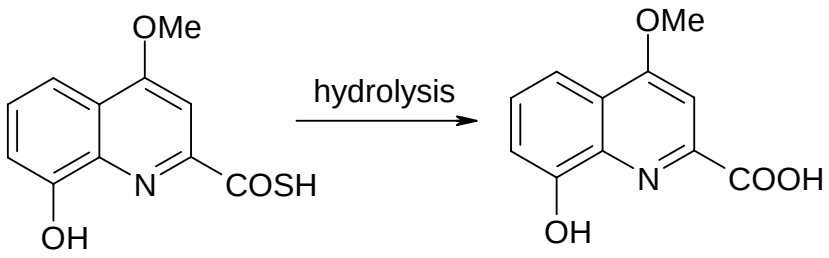

Thio-quinolobactin Quinolobactin

Figure 1.1 Structures of quinolobactin and thio-quinolobactin, which are produced by *P. fluorescens* ATCC 17400.

All of the work done to characterize the iron binding of these molecules has been done with quinolobactin, not the thiocarboxylate due to the latter's reported low stability. Though once it is ionized, the thio-acid should be stable. It was shown that quinolobactin does indeed chelate iron; however it has a much lower affinity for ferric iron than pyoverdine. Quinolobactin has a pFe value of 18.2, while that of pyoverdine is 27.[9, 10] pFe is defined as the -log[uncomplexed Fe^{3+}_{aq}] at pH 7.4, with 1μM total Fe^{3+} and 10μM total ligand. This partially reflects the denticity of the ligands. Pyoverdine is hexadentate and therefore able to fully satiate the six-coordination sites of Fe^{3+}. Although quinolobactin could be either bi- or tri- dentate, titration with Fe^{3+} showed that it is bi-dentate and it coordinates through the nitrogen of the quinoline ring and the hydroxyl group. It is believed that quinolobactin complexes Fe^{3+} in a 2:1

ligand:iron ratio, leaving two coordination sites open. However, other quinolines do possess tridentate binding through the quinoline nitrogen, the hydroxyl group, and also the carboxylate.[11] In addition, the pyridine siderophore, pyridine-2,6-(bis)monothiocarboxylic acid (PDTC), from *P. stutzeri* chelates ferric iron through two thio-acids and a pyridine nitrogen. Although there is no evidence for participation of the carboxylate in iron coordination, it may be possible that the thiocarboxylate would be able to coordinate iron.

Quinolobactin is described as a secondary siderophore because it is produced in lower amounts and it has a lower affinity for ferric iron than pyoverdin, the other siderophore utilized by *P. fluorescens.* The role of secondary siderophores is unclear, though it has been suggested that they provide rescue iron uptake systems since their role in iron acquisition is greatly increased in mutants unable to make their primary siderophore.[12, 13] An alternative hypothesis would be that different siderophores are made by the same organisms in order to solubilize different forms of iron found in the environment such as hematite (Fe_2O_3), magnetite (Fe_3O_4), and also iron hydroxide ($Fe(OH)_3$).[14, 15]

1.3 Biosynthesis of thio-quinolobactin

After the identification of thio-quinolobactin and quinolobactin, a cluster of genes responsible for its biosynthesis, uptake and transport were identified, cloned and sequenced.[16] The cluster contained two operons with twelve open-reading frames (figure 1.2). When a cosmid containing the cluster was introduced into mutants unable to make both pyoverdine and quinolobactin,

the production of quinolobactin and the ability to grow in the absence of iron was restored.

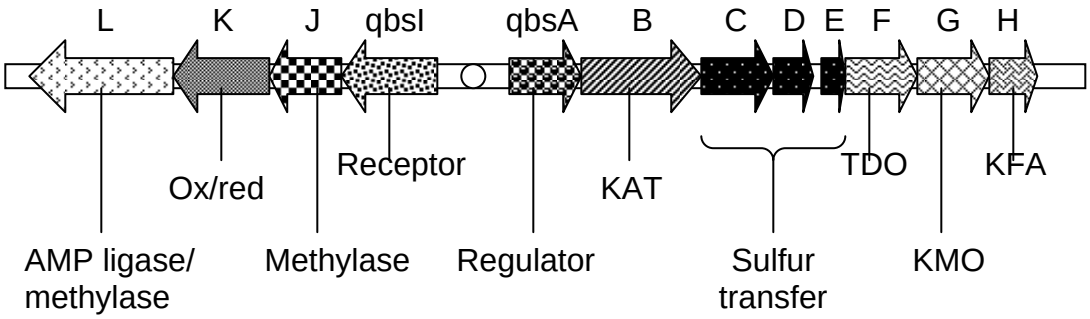

Figure 1.2 Gene cluster responsible for the biosynthesis of thio-quinolobactin. There are two divergent operons. The genes are named *qbs* for *q*uinolo*b*actin *s*ynthesis. The circle between the operons is the putative *fur* (ferric uptake regulator) binding site. Putative gene functions are given below the gene. Abbreviations: Ox/red: oxido-reductase, KAT: kynurenine amino-transferase, TDO: tryptophan-2,3-diooxygenase, KMO: kynurenine monooxygenase, KFA: kynurenine formamidase.

Though the genes responsible for the biosynthesis of thio-quinolobactin have been identified, no functions of the gene products of this cluster have been experimentally investigated. Putative functions were assigned to each of the gene products based on homology searching, and it appears as though the biosynthesis of thio-quinolobactin is a combination of two pathways that have been studied previously in the Begley lab. The first involves tryptophan catabolism to hydroxykynurenine, which is part of the nicotinamide biosynthetic pathway found primarily in eukaryotes. [17] The latter part of the pathway is the formation of thio-quinolobactin from quinolobactin by a ubiquitin/sulfurylation mechanism, similar to that found in thiazole and molybdopterin biosynthesis.[18]

A proposed pathway for the catabolism of tryptophan with gene products that are putatively involved is given in figure 1.3. The homology of the genes involved in quinolobactin biosynthesis and nicotinamide biosynthesis is very high, and as such, the steps are expected to be very similar.

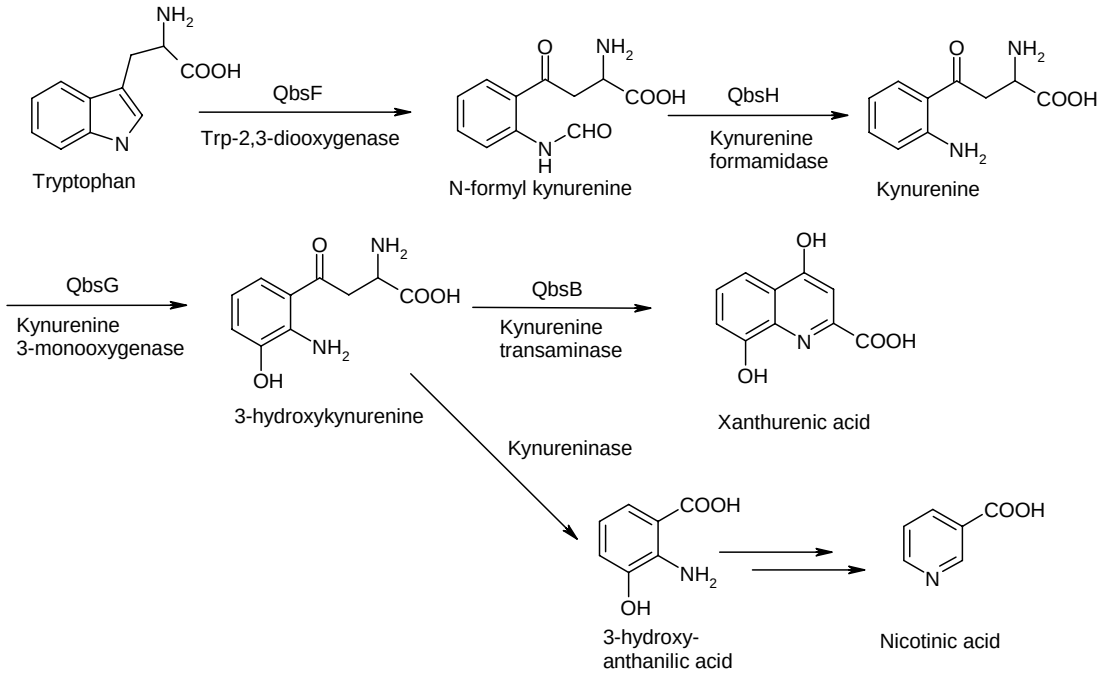

Figure 1.3 Tryptophan catabolism to xanthurenic acid through the common nicotinamide biosynthetic intermediate 3-hydroxykynurenine.

The first step involves the oxidation of tryptophan to N-formyl kynurenine by QbsF, which is 75% homologous to a tryptophan 2,3-diooxygenase from *P. aeruginosa*. Deformylation by QbsH, with similarity to metal-dependent hydrolases, yields kynurenine. The ring can then by hydroxylated by QbsG, which is similar to other kynurenine-3-monooxygenases. Up to this point, the biosynthetic pathways for nicotinamide and thio-quinolobactin are identical. In the nicotinamide pathway, 3-hydroxy-anthranilic acid is formed from 3-hydroxy-kynurenine by kynureninase, which then proceeds on to nicotinic acid.

In the quinolobactin pathway, the quinoline ring is formed by the QbsB dependent deamination of 3-hydroxykynurenine, forming the α-keto acid that can spontaneously cyclize to form xanthurenic acid, a stable intermediate along the biosynthetic pathway. Xanthurenic acid is made in a number of other systems in which it functions as a gametocyte activating factor for *Plasmodium falciparum* (malaria) and as an intermediate along the ommochrome biosynthetic pathway in *Drosophilia*.[19] [20]

The catabolism of tryptophan to 3-hydroxy-kynurenine and the formation of xanthurenic acid have been demonstrated in mammalian and bacterial systems, but the subsequent conversion to thio-quinolobactin has not been characterized. A proposed pathway from xanthurenic acid to thio-quinolobactin is given below (figure 1.4). QbsL, which contains a SAM binding domain, can methylate xanthurenic acid in a SAM dependent reaction to form quinolobactin. In order for sulfurylation of the carboxylic acid of quinolobactin to occur, it must first be activated. This activation can take place through adenylation that is catalyzed by QbsL, which also possesses an AMP-binding domain. Transfer of sulfur to the acyl adenylate is probably mediated through QbsC, QbsD, and QbsE. These putative sulfur transfer proteins are similar to the ubiquitin/sulfurylation system that is found in the biosynthesis of sulfur containing small molecules such as thiazole, cysteine (one of the biosynthetic pathways), and molybdopterin.

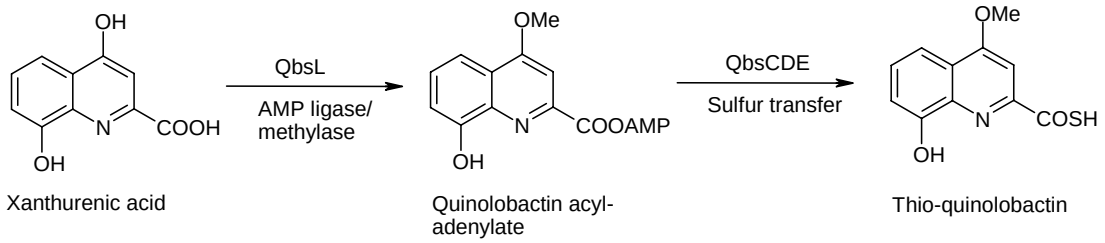

Figure 1.4 Conversion of xanthurenic acid to thio-quinolobactin.

1.4 Incorporation of sulfur into natural products

There are a number of naturally occurring molecules of diverse structure that contain sulfur, including thiamin, molybdopterin, cysteine, and pyridine-2,6-(bis)monothiocarboxylic acid (PDTC), a thio-acid siderophore from *P. stutzeri*. (figure 1.5) The biosynthesis of these molecules takes place without the use of free sulfide, employing a series of sulfur activating and carrying proteins instead. In the case of cysteine, there is more than one pathway by which it is made, and one of them uses proteins in a sulfur transfer system, and not sulfide.

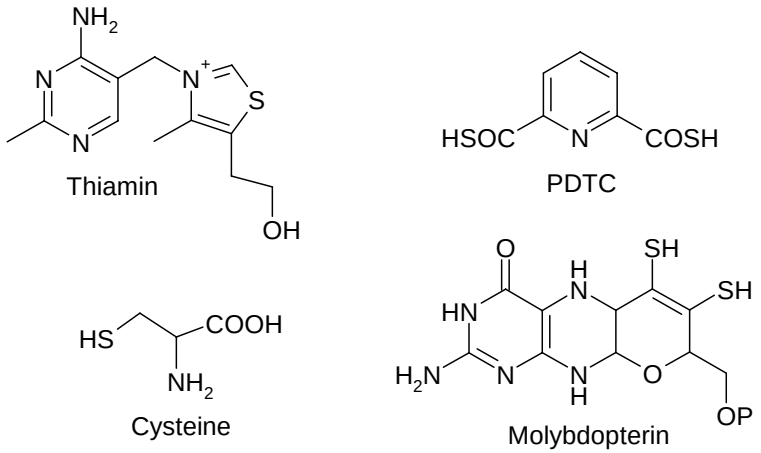

Figure 1.5 Structures of various naturally occurring, sulfur containing small molecules.

Nature has evolved routes for the transfer of sulfur that do not involve sulfide, though the exact reasons are not known. The mechanism of sulfur transfer has been fairly well characterized in the biosynthesis of all of these sulfur-containing molecules except for PDTC. In these systems, a small sulfur carrier protein (ThiS-thiamin, MoaD-molybdopterin, and CysO-cysteine) is responsible for the delivery of sulfur to the small molecule. [21-23] The chemistry of these systems is based on what is observed in the ubiquitin targeting of doomed proteins to the proteosome (figure 1.6).[18] Rather than a thio-ester as found in the ubiquitin system though, these proteins carry sulfide as a thio-carboxylate on their C-terminus.

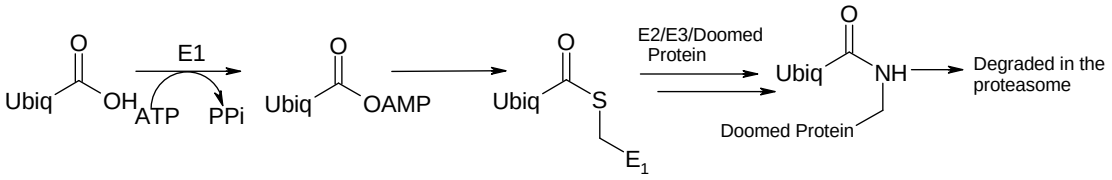

Figure 1.6 Ubiquitin targeting of doomed proteins to the proteasome for degradation. The C-terminal glycine of ubiquitin (Ubiq) is activated by E1, a sequence specific adenylating protein. Ubiquitin is then linked to E1 through a thioester by attack of an E1-cysteine on the ubiquitin acyl adenylate. Eventually ubiquitin is attached to the doomed protein in an amide linkage through the ε-amino group of a lysine on the doomed protein.

In thiamin and molybdopterin biosynthesis, the small sulfur carrier protein (ThiS, MoaD) clusters with an adenylating protein (ThiF, MoeB) within the biosynthetic operon. The sulfur carrier protein, usually about 10kDa, is responsible for holding onto and delivering the sulfur to its target molecule. The C-terminus of each of the proteins has a highly conserved -GG-COOH. The diglycine at the C-terminus gives the protein a ‘floppy tail,’ onto which the sulfur can be placed and subsequently transferred. Before the sulfur is placed on the sulfur-carrier protein, the C-terminus must be activated to accept it. For

the examples given, the activation is done through the formation of a C-terminal acyl adenylate via the adenylating enzymes (ThiF, MoeB) that cluster with the sulfur carrier protein (figure 1.7). Cysteine desulfurases remove the sulfur from cysteine, generating a protein bound persulfide. The sulfane sulfur of the persulfide is then transferred to the sulfur-carrier protein acyl adenylate, forming a C-terminal thiocarboxylate.[24]

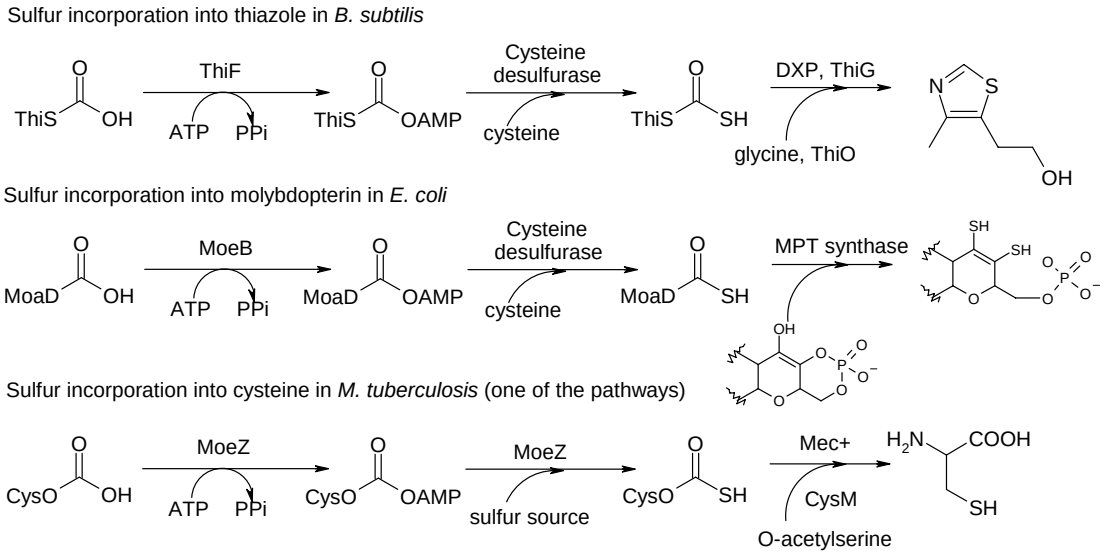

Figure 1.7 Comparison of the sulfur incorporation into thiazole, molybdopterin and cysteine. In all of the examples, a small sulfur carrier protein is used (ThiS, MoaD, or CysO) to deliver the sulfur to its target molecule.

The thio-quinolobactin biosynthetic gene cluster contains a similar small protein, QbsE, to those found in thiamin, molybdopterin, and cysteine biosynthesis (ThiS, MoaD, CysO). Clustered with QbsE is an adenylating enzyme, QbsC, which is similar to the adenylating enzymes ThiF, MoeB, and MoeZ. We propose that QbsC is able to adenylate the C-terminus of QbsE. A sulfide equivalent is then transferred to the activated QbsE, again by QbsC. This could attack the activated quinolobactin acyl adenylate, forming thio-

quinolobactin (figure 1.8). A possible role for QbsD, a putative metal containing hydrolase, is to cleave the covalent intermediate formed between QbsE and quinolobactin, or it could have a role in the processing of QbsE. Unlike the sulfur carrier proteins in thiamin (ThiS), molybdopterin (MoaD), and cysteine (CysO), which have diglycine at their C-termini, QbsE possesses two additional amino acids. QbsD may be involved in removing these extra amino acids, free the diglycine C-terminus of QbsE. We were interested in determining if sulfur is incorporated into quinolobactin via a similar mechanism as is found in thiamin, molybdopterin, and cysteine.

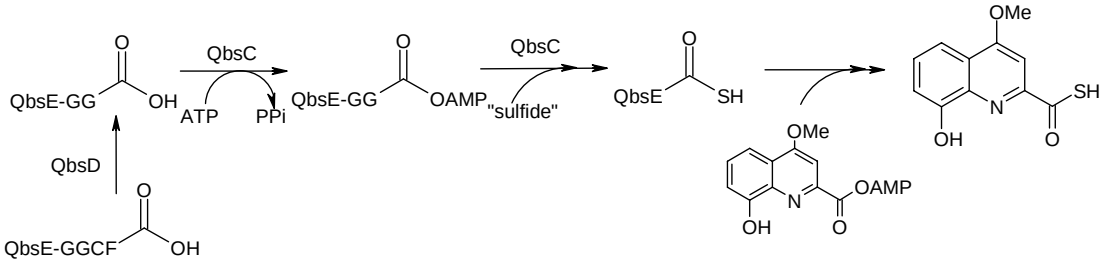

Figure 1.8 Proposed steps in the transfer of sulfur in thio-quinolobactin biosynthesis.

One could ask why sulfur is even incorporated into quinolobactin at all. The carboxylate of quinolobactin does not bind to the ferric iron, and the thio-carboxylate might not either. In addition, Fe^{3+} is a 'hard' atom that prefers to coordinate with other hard atoms, like oxygen, not sulfur which is 'soft'. Little work has been done with thio-quinolobactin due to its instability and rapid hydrolysis in buffer back to the carboxylic acid.[7] Obviously the thio-carboxylate plays some role or the organism would not expend the energy to incorporate it at all. PDTC, also a thio-acid containing siderophore, binds to Cu^{2+} and utilizes it to convert CCl_4 to HCl and CO_2.[25] A thio-quinolobactin-copper complex could reduce ferric iron to ferrous iron, making it much more

soluble. The more soluble Fe^{2+} can either be transported directly into the cell or be bound by a siderophore.[26] Though the low stability of the thio-carboxyolate in solution could mean that the thio-carboxylate does not play a role in metal binding at all. Another possible function for the thio-carboxylate would be an *in vivo* regulatory role. The thio acid could form an acyl-persulfide with a protein that would get transported to the siderophore exporter, and then cleaved just prior to excretion. This would protect the siderophore inside of the cell, preventing it from binding iron under already iron limiting conditions. There is no experimental evidence regarding the true role of the thiocarboxylate.

1.5 Investigating the biosynthesis of thio-quinolobactin

We are interested in investigating the biosynthesis of thio-quinolobactin starting from the 3-hydroxykynurenine aminotransferase, QbsB (figure 1.9). This represents the part of the pathway that is least understood. The tryptophan catabolic gene products, QbsF, QbsH, and QbsG, have high homology with previously characterized proteins, and will not be the focus of this study. We are satisfied based on homology that they are catalyzing their assigned reactions. Work will be described elucidating the functions of the proteins QbsB (aminotransferase) and QbsL (AMP-ligase/O-methyltransferase), and their role in the formation of quinolobactin. We want to elucidate the mechanism of sulfur activation, probably occurring through QbsC, QbsD, and QbsE, and transfer to quinolobactin, because there are only a few examples where sulfur incorporation is well understood.

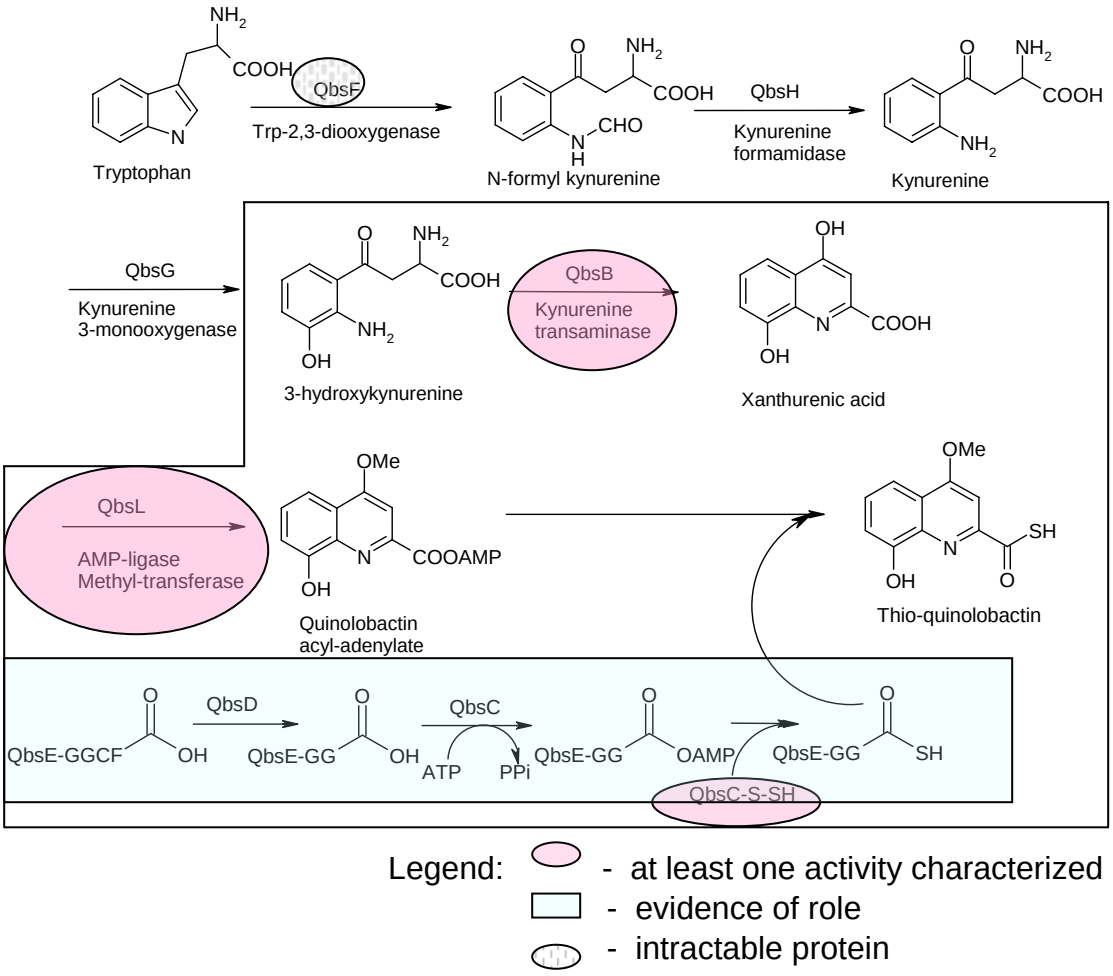

Figure 1.9 Thio-quinolobactin biosynthetic pathway. We are interested in studying the pathway starting with 3-hydroxykynurenine and QbsB (outlined in box). Proteins that are in circles have had at least one of their activities characterized, proteins in dotted boxes have been studied and We have some evidence of their roles/existence, and proteins in a circle with lines have been over-expressed but were intractable.

We began our studies with the putative aminotransferase, QbsB, which appeared to be responsible for the deamination and subsequent cyclization of 3-hydroxykynurenine to xanthurenic acid. When the enzyme was heterologously overexpressed in *E. coli*, it was completely intractable due to its insolubility. When a tag was added to the protein to improve solubility, we obtained soluble protein that was able to catalyze the conversion of 3-

hydroxykynurenine to xanthurenic acid. Cleavage of the tag from QbsB resulted in insoluble protein.

The next enzyme in the pathway, QbsL, appeared to have two functions: one as a methyltransferase and another as an AMP-ligase. We believed that QbsL was responsible for the methylation of the 4-hydroxy position of xanthurenic acid to generate quinolobactin, and that it could also activate the carboxylic acid to an acyl adenylate readying the molecule for sulfurylation. Like QbsB, this enzyme also has solubility problems, but appropriate growth conditions were found where we obtained soluble protein. We were able to see methylation of xanthurenic acid in clarified crude cell lysate of a QbsL *E. coli* overexpression strain, and also a small amount of methylation with purified enzyme by incorporation of a radioactive (^{14}C) methyl group. We also have evidence that QbsL was able to adenylate the carboxylic acid of xanthurenic acid.

Verification of sulfur transfer proved much more elusive and though We have evidence that the sulfur transfer follows the motifs seen in thiamin and molybdopterin biosynthesis, We have not reconstituted transfer to quinolobactin. All three sulfur transfer proteins had minimal solubility when they were overexpressed heterologously in *E. coli*. However, when the proteins QbsC and QbsE were co-overexpressed, we observed a marked increase in solubility. We have data both from pull-downs that identify protein-protein interactions and mass spectrometry, that QbsC and QbsE, two proteins believed to be involved in sulfur transfer, interacted with each other, similar to what was observed in thiamin biosynthesis.[27] We were able to

conclusively show that QbsC can activate sulfur from thiosulfate in the form of a persulfide, a key step in the hypothesized sulfur transfer mechanism. Additionally, when QbsD and QbsE were co-overexpressed, their solubility increased and QbsE purified out with its two C-terminal amino acids hydrolyzed, as QbsE-GG-COOH. This confirmed the function of the JAMM motif protein QbsD, making this the second protein with such a motif to have its function identified in prokaryotes.

We were able to reconstitute the sulfur transfer to QbsE mediated by QbsC and QbsD, identifying the QbsE-thiocarboxylate. A proposed pathway for this sulfur transfer is seen in figure 1.10; however, complete characterization of this sulfur transfer remains to be done.

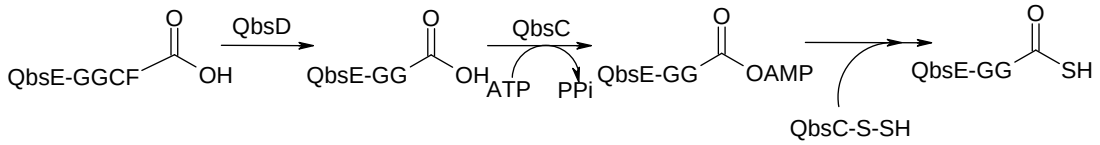

Figure 1.10 Proposed steps in the transfer to the modified C-terminal end of QbsE.

We have shown the formation of the diglycine C-terminal thiocarboxylate on QbsE by ESI-FTMS, QbsE-GG-COSH. This thiocarboxylate is only formed in the presence of QbsD. Therefore we propose that the two terminal amino acids of QbsE (cysteine and phenylalanine) are hydrolyzed to generate the diglycine at the C-terminus by the hydrolase QbsD. The modified C-terminus can be activated as the acyl adenylate by QbsC, readying it for sulfur transfer, again by QbsC.

Overexpression of the proteins individually in the heterologous host, *E. coli*, is not ideal, as it consistently yielded only small amounts of soluble protein. The ability to obtain larger amounts of soluble protein when the genes are overexpressed individually would greatly aid in the characterization of their activities. We are currently exploring overexpressing these proteins other *Psuedomonads*, which are more similar to the native organism, and may yield more soluble protein.

1.6 References

1. Neilands, J.B., *Siderophores of bacteria and fungi.* Microbiological Sciences, 1984. **1**(1): p. 9-14.

2. Neilands, J.B., *Siderophores.* Archives of Biochemistry and Biophysics, 1993. **302**(1): p. 1-3.

3. Pfeifer, B.A., et al., *Biosynthesis of yersiniabactin, a complex polyketide-nonribosomal peptide, using Escherichia coli as a heterologous host.* Applied and Environmental Microbiology, 2003. **69**(11): p. 6698-6702.

4. Barton, L.L., B.C. Hemming, and Editors, *Iron Chelation in Plants and Soil Microorganisms*. 1993. 490 pp.

5. Propper, R., S. Shurin, and D. Nathan, *Reassessment of the use of desferrioxamine B in iron overload.* New England Journal of Medicine, 1976. **294**(26): p. 1421-1423.

6. Girijavallabhan, V. and M.J. Miller, *Therapeutic uses of iron(III) chelators and their antimicrobial conjugates.* Iron Transport in Bacteria, 2004: p. 413-433.

7. Neuenhaus, W., et al., *Bacterial components. Part IX. 8-Hydroxy-4-methoxymonothioquinaldic acid - a further thioacid from Pseudomonas.* Zeitschrift fuer Naturforschung, Teil B: Anorganische Chemie, Organische Chemie, 1980. **35B**(12): p. 1569-71.

8. Mossialos, D., et al., *Quinolobactin, a new siderophore of Pseudomonas fluorescens ATCC 17400, the production of which is repressed by the cognate pyoverdine.* Applied and Environmental Microbiology, 2000. **66**(2): p. 487-492.

9. du Moulinet D'Hardemare, A., G. Serratrice, and J.L. Pierre, *Synthesis and iron-binding properties of quinolobactin, a siderophore from a pyoverdine-deficient Pseudomonas fluorescens.* BioMetals, 2004. **17**(6): p. 691-697.

10. Albrecht-Gary, A.-M., et al., *Bacterial Iron Transport: Coordination Properties of Pyoverdin PaA, a Peptidic Siderophore of Pseudomonas aeruginosa.* Inorganic Chemistry, 1994. **33**(26): p. 6391-402.

11. Perkampus, H.H. and K. Kortum, *Uber eleckronenanregungsspekten einiger Metall-8-hydroxy-chinolate, -4hydroxy-acridinate und -4-hydroxy-phenazinate.* Z. Anal. Chem., 1962. **190**: p. 111-126.

12. Gensburg, K., K. Hughes, and A.W. Smith, *Siderophore-specific induction of iron uptake in Pseudomas aeruginosa.* Journal of General Microbiology, 1992. **138**: p. 2381-2387.

13. Meyer, J.M., P. Azelvandre, and C. Georges, *Iron metabolism in Pseudomonas: salicylic acid, a siderophore of Pseudomonas fluorescens CHA0.* BioFactors, 1992. **4**: p. 23-27.

14. Hershman, L., P. Maurice, and G. Sposito, *Iron acquisition from hydrous Fe(III)-oxides by an aerobic Pseudomonas sp.* Chemical Geology, 1996. **132**: p. 25-31.

15. Hershman, L., et al., *Siderophore Production and Iron Reduction by Pseudomonas mendocina in Response to Iron Deprivation.* Geomicrobiology Journal, 2000. **17**: p. 261-273.

16. Matthijs, S., et al., *The Pseudomonas siderophore quinolobactin is synthesized from xanthurenic acid, an intermediate of the kynurenine pathway.* Molecular Microbiology, 2004. **52**(2): p. 371-384.

17. Kurnasov, O., et al., *NAD biosynthesis: Identification of the tryptophan to quinolinate pathway in bacteria.* Chemistry & Biology, 2003. **10**(12): p. 1195-1204.

18. Hershko, A. and A. Ciechanover, *The ubiquitin system.* Annual review of biochemistry, 1998. **67**: p. 425-479.

19. Billker, O., et al., *Identification of xanthurenic acid as the putative inducer of malaria development in the mosquito.* Nature, 1998. **392**(6673): p. 289-92.

20. Real, M.D. and J. Ferre, *Analysis of kynurenine transaminase activity in Drosophila by high performance liquid chromatography.* Insect Biochemistry, 1991. **21**(6): p. 647-52.

21. Park, J.-H., et al., *Biosynthesis of the Thiazole Moiety of Thiamin Pyrophosphate (Vitamin B1).* Biochemistry, 2003. **42**(42): p. 12430-12438.

22. Burns, K.E., et al., *Reconstitution of a new cysteine biosynthetic pathway in Mycobacterium tuberculosis.* Journal of the American Chemical Society, 2005. **127**(33): p. 11602-11603.

23. Wuebbens, M.M. and K.V. Rajagopalan, *Mechanistic and Mutational Studies of Escherichia coli Molybdopterin Synthase Clarify the Final Step of Molybdopterin Biosynthesis.* Journal of Biological Chemistry, 2003. **278**(16): p. 14523-14532.

24. Behshad, E., S.E. Parkin, and J.M.J. Bollinger, *Mechanism of Cysteine Desulfurase Slr0387 from Synechocystis sp. PCC 6803: Kinetic Analysis of Cleavage of the Persulfide Intermediate by Chemical Reductants.* Biochemistry, 2004. **43**: p. 12220-12226.

25. Stolworthy, J.C., et al., *Metal binding by pyridine-2,6-bis(monothiocarboxylic acid), a biochelator produced by Pseudomonas stutzeri and Pseudomonas putida.* Biodegradation, 2001. **12**(6): p. 411-8.

26. Budzikiewicz, H., *Heteroaromatic monothiocarboxylic acids from Pseudomonas spp.* Biodegradation, 2003. **14**(2): p. 65-72.

27. Taylor, S.V., et al., *Thiamin biosynthesis in Escherichia coli. Identification of the thiocarboxylate as the immediate sulfur donor in the thiazole formation.* Journal of Biological Chemistry, 1998. **273**(26): p. 16555-16560.

CHAPTER 2:

HYDROXYKYNURENINE AMINOTRANSFERASE (QbsB)

2.1 Introduction

Thio-quinolobactin is a secondary metabolite formed from the catabolism of the amino acid tryptophan. Nicotinamide adenine dinucleotide (NAD) is another tryptophan metabolite with the same initial steps in the breakdown of tryptophan.[1] The point where the biosynthetic pathways of these two molecules diverge is 3-hydroxykynurenine (figure 2.1).

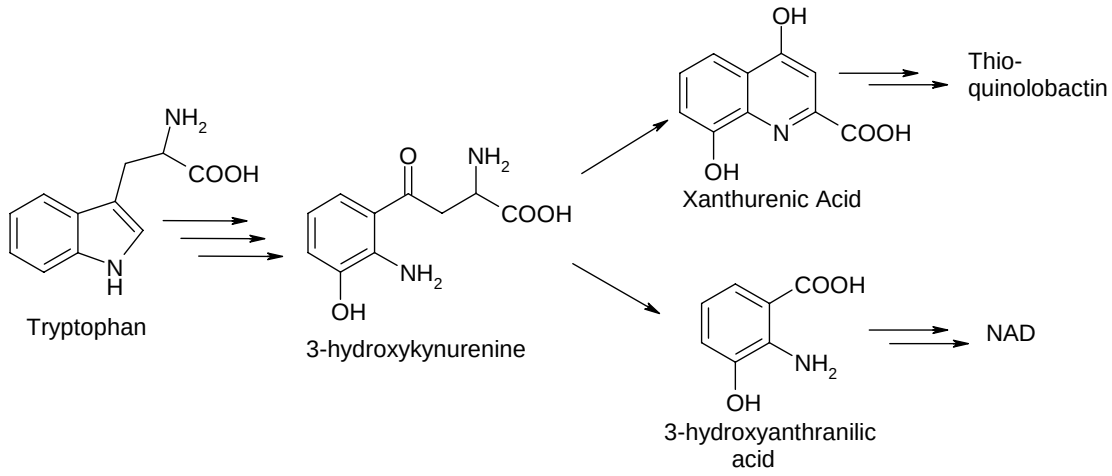

Figure 2.1 Highlights the common biosynthetic features of NAD and thio-quinolobactin biosynthesis.

At this juncture, 3-hydroxykynurenine loses an amino group and cyclize to form xanthurenic acid, the quinoline core of quinolobactin. The biosynthetic gene cluster of thio-quinolobactin contains only one putative amino-transferase, QbsB. This enzyme does not align with any known and

characterized kynurenine aminotransferases. It does however show similarity to histidinol phosphate aminotransferases, and contains a PLP binding aminotransferase domain. The proposed catalysis of QbsB is outlined in figure 2.2.

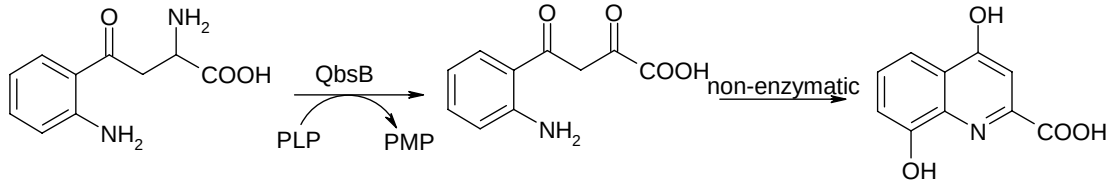

Figure 2.2 Proposed reaction sequence for the cyclizing aminotransferase, QbsB.

3-Hydroxykynurenine is deaminated by QbsB in a PLP dependent reaction forming the α-ketoacid. The α-ketoacid can then non-enzymatically cyclize to form the quinoline core of quinolobactin. Xanthurenic acid is made in a number of other systems by a 3-hydroxykynurenine aminotransferase including as a gametocyte activating factor for *Plasmodium falciparum* (malaria) and as an intermediate along the ommochrome biosynthetic pathway in *Drosophilia*.[2],[3]

2.2 Cloning and overexpression of hydroxykynurenine aminotransferase, QbsB, in *E. coli*

2.2.1 Cloning

QbsB was cloned by the Cornell Protein Purification Facility. The *qbsB* gene was PCR amplified from *P. fluorescens* ATCC 17400 genomic DNA using the following primers: forward 5'-CAC CAT GAA ATT CTC CAA CTT CTT TAG AAA CAG CC-3' and reverse 5'-CTA TCA GAT CGG GTA GAA GAG CCC

GTG ATG GTG CG-3'. The PCR product was purified and clones were screened by restriction digest and verified by sequencing. A correct clone was used in an LR reaction (Gateway cloning system) with the plasmid pDESTF1 and named pPfQbsB.XF1.

2.2.2 Overexpression and solubilization trials

QbsB overexpressed extremely well, but yielded no soluble protein when grown in *E. coli* Tuner (DE3) at reduced temperatures. Reduced amounts of IPTG and the use of various additives such as 0.1% sorbitol, pyridoxal, 1% glucose, 1% sucrose or 3-hydroxykynurenine failed to give any soluble protein. Lysis with the substrate hydroxykynurenine, the cofactor PLP, the product xanthurenic acid or with nonionic detergents such as triton X-100 again failed to give any soluble protein, even with lysis of many liters of cell pellets.

In an attempt to obtain soluble protein, various methods of solubilization via denaturation followed by subsequent refolding were investigated. Cells were lysed in the presence of 6M urea, yielding denatured protein. This was bound to the Ni-NTA column, washed, and eluted under denaturing conditions. When the urea was removed by dialysis to refold the protein, a large amount of precipitate was observed. When the soluble portion was concentrated and run on an SDS-PAGE gel, very little protein of the correct molecular weight appeared to be soluble; however, the insoluble, precipitated protein turned out to be the desired QbsB (figure 2.3).

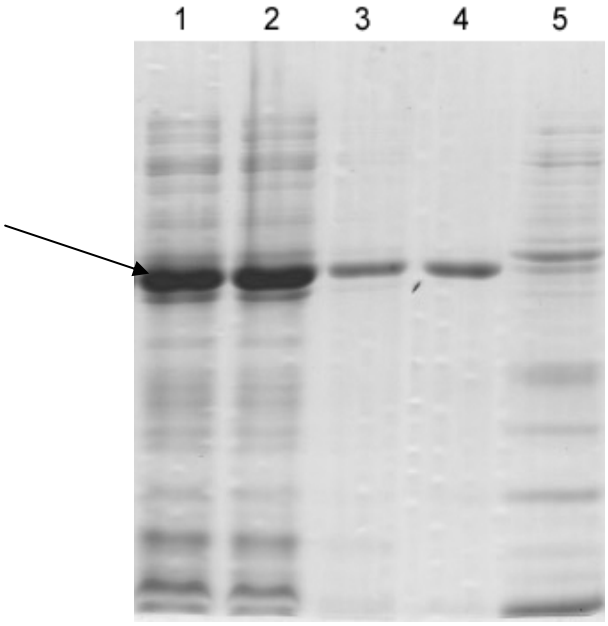

Figure 2.3 SDS gel electrophoresis (12%) analysis of the overexpression and purification of QbsB under denaturing conditions. Lane 1: supernatant Lane 2: flowthrough Lane 3: elution Lane 4: precipitated protein with dialysis Lane 5: concentrated soluble fraction after dialysis. QbsB is indicated with a black arrow.

Since traditional denaturation followed by refolding yielded no soluble protein, probably due to aggregation, an on-column refolding was attempted. The on-column refolding was performed according to the published procedure.[4] Unfortunately, no soluble protein was obtained from the procedure.

2.2.3 Use of fusion proteins to increase solubility

Because all previous attempts to obtain soluble protein were unsuccessful, protein fusion tags were used to obtain soluble QbsB. Two such fusion tags were tested: the protein responsible for the catabolism of maltodextins, maltose-binding protein (MBP) and the bacteriophage lambda RNA binding protein, NusA.[5, 6] Overexpression with the MBP-tag failed to yield full length

protein, probably due to proteolysis. The use of protease inhibitors during lysis and purification still did not yield any full length protein, so the cleavage was probably occurring *in vivo*. Fusion with the NusA protein with a 6x-His tag did yield full length, soluble protein that could be purified by Ni-NTA affinity chromatography (figure 2.4). Full length protein was obtained in greater yield when protease inhibitors were included in the purification buffers. The addition of 25% glycerol to the lysis buffer and all purification buffers also aided in solubility and stability.

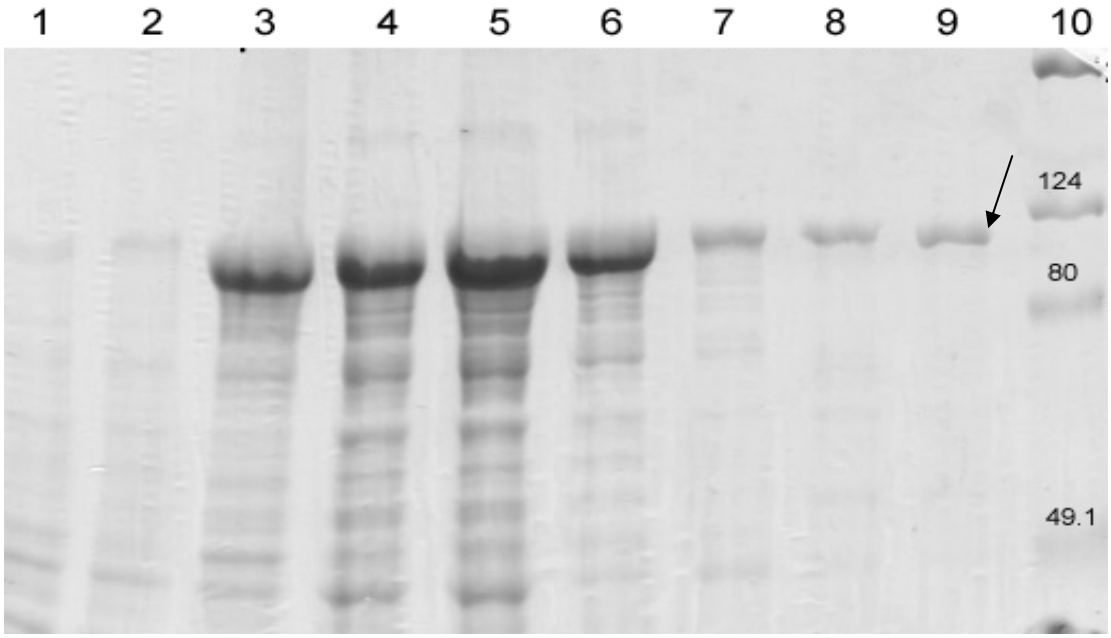

Figure 2.4 SDS gel electrophoresis (8%) analysis of the overexpression and purification of NusA-6x-his-QbsB construct. Lane 1: Pre-induction Lane 2: Post-induction Lane 3: Insoluble pellet Lane 4: Soluble supernatant Lane 5: desalted supernatant Lane 6: Column flowthrough Lane 7: Ni-NTA Column wash Lane 8: Elution Lane 9: Dialyzed eluate Lane 10: molecular weight markers (kDa). NusA-QbsB is indicated with a black arrow.

Figure 2.4 shows that soluble, full-length protein was obtained in reasonable yield (about 8mg/liter of cell culture). However, a considerable amount of the

soluble protein did not bind to the Ni-NTA resin, or was removed in the wash step. This was attributed to the construction of the overexpression vector. The construct was ordered as NusA-6x-His-QbsB, and since the 6x-His-tag was placed between NusA and QbsB, it might not have been completely exposed for binding to the Ni-NTA resin. This explained the decreased affinity the overexpressed protein had for the resin, and why so much eluted in the flow-through and wash. It was also found that the addition of 500mM NaCl significantly increased the stability of the construct, helping to slow aggregation and precipitation.

2.3 Characterization of the NusA-QbsB construct

Interestingly, QbsB has no significant homology to other structurally characterized kynurenine or hydroxykynurenine aminotransferases; rather it shows similarity to histidinol phosphate aminotransferases. To this end, we needed to verify that QbsB did indeed have the putative cyclizing amino-transferase activity seen in figure 2.5.

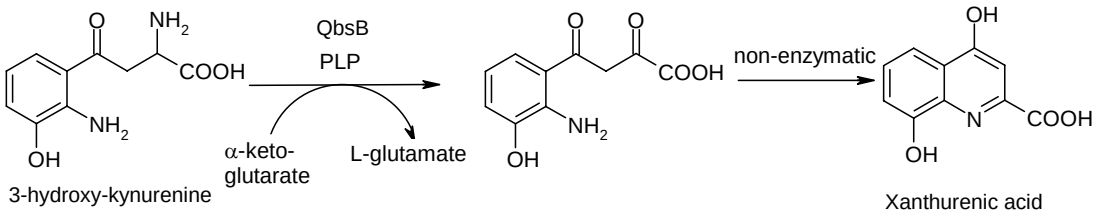

Figure 2.5 Conversion of hydroxykynurenine to xanthurenic acid, dependent upon the cofactor PLP and α-ketoglutarate.

In this reaction, the 3-hydroxykynurenine is deaminated in a PLP dependent mechanism to give the α-keto acid, which then cyclizes non-enzymatically with the aromatic amino group, yielding xanthurenic acid.

2.3.1 Verification of activity via detection of the cyclized product

The initial activity assay was performed with purified NusA-QbsB overexpressed in *E. coli*. In these assays, cultures containing the *nusA-qbsB* overexpression strain were lysed, centrifuged to remove cellular debris and purified by Ni-NTA affinity chromatography. DL-3-hydroxykynurenine, PLP, and α-ketoglutarate were added to NusA-QbsB and the reaction was monitored by detecting formation of xanthurenic acid by HPLC (figure 2.6).[1]

With these reaction conditions there was a significant amount of turnover to product that was dependent on the presence of α-ketoglutarate. If α-ketoglutarate was omitted form the reaction, there was a small but detectable amount of turnover that was approximately equivalent to the amount of PLP that was added to the reaction. When the cofactor PLP was left out of the reaction, the enzyme displayed approximately the same amount of activity, probably due to pyridoxamine phosphate being bound at the enzyme active site.

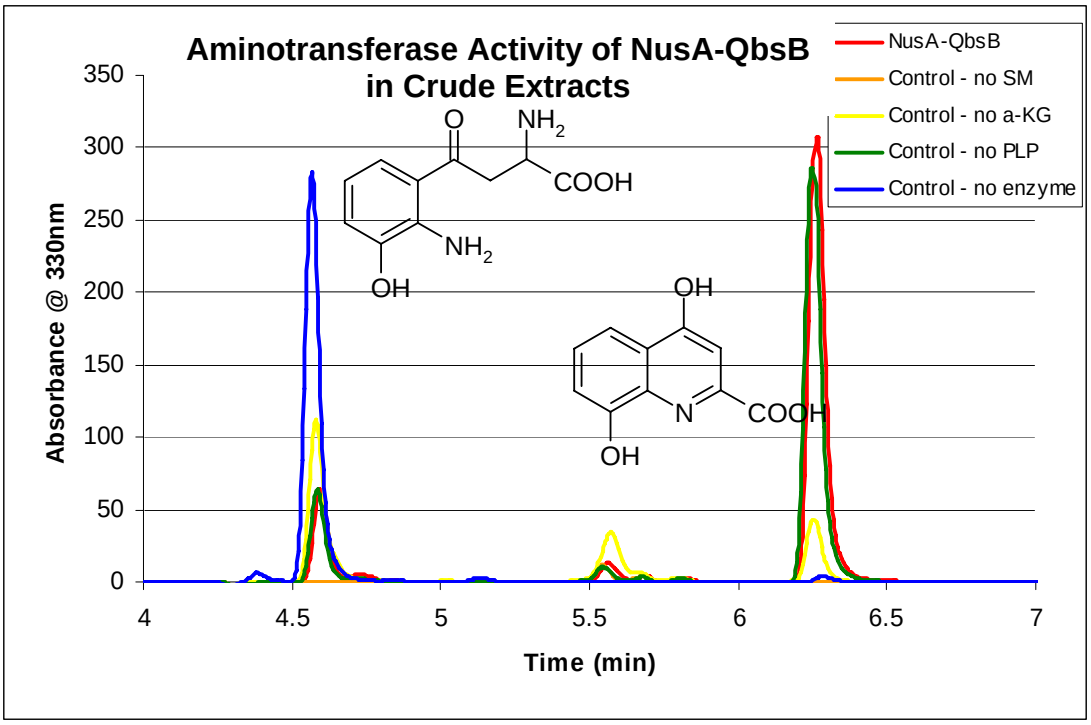

Figure 2.6 Formation of xanthurenic acid in the presence of NusA-QbsB (purified), DL-3-hydroxykynurenine, PLP, and α-ketoglutarate. Reactions are run at room temperature overnight. Red – NusA-QbsB + hydroxykynurenine + PLP + α-ketoglutarate; Orange – NusA-QbsB + PLP + α-ketoglutarate; Yellow - NusA-QbsB + hydroxykynurenine + PLP; Green – NusA-QbsB + hydroxykynurenine + α-ketoglutarate; Blue – hydroxykynurenine + PLP + α-ketoglutarate (no enzyme). DL-3-hydroxykynurenine elutes at ~4.6 min and xanthurenic acid at ~6.3 min.

A UV scan of the purified enzyme shows a broad peak at about 320 nm, which indicates the presence of pyridoxamine (figure 2.7). Only about half of the DL-3-hydroxykynurenine was converted to product based on the HPLC trace, even after overnight incubation with the enzyme. This was expected since the enzyme should be specific for only the L-form of the amino acid derivative.

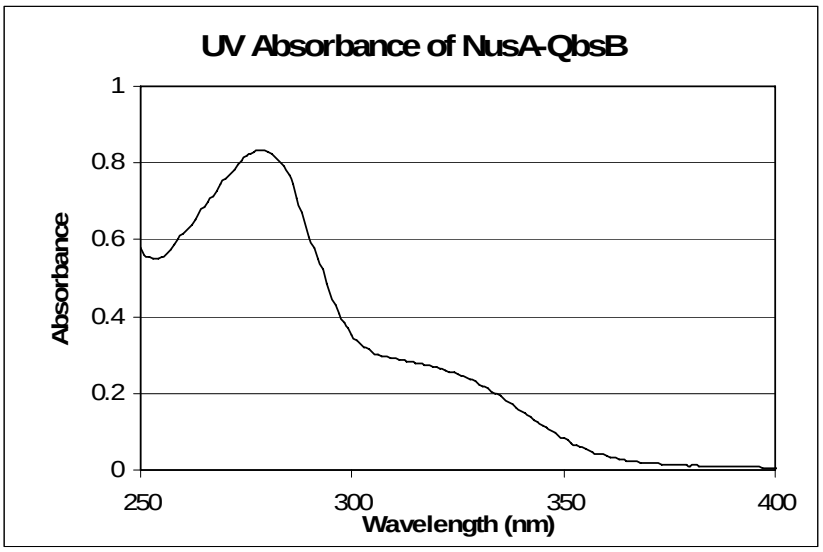

Figure 2.7 UV-Vis trace of the purified NusA-QbsB enzyme showing a broad peak at about 320 nm, indicating the presence of pyridoxamine phosphate.

Once product formation was confirmed via HPLC, a continuous UV-Vis based assay was used to monitor the formation of xanthurenic acid.[7] The product formation observed was also dependent on the concentration of enzyme added to the reaction. This enzyme dependence and the inability of heat denatured enzyme or bovine serum albumin to catalyze the formation of product, indicated that NusA-QbsB is responsible for the product turnover.

Since the enzyme has high homology to histidinol phosphate aminotransferase other substrates were tested (figure 2.8). When NusA-QbsB was incubated with L-tyrosine or L-phenylalanine no enzymatic activity was observed. However, the protein did accept L-histidine as a substrate, but the rate of amount of product turnover was lower than that for DL-3-hydroxykynurenine. NusA-QbsB did not take the D-form of histidine as a

substrate (not shown), lending further support to the enzyme's ability to only accept the L-form of 3-hydroxykynurenine as a substrate.

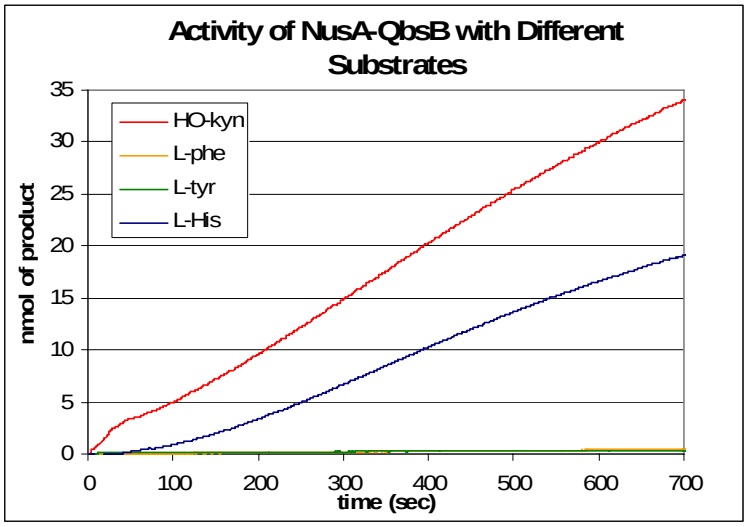

Figure 2.8 Activity of NusA-QbsB with different substrates. Reactions are run at room temperature with 250nmol of substrate and 3.5μM NusA-QbsB. Red: DL-3-hydroxykynurenine; Orange: L-phenylalanine; Green: L-tyrosine; Blue: L-histidine.

2.3.2 Monitoring the formation of xanthurenic acid by NMR

To further confirm the enzyme catalyzed formation of xanthurenic acid from hydroxykynurenine, the reaction was monitored by NMR (figure 2.9). Again, since the starting material is DL and the enzyme appears to only accept one of the enantiomers only about half of the starting material was consumed during the course of the reaction. The NMR spectrum clearly showed the aromatic protons of the product (Hd, He, Hf, Hg) growing in, while those corresponding to the starting material (Ha, Hb, Hc) were decreasing in intensity. The increase is most obvious in the case of Hg (singlet, 6.76 ppm).

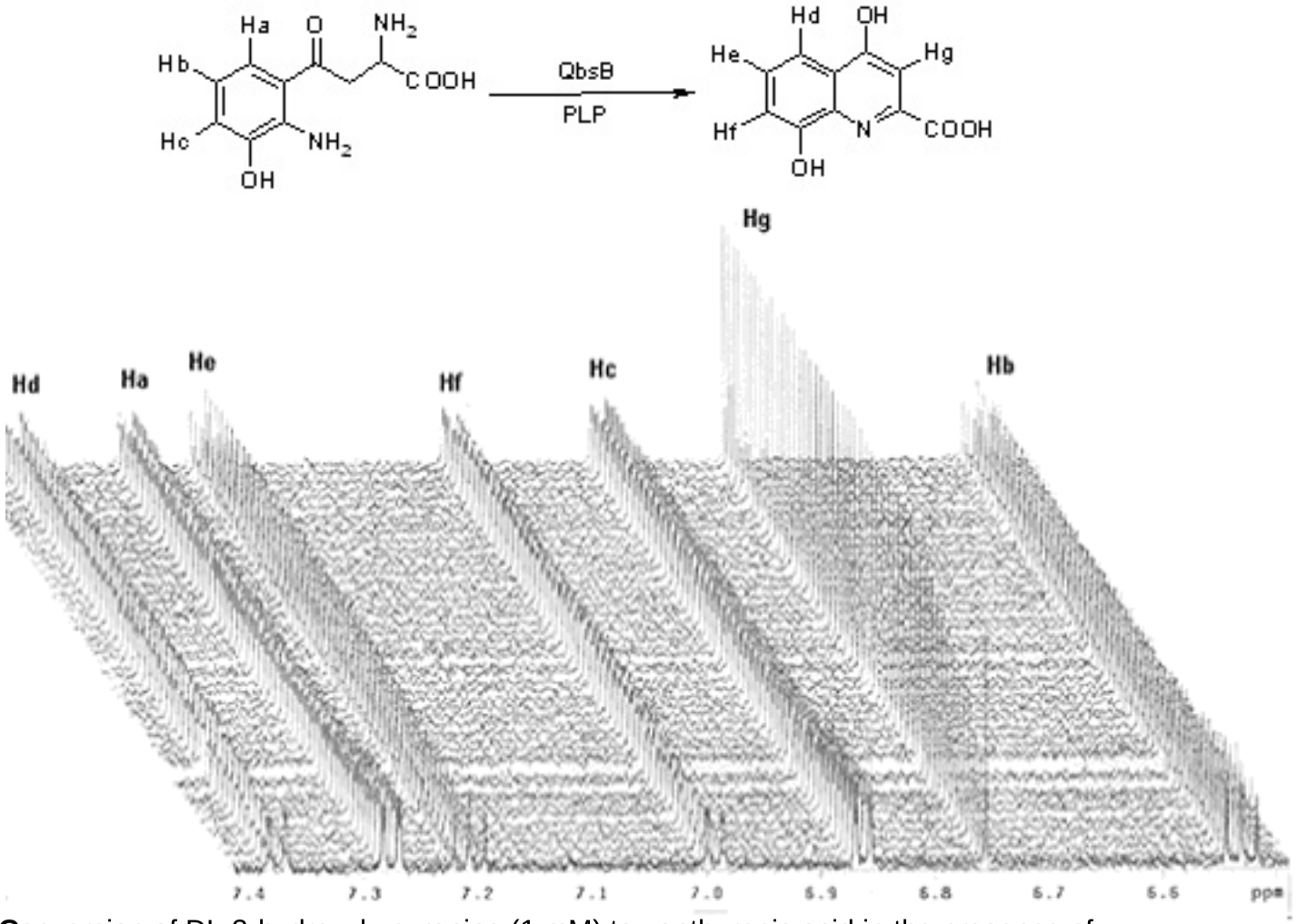

Figure 2.9 **C**onversion of DL-3-hydroxykynurenine (1 mM) to xanthurenic acid in the presence of α-ketoglutarate (5 mM) and NusA-QbsB (~10 uM). The reaction takes place in about an hour.

2.3.3 Kinetic characterization of the cyclizing aminotransferase activity

In order to fully characterize the enzyme, the kinetic parameters were determined. It was necessary to use the NusA-QbsB construct since any attempt to cleave off the NusA tag resulted in insoluble protein. The initial rates were determined with UV-Vis spectroscopy by monitoring the formation of xanthurenic acid, which caused an increase in absorbance at 330 nm. The enzyme has a specific activity of 700 nmol min^{-1} mg^{-1} with DL-3-hydroxykynurenine. K_m and k_{cat} were determined by plotting the initial rates as monitored by UV spectroscopy versus the substrate concentrations in GraFit (figure 2.10).

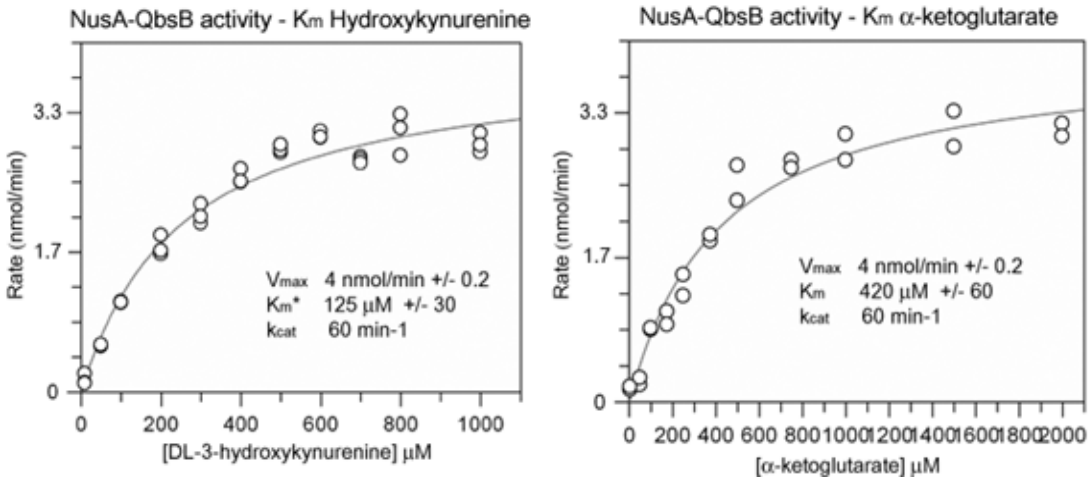

Figure 2.10 Plot of substrate concentrations versus initial rates for NusA-QbsB. The enzyme concentration used in the reactions was 135 nM. The concentration of DL-3-hydroxykynurenine was varied to determine its K_m, and likewise the concentration of α-ketoglutarate was varied to determine its K_m. The concentration of the constant substrate was added to approximately five times its K_m. All data points were determined in triplicate. *****The reported K_m for 3-hydroxykynurenine is half the K_m determined for DL-3-hydroxykynurenine owing to the enzyme specificity for the L-enantiomer.

The kinetic parameters for the cyclizing aminotransferase were determined to be: K_m(L-3-hydroxykynurenine) 125 μM +/- 30, K_m(α-ketoglutarate) 420 μM +/- 60, k_{cat} 60 min^{-1}. It is assumed that the actual substrate of the enzyme is the L-enantiomer of 3-hydroxykynurenine, based on the enzyme accepting L-kynurenine but no D-amino acids, and more generally, what amino-acids are available in the cell.

2.4 Conclusions

QbsB alone proved to be completely insoluble under all of the overexpression and purification conditions attempted. When the protein was expressed with a NusA tag as the construct NusA-6x-his-QbsB, full-length soluble protein was obtained when the cells were lysed with protease inhibitors. The protein purifies with pyridoxamine phosphate bound, was only stable under high salt conditions, and precipitated on storage at 4ºC overnight.

NusA-QbsB was shown to have cyclizing aminotransferase activity, and has a specific activity of 700 nmol min^{-1} mg^{-1} with DL-3-hydroxykynurenine. The enzyme was able to take L-histidine as a substrate in addition to L-kynurenine and DL-3-hydroxykynrenine. D-histidine, L-phenylalanine, and L-tyrosine were not substrates. The kinetic parameters were determined to be K_m(L-3-hydroxykynurenine) 125 μM +/- 30, K_m(α-ketoglutarate) 420 μM +/- 60, k_{cat} 60 min^{-1}.

2.5 Materials and experimental procedures

All materials were obtained from Sigma-Aldrich unless otherwise indicated.

2.5.1 Cloning of QbsB and the NusA-6xHis-QbsB construct

Cloning was performed in the Cornell Protein Purification Facility. The *P. fluorescens qbsB* gene was amplified from genomic DNA by PCR with the following primer pair: 5'-CAC CAT GAA ATT CTC CAA CTT CTT TAG AAA CAG CC-3' and 5'-CTA TCA GAT CGG GTA GAA GAG CCC GTG ATG GTG CG-3'. The PCR product was purified and reacted with pENTR/TEV/D-TOPO (Invitrogen), essentially following the manufacturer's instructions. Clones were screened by restriction digest and verified by sequencing. A correct clone was used in an LR reaction with the plasmid pDESTF1 and, separately, with pDEST544, which is a Gateway adapted vector based on the pET-system from Novagen. The plasmid pDESTF1 encodes an N-terminal 6xHis tag and pDEST544 encodes the NusA protein with an N-terminal 6xHis tag. Both plasmids are under the control of the T7*lac* promoter. Again, clones were screened by restriction digest. Correct clones were named pPfQbsB.XF1 and pPfQbsB.X544.

2.5.2 Overexpression and purification of NusA-QbsB

All cultures contained 100 mg/L ampicillin. 10 mL of LB/Amp were inoculated with a single colony of pPfNusA.QbsB.XF1 in *E. coli* tuner (DE3) cells and grown at 37 ºC for 7 hours with agitation. The entire starter culture was used to inoculate 1 L of LB/Amp media. The culture was grown at 37 ºC to an OD_{600} of 0.4, at which point the temperature was decreased to 15 ºC. At an OD_{600} of 0.6, overexpression was induced by the addition of 500 μM IPTG and growth was continued overnight. The cells were harvested by centrifugation at 7800xg for 12 min at 4 ºC and then stored at -20 ºC.

Purification of the protein was carried out by Ni-NTA chromatography (Qiagen). The cell pellet was resuspended and lysed in 50 mM sodium phosphate buffer, pH 8, 300 mM NaCl, 10 mM imidazole, 25% glycerol with sonication on ice. To all purification buffers was added 100 μM benzamidine and 100 μM PMSF (protease inhibitors). The cellular debris was removed by centrifugation at 27000xg for 30 min at 4 ºC and the supernatant was loaded onto a Ni-NTA column pre-equilibrated in lysis buffer. The column was washed with 20 column volumes of wash buffer, 50 mM sodium phosphate pH 8, 300 mM NaCl, 25 mM imidazole, 25% glycerol, and the protein was eluted with 50 mM sodium phosphate, 10% glycerol, 300 mM NaCl and 250 mM imidazole. The protein was only stable under relatively high salt concentrations, and 500 mM NaCl was usually used. NusA-QbsB is typically desalted into 50 mM Tris pH 7.8 with 500 mM NaCl. After storage at 4 ºC overnight, a considerable amount of protein precipitates. The protein was stable at -20 °C in 20% glycerol for at least one month.

2.5.3 Identification of xanthurenic acid by HPLC

A typical reaction mixture for the purified system contained 200 μM xanthurenic acid, 1 mM α-ketoglutarate, 12 μM PLP, 1.5 μM NusA-QbsB and 50 mM Tris pH 8 with 500 mM NaCl. Controls were performed by omitting reaction substrates. The enzymatic reaction was quenched by rapid freezing in dry ice/acetone bath. The samples were kept frozen until ready for use. Prior to analysis, the thawed samples were centrifuged at 14,000 rpm for 5 min to remove the precipitated protein, and then filtered with microcon YM-3 filters (Amicon). A 500 μL sample of the protein-free reaction mixture was analyzed by HPLC (Supercosil LC-18T 15 cm x 4.6 mm, 3 μm) using the

following gradient: solvent A: 20mM Phosphoric acid 20mM acetic acid pH 4.5 solvent B: 100% acetonitrile, Gradient: 100% A -> 50% A/ 50% B over 15 min, 50% A/50% B ->100% A over 1 min. Both 3-hydroxykynurenine and xanthurenic acid were detected at 330nm (ref 500 nm +/- 5 nm), and eluted from the column at 4.6 and 6.4 min respectively.

2.5.4 Characterization of enzymatic activity by NMR

The enzymatic reaction consisted of 7.5 μM NusA-QbsB, 1 mM DL-3-hydroxykynurenine, 2 mM α-ketoglutarate, 12 μM PLP, 50 mM Tris (fully deuterated) pH 8, and 150 mM NaCl. All substrate stocks were made in deuterium oxide and all water was carefully excluded. The enzyme was desalted into 50 mM fully deuterated Tris in deuterium oxide with 150 mM NaCl with Centri*Spin 10 size exclusion chromatography columns equilibrated in deuterated buffer (Princeton Separations). All reagents except for the enzyme were added to the NMR tube and the sample was locked and shimmed. After addition of the enzyme, the sample was mixed thoroughly and shimmed again. A spectrum was acquired every minute for one minute each over the course of one hour. The spectra were acquired on a Varian 600MHz spectrometer at room temperature.

2.5.5 UV-Vis assay for the formation of xanthurenic acid

A typical reaction for the K_m/k_{cat} determination with DL-3-hydroxykynurenine consisted of 135 nM NusA-QbsB, 2.5 mM α-ketoglutarate, 100 μM PLP, 50 mM Tris pH 8, and 500 mM NaCl. The concentration of DL-3-hydroxykynurenine was varied from 10 μM to 1 mM. A typical reaction for the K_m/k_{cat} determination with α-ketoglutarate consists of 135 nM NusA-QbsB,

1.25 mM DL-3-hydroxykynurenine, 100 μM PLP, 50 mM Tris pH 8, and 500 mM NaCl. The concentration of α-ketoglutarate is varied from 1 μM to 2 mM. Initial rates were measured by monitoring the change in absorbance at 330 nm, which was the formation of product. All data points were obtained in triplicate and kinetic parameters were determined by fitting with GraFit.

2.6 References

1. Kurnasov, O., et al., *NAD biosynthesis: Identification of the tryptophan to quinolinate pathway in bacteria.* Chemistry & Biology, 2003. **10**(12): p. 1195-1204.

2. Billker, O., et al., *Identification of xanthurenic acid as the putative inducer of malaria development in the mosquito.* Nature, 1998. **392**(6673): p. 289-92.

3. Real, M.D. and J. Ferre, *Analysis of kynurenine transaminase activity in Drosophila by high performance liquid chromatography.* Insect Biochemistry, 1991. **21**(6): p. 647-52.

4. Oganesyan, N., S.-H. Kim, and R. Kim, *On-column Refolding of Proteins.* PharmaGenomics, 2004. **9**: p. 22-25.

5. di Guan, C., et al., *Vectors that facilitate the expression and purification of foreign peptides in Escherichia coli by fusion to maltose-binding protein.* Gene, 1988. **67**: p. 21-30.

6. De Marco, V., et al., *The solubility and stability of recombinant proteins are increased by their fusion to NusA.* Biochemisty and Biophysics Research Communications, 2004. **322**: p. 766-771.

7. Miller, I.L., M. Tsuchida, and E.A. Adelberg, *The transamination of kynurenine.* Journal of Biological Chemistry, 1953. **203**: p. 205-11.

CHAPTER 3:

XANTHURENIC ACID METHYLTRANSFERASE AND AMP LIGASE (QbsL) – A DUAL FUNCTIONAL ENZYME

3.1 Introduction

An interesting enzyme along the thio-quinolobactin biosynthetic pathway is the dual domain protein QbsL. This protein has two conserved domains, an AMP-binding domain and a methyltransferase domain (figure 3.1)

Figure 3.1 Structural domains found in QbsL (created with BLAST http://www.ncbi.nih.gov/BLAST/).

Mutation of this gene in *P. fluorescens* renders the organism unable to produce thio-quinolobactin.[1] There are a number of families of methyltransferases, including O-, N-, and C- methyltransferases.[2] The methyltransferase domain of QbsL has homology to some characterized O-methyltransferases, suggesting that this domain may be able to transfer a methyl group to the 4-hydroxy position on xanthurenic acid in a SAM-dependent reaction, generating quinolobactin. The AMP-binding domain of QbsL exhibits significant homology to AMP ligases involved in vibriobactin and enterobactin biosynthesis. With this domain of QbsL, the carboxylic acid of quinolobactin can be activated as the acyl adenylate, using ATP. This

reaction forms the quinolobactin-AMP ester, which is ready to undergo sulfurylation via a sulfide donor to form the thiocarboxylate (figure 3.2).

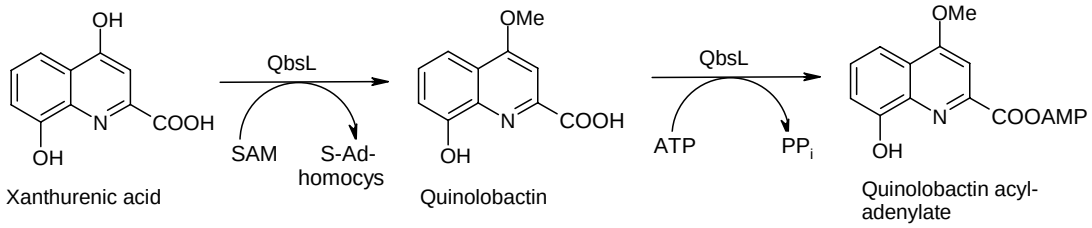

Figure 3.2 Proposed transformations catalyzed by the two domains of QbsL. The first involves the SAM dependent O-methylation of xanthurenic acid by the methyltransferase domain of QbsL and the second is catalyzed by the AMP ligase domain, activating the carboxylic acid of quinolobactin as the acyl adenylate.

3.2 Cloning, overexpression, and purification of the xanthurenic acid methyltransferase and AMP ligase, QbsL in *E. coli*

3.2.1 Cloning

The *qbsL* gene was PCR amplified from *P. fluorescens* ATCC 17400 genomic DNA using the following primers: forward 5'- GAT TTC CAA CAT ATG AAT GGC GCC TTA TTG GCC-3' and reverse 5'- CA ATG CTC ATG GAA TTC TCC AGA CAA TAA AAA GCC-3'. The NdeI/EcoRI cut PCR product was ligated into a similarly digested pET28a vector and transformed into Top10 Cells. Colonies were screened for insert and the hits were sent for sequencing to verify the correct gene sequence. A clone with the correct sequence was identified and named pPfQbsL.28a.

3.2.2 Overexpression trials

Suitable conditions for overexpression of soluble QbsL needed to be identified so that its activity could be studied. Standard overexpression conditions of

37 ºC for 6 hrs in *E. coli* BL21 with 1 mM IPTG in LB/Kan media yielded completely insoluble protein (Figure 3.3).

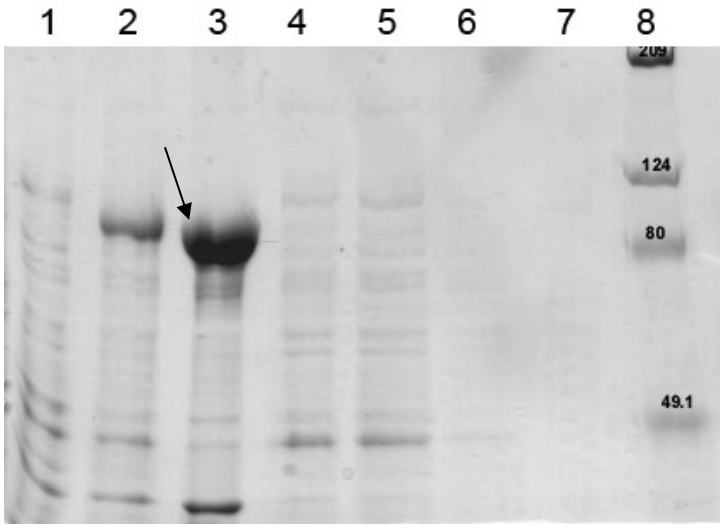

Figure 3.3 SDS gel electrophoresis (8%) analysis of the overexpression and purification of QbsL. Lane 1: Pre-induction Lane 2: Post-induction Lane 3: Insoluble pellet Lane 4: Soluble supernatant Lane 5: Column flow-through Lane 6: Ni-NTA Column wash Lane 7: Elution Lane 8: molecular weight markers (kDa). QbsL is indicated by an arrow.

QbsL overexpressed well, but formed insoluble inclusion bodies. In order to express the protein solubly, a variety of growth and lysis conditions were explored. By overexpressing the protein in *E. coli* tuner (DE3) cells with a lower amount of IPTG (500 μM) and at a reduced temperature (15 ºC) for a longer time (12 hrs), some soluble protein was obtained. However, the highest yield of soluble protein was achieved when the cells were lysed with 1% Triton X-100, and when sorbitol (0.1%) and xanthurenic acid (0.01%) were added to the growth media. The *qbsL* gene product was then purified by Ni-NTA chromatography (Figure 3.4)

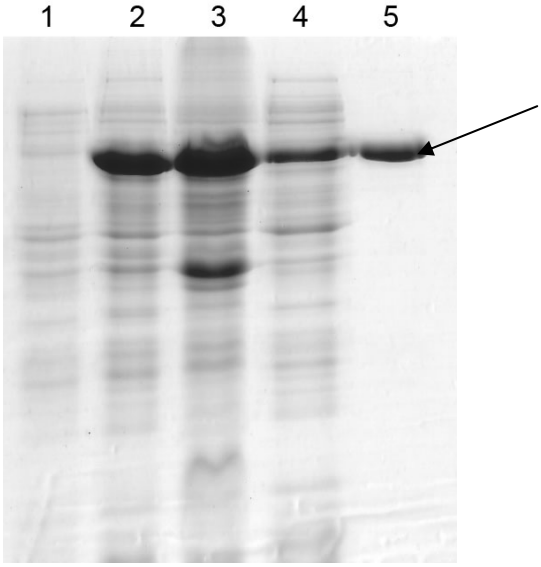

Figure 3.4 SDS gel electrophoresis (12%) analysis of the overexpression and purification of QbsL. Lane 1: Pre-induction Lane 2: Post-induction Lane 3: Insoluble pellet Lane 4: Soluble supernatant Lane 5: Elution. QbsL is indicated by an arrow.

Though the protein was soluble, it did appear as if it was not all binding to the Ni-NTA resin as some eluted in the flow-through and during the column wash step (not shown). This may be due to improper folding of the protein, or low availability of the 6x-His tag of QbsL on the protein surface since QbsL is a rather large protein (~100 kDa). The yield of soluble QbsL was approximately 2-3 mg/liter of cell culture.

3.3 Characterization of the methyltransferase activity of QbsL

Based on the sequence homology of QbsL with other SAM dependent methyltransferases, it was hypothesized that QbsL should be able to transfer a methyl group from SAM to xanthurenic acid, seen in figure 3.5.

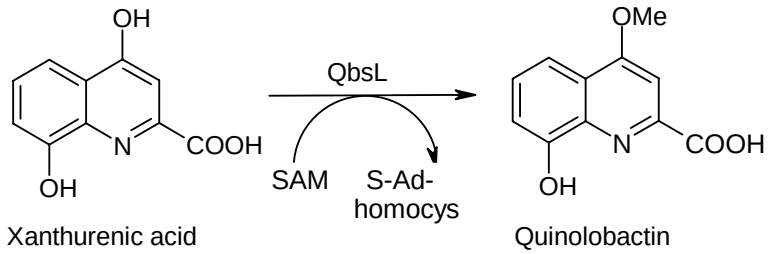

Figure 3.5 One of the reactions catalyzed by QbsL, transfer of a methyl group from SAM to xanthurenic acid to give quinolobactin and S-adenosyl homocysteine (S-Ad-homocys).

3.3.1 Detection of methyltransfer with QbsL crude lysate

The initial activity assay was performed in the clarified crude cell lysate of QbsL overexpressed in *E. coli*. In these assays, cultures containing the *qbsL* overexpression strain were lysed, centrifuged to remove cellular debris, and small molecules were removed by desalting. Xanthurenic acid and SAM were added and the reaction was monitored by detecting formation of quinolobactin by HPLC.[3] With these reaction conditions, no detectable methyl transfer took place. However, given the position of the enzyme in the overall biosynthetic pathway, QbsL may require some of the other biosynthetic enzymes to be present in order for it to function properly. The putative sulfur transfer proteins (QbsCDE) were likely candidates since the final product of QbsL, the quinolobactin acyl adenylate, is not a particularly stable species and would likely be shuttled directly to the next enzymatic step.

Hence, the methyltransferase activity of QbsL in crude cell lysate was again assayed in the presence of clarified crude cell lysate of QbsCDE overexpressed in *E. coli*. Xanthurenic acid and SAM were added and the formation of quinolobactin was monitored via HPLC (Figure 3.6).

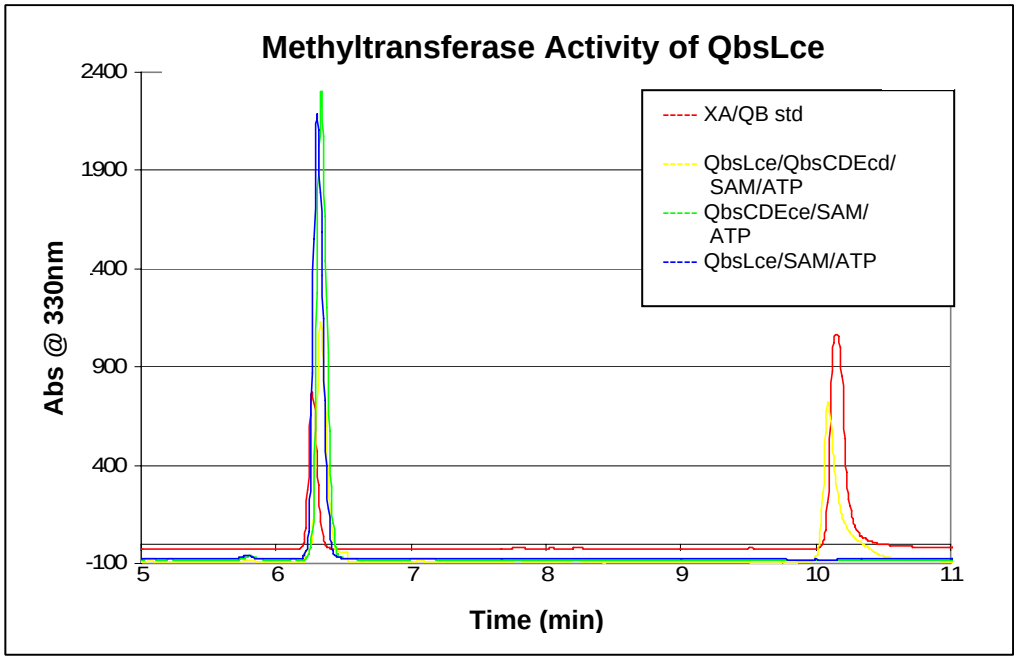

Figure 3.6 Formation of quinolobactin in the presence of QbsL (crude extracts), xanthurenic acid, and SAM. Red – Standards of xanthurenic acid (6.7 min) and quinolobactin (11.2 min); Yellow – QbsL crude extract + QbsCDE crude extract + xanthurenic acid + SAM +ATP; Green – QbsCDE crude extract + xanthurenic acid + SAM + ATP; Blue – QbsL crude extract + xanthurenic acid + ATP + SAM.

When the crude extracts from a QbsCDE overexpression strain were added, a significant amount of quinolobactin (about 74% conversion) formed after overnight incubation. This supported the idea that QbsL was not constitutively active, but rather its activity required the presence of later biosynthetic proteins. However, no methyl transfer took place when either QbsL or SAM were left out of the reaction. Upon heat denaturation no methyltransferase activity was observed. The amount of quinolobactin formed from xanthurenic acid was dependent on the amount of QbsL added to the reaction; higher concentrations of QbsL gave more product turnover. This clearly

demonstrated that QbsL crude extracts alone were not sufficient to produce a detectable amount of quinolobactin.

3.3.2 Detection of methyltransfer with purified QbsL

The next logical step was to look for methyltransfer in a purified system. Presumably, the enzyme that was most likely to interact directly with QbsL was the small putative sulfur carrier protein, QbsE. Given the increase in activity when QbsCDE were present in the crude cell lysate reactions, purified QbsE or a thiocarboxylate mimic, thioacetate, was added to the reaction mixture containing purified QbsL to determine if they had any affect on quinolobactin production. The reactions were run with xanthurenic acid and SAM and the formation of quinolobactin was monitored. Purified QbsL did not have any detectable methyltransferase activity by HPLC, meaning the no quinolobactin formation was detected. The addition of neither purified QbsE nor thioacetate to the reaction gave any detectable amount of quinolobactin. From these experiments, it was unclear if QbsL was simply not active in its purified form or if QbsE and the thiocarboxylate analog were not sufficient to induce activity in QbsL. To test this, further experiments were done with purified QbsL, QbsC, QbsD, and QbsE. No detectable methyltransferase activity was observed via HPLC, implying that QbsL was not appreciably active in its purified form, even when the putative sulfur transfer proteins were added.

A more sensitive approach to look for methyltransferase activity of purified QbsL was to use ^{14}C-(methyl)-SAM. This method was able to detect low amounts of product turnover. Reactions were run with purified QbsL,

xanthurenic acid, DTT, and ^{14}C-SAM. Given the effect the putative sulfur transfer proteins had on the reactions in crude cell extract, these experiments were performed in the presence of purified QbsC and QbsE to determine if they had any affect on product formation (figure 3.7). It was also found that DTT had an accelerating affect on the reaction, something that was not observed in the crude cell extracts.

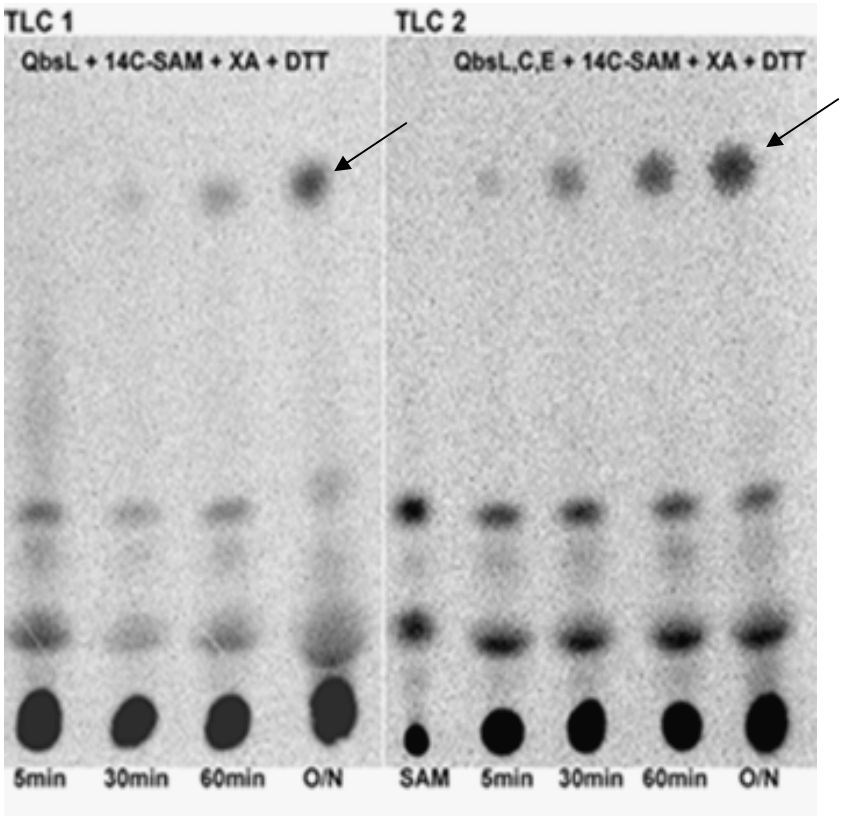

Figure 3.7 Time course of methyltransferase activity of purified QbsL using ^{14}C-SAM. The time course in TLC 1 has QbsL (purified) + ^{14}C-SAM + xanthurenic acid (XA) + DTT, while that in TLC 2 additionally contains QbsC and QbsE (purified). The black arrow indicates where the product, quinolobactin runs on the TLC plate. Spots at the bottom of the plate were not identified and were present in the purchased SAM.

These results indicated that purified QbsL did have some level of methyltransferase activity even without QbsC and QbsE, although it was very low. Even after only thirty minutes some amount of product formation was observed. By comparison, when QbsC and QbsE were added product formation was observed in as little as five minutes. Overall, it appeared as though the presence of QbsC and QbsE increased the amount of product formation. This reinforced the results obtained when assaying the clarified crude cell lysate.

3.3.3 Kinetics of the methyltransfer

Firm kinetic parameters could not be obtained in the crude extract, but a time course of the methyltransferase reaction was carried out (figure 3.8).

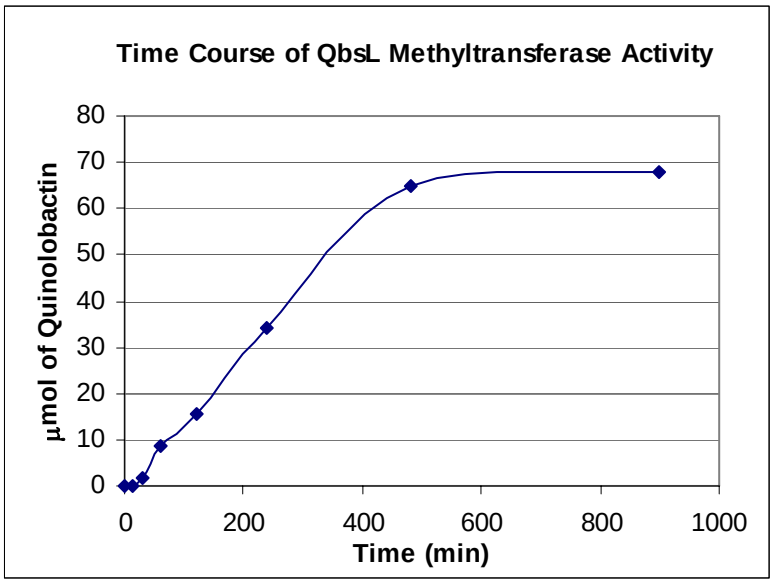

Figure 3.8 Amount of quinolobactin formed with time by QbsL crude extracts with QbsCDE crude extracts. The total amount of starting material used was 475µmol.

Enzymatic turnover was extremely slow and also very low. This indicated that we have not fully identified the binding partners that QbsL may have that were required for it to be fully active. The low activity may also be caused by improper folding of the protein, resulting in a large inactive population. Though product formation was very slow, it was detectable and well above background.

3.4 Characterization of the acyl adenylate formed by QbsL

QbsL also contains an AMP-binding domain that could be capable of activating the carboxylic acid on xanthurenic acid as the acyl adenylate (figure 3.9). This would activate the xanthurenic acid for subsequent sulfur transfer to form the final product, thio-quinolobactin.

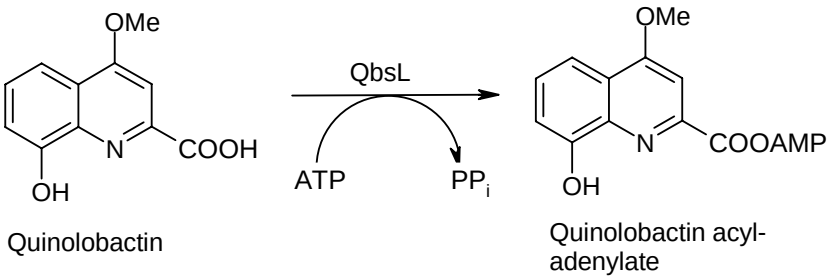

Figure 3.9 Activation of the carboxylic acid of quinolobactin with AMP to form the acyl adenylate, in and ATP dependent reaction.

3.4.1 Detection of acyl adenylate formation with QbsL crude extracts

In order to detect the acyl-adenylation activity of QbsL we needed to detect the unstable quinolobactin acyl adenylate product. Due to its instability this species was difficult to isolate and characterize, so secondary methods of detection were used to detect its formation. Since the initial activity was being determined in crude cell extracts, we could not directly look for the formation of

AMP due to high background hydrolysis of ATP to AMP. An alternative method was developed that took advantage of the reactivity of the quinolobactin acyl adenylate to form a more stable species that linked quinolobactin to dansylhydrazine through an amide bond (figure 3.10).

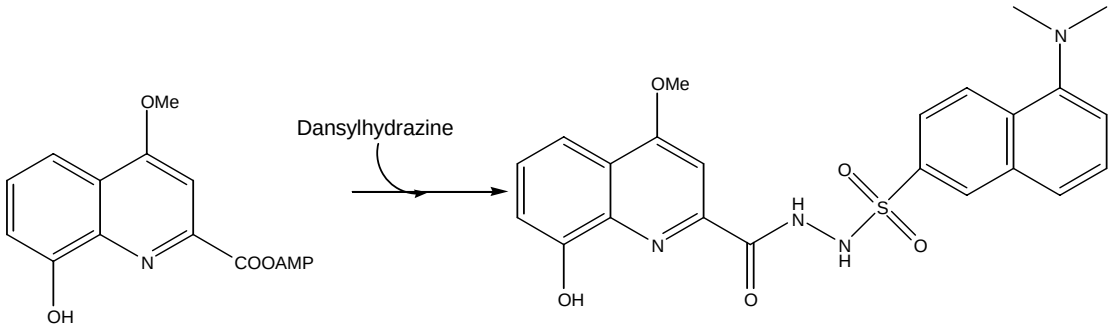

Figure 3.10 Method used to detect the unstable quinolobactin acyl adenylate by forming a stable conjugate with dansylhydrazine.

The reaction mixture contained QbsL crude extracts, QbsCDE crude extracts, quinolobactin, ATP, and dansylhydrazine. Dansylhydrazine in the reaction mixture ensured that if the quinolobactin acyl adenylate was released from QbsL, it had a chance of reacting before it was hydrolyzed. The quinolobactin-dansylhydrazine conjugate was synthesized chemically as a standard and the enzymatic formation was monitored by HPLC (figure 3.11).

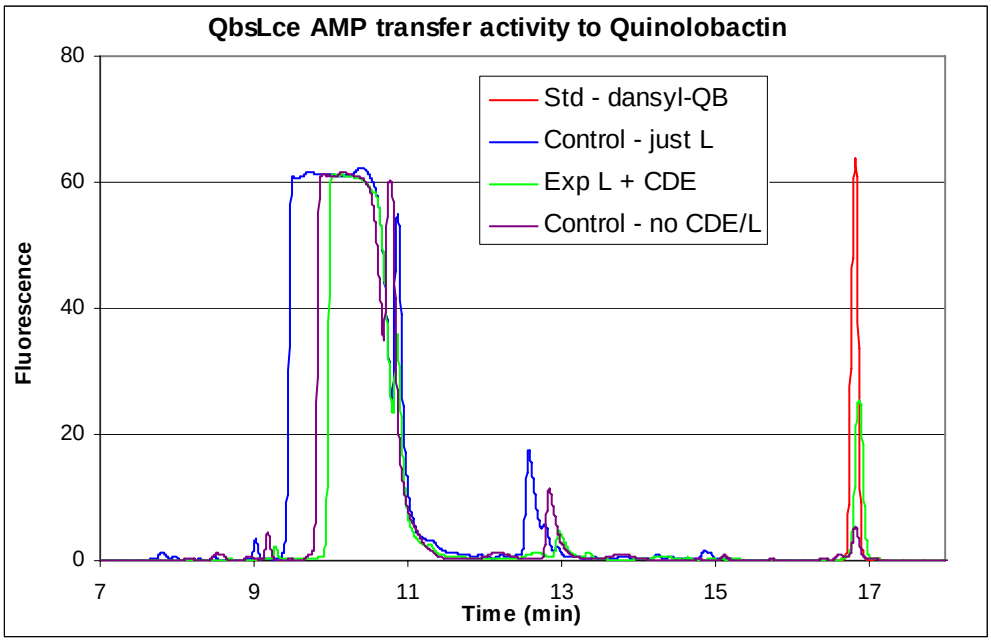

Figure 3.11 Formation of quinolobactin-dansylhydrazine conjugate. Red – Standard quinolobactin-dansylhydrazine (16.9min) Blue – QbsL (crude extracts) + quinolobactin + ATP + dansylhydrazine Green – QbsL (crude extracts) + QbsCDE (crude extracts) + quinolobactin + ATP + dansylhydrazine Purple - quinolobactin + ATP + dansylhydrazine. Dansyl-hydrazine elutes at about 10min.

The HPLC trace showed that the quinolobactin-dansylhydrazine conjugate (17 min) is formed only in the presence of crude cell lysates of both QbsL and QbsCDE. Again this supported the idea that QbsL required the presence of later biosynthetic enzymes in order to exhibit enzymatic activity. That the amount of conjugate formed was relatively small compared to the amount of quinolobactin added to the reaction can be explained in two ways. One is that the quinolobactin acyl adenylate is not released from the enzyme unless the components for sulfur transfer are present so that the thio-quinolobactin can be made. Alternatively, if the quinolobactin acyl adenylate is released, it may

get hydrolyzed before encountering the dansylhydrazine, thus reforming quinolobactin.

3.4.2 Detection of acyl adenylate formation with purified QbsL

If quinolobactin acyl adenylate is released from QbsL it would be hydrolyzed due to its instability. The half-life of similar compounds is less that 30 min in a pH 7 solution.[4] In a purified system, we can directly detect any AMP that is released from the quinolobactin acyl adenylate. When purified QbsL was incubated with α-^{32}P-ATP and quinolobactin there was a small amount of AMP released. QbsL alone, without quinolobactin, did not appear to catalyze any appreciable amount of ATP hydrolysis.

Like with the crude extracts, we ran the QbsL adenylation reaction in the presence of QbsC, QbsD, and QbsE or thioacetate, which acts as a QbsE-thiocarboxylate mimic. Since QbsE is the protein that putatively delivers the sulfur to the small molecule, this species might induce adenylation activity in QbsL. Since QbsE would also be the sulfur carrier, it may help to dislodge the quinolobactin acyl adenylate from the active site of QbsL. This would then make the acyl adenylate more susceptible to hydrolysis. The addition of thioacetate or QbsE alone did not appear to increase the amount of α-^{32}P-AMP detected. When QbsL was mixed with QbsC, QbsD, and QbsE an increase in the amount of AMP was observed (figure 3.12). When just QbsC, QbsD, and QbsE or QbsD and QbsE were combined no formation of α-^{32}P-AMP was detected.

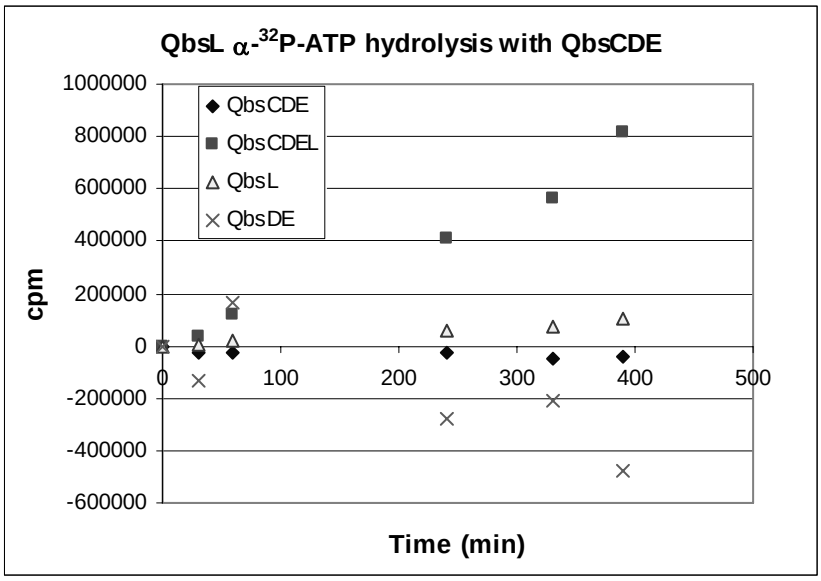

Figure 3.12 α-^{32}P-ATP hydrolysis catalyzed by QbsL. Enzymatic activity was monitored by detection of α-^{32}P-AMP. The amount of α-^{32}P-ATP and quinolobactin used were approximately 50x that of QbsL. Squares – QbsCDE + QbsL + QB + α-^{32}P-ATP; Triangles - QbsL + QB + α-^{32}P-ATP; Diamonds - QbsCDE + QB + α-^{32}P-ATP; X's - QbsDE + QB + α-^{32}P-ATP

It appears that the addition of QbsC, QbsD, and QbsE to the QbsL reaction increased the amount of α-^{32}P-ATP formed. There was a small amount of ATP hydrolyzed by QbsL alone. The presence of auxiliary proteins (like the sulfur transfer proteins) with QbsL appeared to increase the activity of the enzyme.

3.5 Conclusions

We have shown that QbsL was able to catalyze the SAM dependent transfer of a methyl group to xanthurenic acid. The activity was detectable by HPLC in crude extracts, but no quinolobactin is detected with purified QbsL. In order for activity to be seen, even in crude extracts, the putative sulfur transfer proteins must be added. The amount of product turnover was very low and

the amount of QbsL obtained from a protein preparation was small. A minute but detectable amount of methyl transfer was seen with purified QbsL alone when ^{14}C-methyl-SAM was used. In addition, we have evidence that QbsL may also catalyze the formation of the quinolobactin acyl adenylate in an ATP dependent reaction. We have observed QbsL dependent formation of α-^{32}P-AMP with quinolobactin, which implies that QbsL may be activating the carboxylic acid of quinolobactin with AMP. In addition, when dansylhydrazine was added to QbsL crude extracts in the presence of the putative sulfur transfer proteins, quinolobactin, and ATP, we saw a new species by HPLC that migrated with a dansyl-quinolobactin conjugate standard. This provided evidence that QbsL could indeed activate the carboxylic acid of quinolobactin as the acyl adenylate.

3.6 Materials and experimental procedures

All materials were obtained from Sigma-Aldrich unless otherwise indicated.

3.6.1 Cloning of *qbsL* into pET28a

Genomic DNA from *P. fluorescens* ATCC 17400 was isolated using the Wizard^{TM} Plus DNA prep kit. This was used to PCR amplify *qbsL* using the following primers: forward 5'- GAT TTC CAA CAT ATG AAT GGC GCC TTA TTG GCC-3' and reverse 5'- CA ATG CTC ATG GAA TTC TCC AGA CAA TAA AAA GCC-3' (IDT oligs). PCR reactions were carried out using Platinum Pfx Polymerase and dNTPs from Invitrogen according to the literature protocol, except using 100 pmol of each primer and 1μL of enhancer per 10 μL reaction. The PCR product (~2.7 kb) was purified by agarose gel electrophoresis, excised and purified with the Qiagen Gel Extraction kit. PCR

amplified *qbsL* was digested with NdeI and EcoRI, obtained from New England Biolabs. The digested *qbsL* was purified directly from the reaction mixture with the QiaQuick MiniElute PCR purification kit. The cut insert was ligated into a similarly digested pET28a vector (Novagen) that had been purified by gel electrophoresis with T4 DNA ligase (New England Biolabs). Supercompetent *E. coli* Top 10 cells (Invitrogen) were used to transform the ligated pET28a and insert. Standard methods were used for DNA restriction endonuclease digestion, ligation and transformation of DNA. Colonies were then screened for the *qbsL* insert and those colonies that had insert were grown at 37 ºC in LB/Kan media for 8 hrs, and the plasmid harvested. The prepared plasmid was sequenced and a plasmid with the correct sequence was selected and named pPfQbsL.28a. Plasmid DNA was purified with the Qiagen Plasmid purification kit. Plasmid storage and propagation was performed using *E. coli* Mach1 $T1^R$ cells (Invitrogen).

3.6.2 Overexpression and purification of QbsL

All cultures contained 50 mg/L kanamycin sulfate. 10 mL of LB(VWR)/Kan were inoculated with a single colony of pPfQbsL.28a in *E. coli* tuner (DE3) cells and grown at 37 ºC for 7 hrs with agitation. The entire starter culture was used to inoculate 1L of LB/Kan media with 0.1% sorbitol (VWR) and 0.01% xanthurenic acid. The culture was grown at 37 ºC to an OD_{600} of 0.4, at which point the temperature was decreased to 15 ºC. At an OD_{600} of 0.6, overexpression was induced by the addition of 500 μM IPTG and growth was continued overnight. The cells were harvested by centrifugation at 7800xg for 12 min at 4 ºC and then stored at -20 ºC.

Purification of the protein was carried out by Ni-NTA chromatography (Qiagen). The cell pellet was resuspended and lysed in 50 mM sodium phosphate buffer, pH 8, 300 mM NaCl, 10 mM imidazole with sonicaiton on ice. The cellular debris was removed by centrifugation at 27000xg for 30 min at 4 ºC and the supernatant was loaded onto a Ni-NTA column pre-equilibrated in lysis buffer. The column was washed with 20 column volumes of wash buffer, 50 mM sodium phosphate pH 8, 300 mM NaCl, 25 mM imidazole, and the protein was eluted with 50 mM sodium phosphate, 300 mM NaCl and 250 mM imidazole. The protein was only stable with a minimum of 50 mM NaCl present in the buffer and was typically desalted into 50 mM Tris pH 7.8 with 50 mM NaCl. After storage at 4 ºC overnight, a considerable amount of protein precipitates. Even when left in the clarified crude cell extract most of the protein precipitated after overnight storage at 4 ºC.

3.6.3 Overexpression and preparation of QbsCDE

QbsCDE was overexpressed as described for QbsL above, but without adding xanthurenic acid to the growth media. The frozen cell pellet was resuspended and lysed in 50 mM sodium phosphate buffer pH 8, 300 mM NaCl, 10 mM imidazole with sonicaiton on ice. The cellular debris was removed by centrifugation at 27000xg for 30min at 4ºC. The supernatant was desalted into 50 mM Tris pH 7.8, 50 mM NaCl using EconoPac DG10 columns (Biorad).

3.6.4 Identification of ^{14}C-methyl-quinolobactin via TLC using ^{14}C-SAM

A typical reaction mixture contained 200 μM xanthurenic acid, 400 μM SAM, 0.5 μCi ^{14}C-methyl-SAM (ARC), 1 mM DTT, 7 μM QbsL (purified), and 50 mM Tris pH 7.8 with 150 mM NaCl. All reagents were mixed except for the SAM

and ^{14}C-SAM, which were added last to initiate the reaction. The reaction was quenched by simply spotting 5 μL onto a silica TLC plate at various time points. The TLC plate was run in 4:1:1 nBuOH:AcOH:water, dried, wrapped in plastic wrap and placed on a phosphorimaging screen from Molecular Dynamics. After exposure, the screen was imaged using a Storm 860 Phosphorimager from Amersham and data was analyzed using ImageQuant.

3.6.5 Identification of quinolobactin formation by HPLC

A typical reaction mixture for the purified system contained 0.5 mM xanthurenic acid, 1 mM SAM, 1 mM ATP, 5 mM $MgCl_2$, 3.8 μM QbsL and 50 mM Tris pH 8 with 50 mM NaCl. To some reactions was added 10μM QbsE or 1 mM thioacetate. The enzymatic reaction was quenched by rapid freezing in dry ice/acetone bath. The samples were kept frozen until ready for use. Prior to analysis, the thawed samples were centrifuged at 14,000rpm for 5 min to remove the precipitated protein, and then filtered with microcon YM-3 filters (amicon). A 500 μL sample of the protein-free reaction mixture was analyzed by HPLC (Supercosil LC-18T 15 cm x 4.6 mm, 3 μm) using the following gradient: solvent A: 20 mM Phosphoric acid 20 mM acetic acid pH 4.5 solvent B: 100% acetonitrile, Gradient: 100% A -> 50% A/ 50% B over 15min, 50% A/50% B ->100% A over 1 min. Both xanthurenic acid and quinolobactin were detected at 330 nm (ref 500 nm +/- 5 nm), and eluted from the column at 6.7 and 11.2 min respectively.

When the reaction was performed in crude cell extracts, they typically contained 0.5 mM xanthurenic acid, 1 mM SAM, 1 mM ATP, 5 mM $MgCl_2$, 50 mM Tris pH 8 with 50 mM NaCl, and 300 μL of QbsL (crude extract). To

some reactions was added 100 μL of QbsCDE (crude extract). The enzymatic reaction was again quenched by rapid freezing in dry ice/acetone bath, and the samples were kept frozen until ready for use. Subsequent treatment and analysis was the same as described above.

3.6.6 Detection of α-^{32}P-AMP from the hydrolysis of quinolobactin acyl adenylate

These reactions were only performed with purified enzyme preparations. A typical reaction contained 100 μM ammonium thiosulfate, 50 μM quinolobactin, 500 μM $MgCl_2$, 100 μM ATP, 75 mM Tris pH 7.8, 50 mM NaCl, and 1.2 μM of each enzyme, QbsC, QbsD, QbsE, and QbsL. To each reaction was added 0.25 μCi of α-^{32}P-ATP (GE-Healthcare) in a stock of cold ATP. Reactions were started by the addition of the ATP. Aliquots of the reaction were taken at various intervals and quenched by direct spotting on a 20x20 cm silica TLC plate. The plates were run in 4:1:1 n-BuOH:water:acetic acid mixture. After drying the plates were wrapped in plastic wrap and then exposed to a phosphorimaging. The screen was developed using the Storm 860 Phosphorimager and quantitated using ImageQuant.

3.6.7 Synthesis of quinolobactin

Quinolobactin was synthesized following the procedure of d'Hardemare, et.al.[5] A suspension of xanthurenic acid (500 mg) in 5 mL of thionyl chloride was refluxed for 14 hrs, yielding a homogenous dark brown solution. The excess thionyl chloride was removed by distillation under aspirator pressure. To the remaining brown residue was added 5 mL of anhydrous methanol, giving a brown-orange solution that was refluxed for 30 min. The solution was

concentrated by rotovapping and 500 mg of sodium dissolved in 5 mL of methanol was added. The resulting brown/orange suspension was refluxed for 3 hrs. The solid was filtered off and the dark brown filtrate was rotavapped to remove the methanol. Water was added to the residue and the quinolobactin methyl ester was exhaustively extracted with ethyl acetate. The combined organic layers were dried with $MgSO_4$ and filtered, and the ethyl acetate was removed by rotovapping, yielding an orange solid. The orange solid was dissolved in aqueous sodium hydroxide and refluxed for 40 min. The solution was cooled to room temperature and the pH adjusted to 2 with HCl, causing a yellow precipitate to form. Quinolobactin was extracted exhaustively with ethyl acetate. Again the organic layers were dried with $MgSO_4$ and filtered. The solution was rotovapped to remove solvent. Yield: 210 mg of a yellow solid. NMR (D_2O with NaOD) δ(7.237 s, 1H); δ(7.201 t, 1H); δ(7.066 d, 1H); δ(6.659 d, 1H); δ(3.882 s, 3H).

3.6.8 Synthesis of the quinolobactin-dansylhydrazine conjugate

Quinolobactin (25 mg) was heated to reflux in 500 μL of thionyl chloride for 2 hrs. The excess thionyl chloride was distilled off under aspirator pressure and the remaining residue was dissolved in 1 mL of anhydrous dichloromethane. A suspension of dansylhydrazine (30 mg) in 1 mL of dichloromethane was added with stirring. The reaction was stirred at room temperature for 6 hrs, and the solvent was removed *in vacuo*. The residue was brought up in a minimal amount of methanol and purified by preparative TLC with 6:1:1 n-BuOH:AcOH:water. Yield 1 mg of a yellow/orange solid. NMR 300MHz CD_3OD δ(8.56, d, 1H); δ(8.27, t, 2H); δ(7.61, q, 2H); δ(7.30, d, 1H); δ(7.24, s, 1H); δ(7.11, t, 1H); δ(7.01, d, 1H); δ(6.61, d, 1H); δ(3.80, s, 3H); δ(2.91, s, 6H).

3.7 References

1. Matthijs, S., et al., *The Pseudomonas siderophore quinolobactin is synthesized from xanthurenic acid, an intermediate of the kynurenine pathway.* Molecular Microbiology, 2004. **52**(2): p. 371-384.

2. Yoon, Y., et al., *Characterization of O-methyltransferase ScOMT1 cloned from Streptomyces coelicolor A3(2).* Biochimica et Biophysica Acta, 2005. **1730**: p. 85-95.

3. Kurnasov, O., et al., *NAD biosynthesis: Identification of the tryptophan to quinolinate pathway in bacteria.* Chemistry & Biology, 2003. **10**(12): p. 1195-1204.

4. Moldave, K., P. Castelfranco, and A. Meister, *The Synthesis and Some Properties of Amino Acyl Adenylates.* Journal of Biological Chemistry, 1959. **234**(4): p. 841-848.

5. du Moulinet D'Hardemare, A., G. Serratrice, and J.L. Pierre, *Synthesis and iron-binding properties of quinolobactin, a siderophore from a pyoverdine-deficient Pseudomonas fluorescens.* BioMetals, 2004. **17**(6): p. 691-697.

CHAPTER 4:

SULFUR ACTIVATING PROTEIN (QbsC)

4.1 Introduction

Nature produces a number of molecules that have sulfur incorporated into them including thiamin, molybdopterin, cysteine, and pyridine-2,6-di-(monothiocarboxylic acid) (PDTC). The final product of the biosynthetic pathway we are studying is thio-quinolobactin, which also possesses sulfur in the form of a thiocarboxylate. There are a few examples of thiocarboxylates that are biosynthesized in various *Pseudomonads spp.*[1] We are interested in investigating how the sulfur is transferred to quinolobactin acyl adenylate that is made by QbsL (figure 4.1).

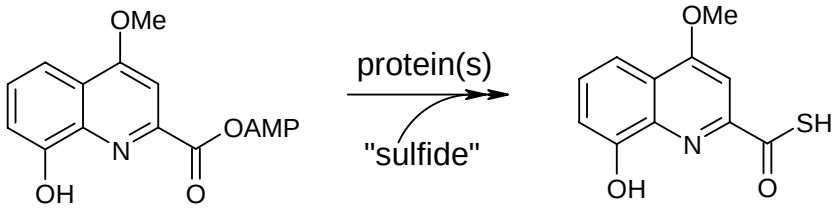

Figure 4.1 Sulfur transfer to the quinolobactin acyl adenylate.

We were first led to look at QbsC as a participant in sulfur transfer because it has significant sequence similarity to ThiF, a protein involved in sulfur transfer in thiamin biosynthesis, and MoeB, which is involved in sulfur transfer in molybdopterin biosynthesis.[2] These proteins are involved in the activation of the small sulfur carrier protein, ThiS and MoaB, respectively. When the

sequence of QbsC is compared with proteins of known function, we find that it has two domains (figure 4.2).

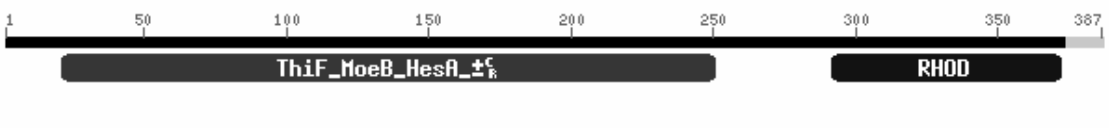

Figure 4.2 Structural domains found in QbsC (created with BLAST http://www.ncbi.nih.gov/BLAST).

The ThiF_MoeB_HesA domain is responsible for the activation of the small sulfur carrier protein by adenylation of its C-terminal end. The second domain found in QbsC is a rhodanese domain. Rhodanese domains are versatile sulfur carriers that are used to fulfill the need for a reactive sulfur species and catalyze the transfer of a sulfane sulfur atom from thiosulfate to cyanide *in vitro*. The presence of this domain indicates that QbsC may be able to activate sulfur that will eventually get transferred to quinolobactin. This rhodanese domain is not always found in ThiF or MoeB proteins, implying that the activation of the sulfur is carried out by another protein in these systems for subsequent delivery to the sulfur carrier protein.

Catalysis by the rhodanese domain occurs via a double displacement mechanism (figure 4.3). An activated cysteine, which is typically part of a six-amino active-site loop, attacks the thiosulfate, displacing sulfite and forming a transient persulfide intermediate on the protein (Cys-S-SH).[3, 4] A nucleophile, such as cyanide, then attacks the protein bound persulfide, regenerating the active site cysteine and forming thiocyanide.

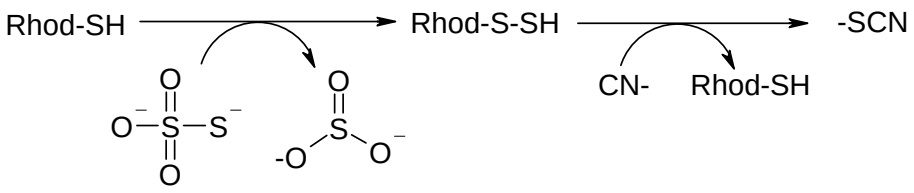

Figure 4.3 Catalytic mechanism employed by rhodanese proteins.

Here we are interested in exploring and characterizing the rhodanese activity of QbsC. We believe that QbsC is able to form a protein bound persulfide using the sulfane sulfur from thiosulfate and transfer that sulfur to the activated small sulfur carrier protein, QbsE.

4.2 Cloning, overexpression, and purification of the sulfur activating protein, QbsC in *E. coli*

4.2.1 Cloning

The *qbsC* gene was PCR amplified from *P. fluorescens* ATCC 17400 genomic DNA using the following primers: forward 5'- GGA ACA CAT ATG CAA CTT CCA CCC TTG GTA GAA GCC -3' and reverse 5'- GC AAC ATA AGC GAA TTC TCA GTA GGC CGG CAG -3'. The NdeI/EcoRI cut PCR product was ligated into an NdeI/EcoRI digested pET28a vector and transformed into Top10 Cells. Colonies were screened for insert and the hits were sent for sequencing to verify the correct gene sequence. A clone with the correct sequence was identified and named pPfQbsC.28a.

4.2.2 Overexpression trials

Suitable conditions for overexpression of soluble QbsC needed to be identified so that its activity could be studied. Like QbsB and QbsL, standard overexpression conditions of 37ºC for 6hrs in *E. coli* BL21 with 1 mM IPTG in

LB/Kan media yielded completely insoluble protein. The putative sulfur donor protein QbsC overexpressed extremely well, but was not appreciably soluble. Further attempts to obtain soluble protein with lowered growth temperatures and reduced amounts of IPTG (250-500 μM) failed. When sorbitol was added to the growth media at 0.1%, and Triton X-100 was added to the resuspended cells during lysis some soluble protein was obtained. The protein was purified by Ni-NTA affinity chromatography (figure 4.4).

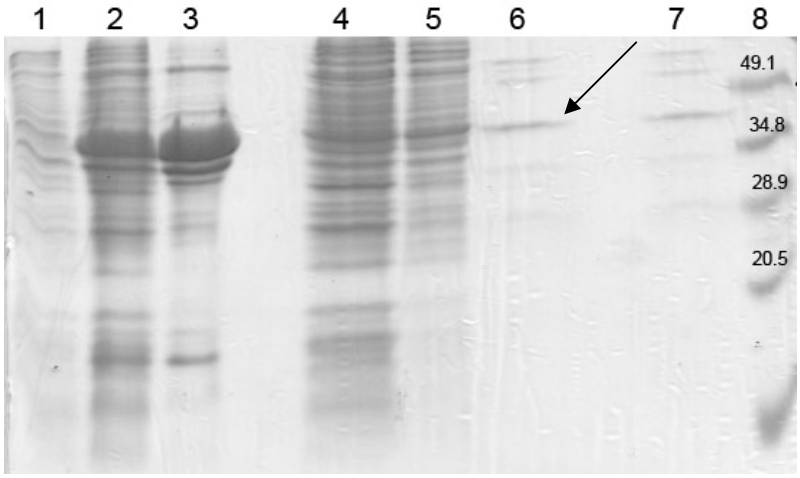

Figure 4.4 SDS gel electrophoresis (12%) analysis of the overexpression and purification of QbsC, which has a molecular weight of ~42 kDa (indicated by arrow). Lane 1: Pre-induction Lane 2: Post-induction Lane 3: Insoluble pellet Lane 4: Soluble supernatant Lane 5: Column flowthrough Lane 6: Ni-NTA Column elution Lane 7: Buffer exchanged protein Lane 8: molecular weight markers (kDa).

Very little soluble protein, typically 1-2 mg/liter of cell culture, was obtained from this preparation.

4.2.3 Improved solubility with co-overexpression with QbsE

Based on the sequence similarity of QbsC with the sulfur donor protein ThiF in thiamin biosynthesis, it was thought that QbsC would require a binding partner to have improved solubility. In the case of ThiF, the binding partner is a small sulfur carrier protein, ThiS.[5] The thio-quinolobactin biosynthetic gene cluster contains a similar small potential sulfur carrier protein, QbsE. We wanted to test if the solubility of QbsC was enhanced by co-overexpression with the ThiS-like protein, QbsE. Two plasmids, one containing QbsC and the other QbsE, (see chapter 5 for cloning) were co-transformed into Tuner (DE3) cells and overexpressed at 15 °C with reduced amounts of IPTG (500 μM) and 0.1% sorbitol added to the media. The cells were lysed with Triton X-100 and purified by Ni-NTA affinity chromatography (figure 4.5).

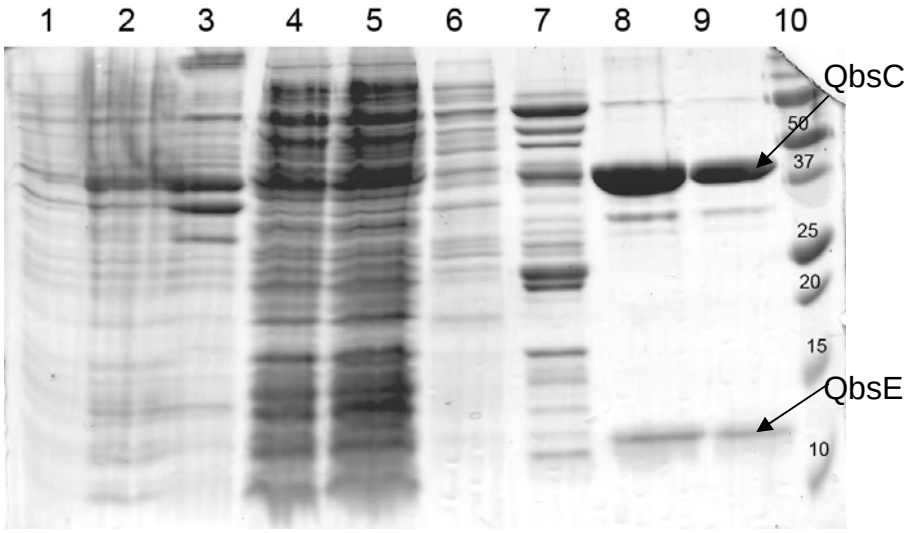

Figure 4.5 SDS gel electrophoresis (12%) analysis of the overexpression and purification of QbsC with co-overexpressed QbsE, which has a molecular weight of ~12 kDa. Lane 1: Pre-induction Lane 2: Post-induction Lane 3: Insoluble pellet Lane 4: Soluble supernatant Lane 5: Column flowthrough Lane 6: Column wash 1 Lane 7: Column wash 2 Lane 8: Column elution Lane 9: Buffer exchanged protein Lane 10: molecular weight markers (kDa).

The protein was considerably more soluble when it was co-overexpressed with QbsE. This seemed to imply that these two proteins could be working together to perform some function in sulfur transfer. The yield of soluble protein, both QbsC and QbsE together, was approximately 8-10 mg/liter of cell culture. Maximum stability is achieved when the proteins are stored in 50 mM Tris pH 7.8 with at least 50 mM NaCl.

4.3 Characterization of sulfur transfer activity of QbsC

4.3.1 Detection of sulfur transfer to cyanide

Since we believed that QbsC was involved in sulfur activation we explored whether it indeed had this activity. As mentioned previously, QbsC has a rhodanese (thiosulfate sulfurtransferase) domain, which catalyzes the transfer of the sulfane atom of thiosulfate to cyanide to form sulfite and thiocyanate. We examined both QbsC expressed alone and QbsC co-overexpressed with QbsE for this activity. The rhodanese activity can be monitored by detection of the product thiocyanate (figure 4.6).[6, 7]

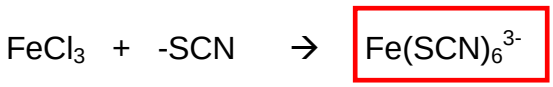

Figure 4.6 When thiocyanate is mixed with an iron(III) species, bright red iron-thiocyanate complexes are formed that can be detected spectrophotometrically at 460 nm.

The activity assays had to be carried out in a purified system since *E. coli* crude extracts have a significant amount of background rhodanese activity.

4.3.1.1 QbsC/QbsE co-overexpressed

The initial activity assay was carried out with the co-overexpressed QbsC and QbsE, primarily because of the higher solubility of the two proteins together over QbsC alone. Detection of thiocyanate formation was monitored spectrophotometrically by complexation with iron(III) as described previously. QbsC with QbsE had robust rhodanese activity when it was incubated with ammonium thiosulfate and potassium cyanide (figure 4.7)

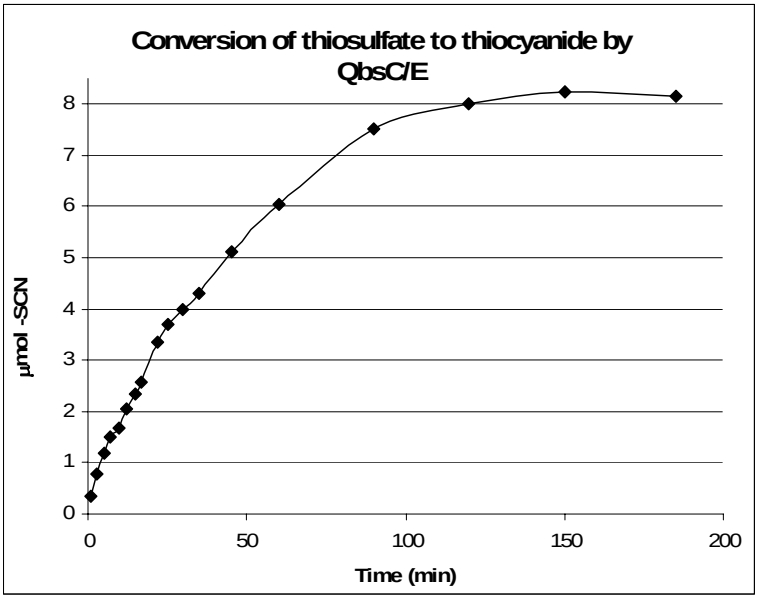

Figure 4.7 QbsC/QbsE dependent conversion of thiosulfate to thiocyanate. The reaction has ~10 μmol of thiosulfate and 75 μg of QbsC/E.

Almost complete conversion to thiocyanate was observed in about two hours. No rhodanese activity was seen with heat denatured protein or when QbsC/E was substituted with BSA. The proteins had a specific activity for thiosulfate of 2 μmol min^{-1} mg^{-1}. It was also determined that reductants such as DTT (1 mM) and TCEP (1 mM) had no effect on the reaction.

4.3.1.2 Alternative substrates for QbsC

Typically rhodanese domain containing proteins only utilize thiosulfate as a small molecule sulfur source *in vitro*. *In vivo* the sulfur is probably donated from another protein that carries sulfur in the form of a persulfide, such as a cysteine desulfurase. Other potential sulfur-donating small molecules were tested to determine if they could be utilized by QbsC to form thiocyanate (figure 4.8).

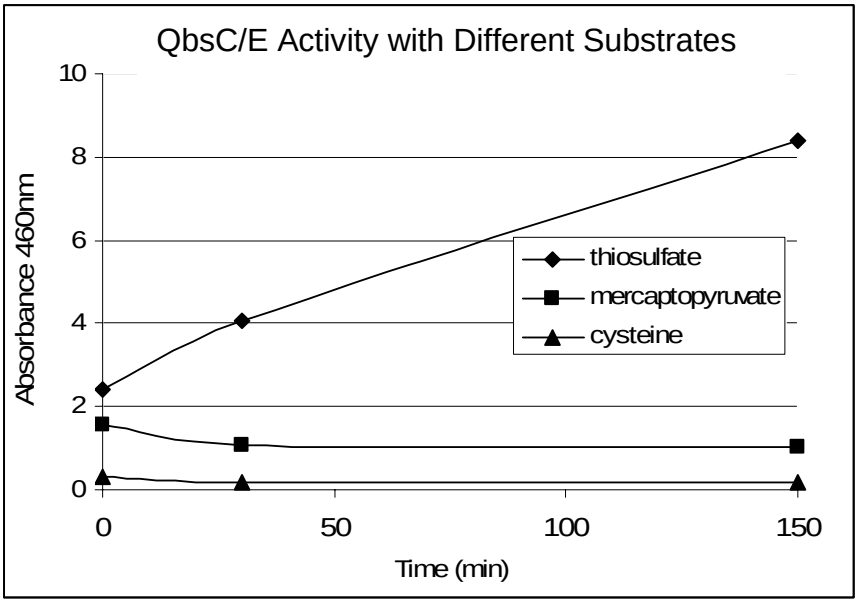

Figure 4.8 Rhodanese activity of QbsC/E co-overexpressed and purified with various potential small molecule sulfur donors (typically 25 mM in each reaction). Diamonds – thiosulfate; Squares – mercaptopyruvate; Triangles – cysteine.

The only sulfur-containing small molecule that was utilized by QbsC was thiosulfate. No thiocyanate was formed when either mercapto-pyruvate or cysteine was used as a sulfur donor.

4.3.1.3 QbsC

Once appropriate overexpression and purification conditions were determined to obtain soluble QbsC alone, the protein was tested for its rhodanese activity. We wanted to determine if the small sulfur carrier protein, QbsE, which was present in the previous assays was necessary for the QbsC rhodanese activity. Detection of thiocyanate formation by QbsC using thiosulfate and cyanide was monitored spectrophotometrically by complexation with iron(III) as described above (figure 4.9).

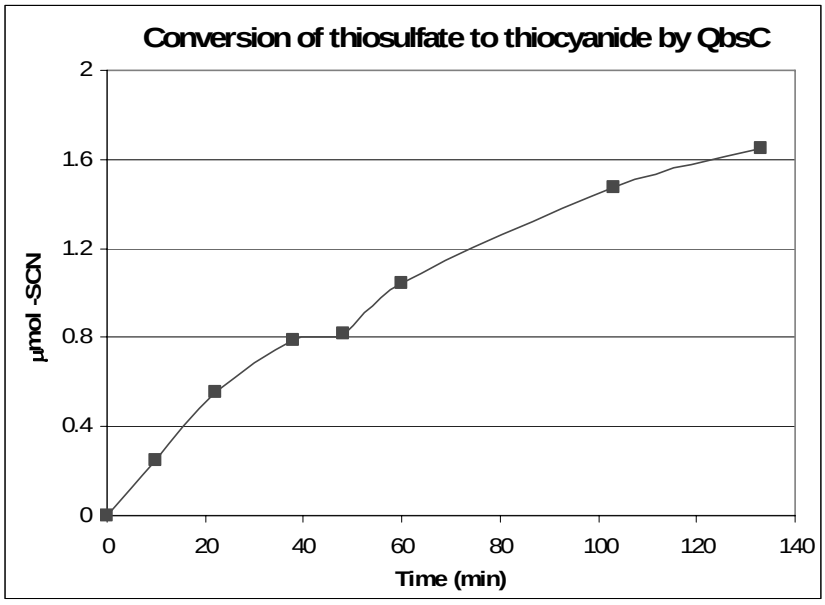

Figure 4.9 QbsC dependent conversion of thiosulfate to thiocyanate. The reaction has ~4 μmol of thiosulfate and 75 μg of QbsC.

QbsC alone has similar rhodanese activity to the co-overexpressed and purified QbsC/E. QbsC does not require QbsE to have rhodanese activity. The specific activity of QbsC alone with thiosulfate was about 4.2 μmol min^{-1} mg^{-1}. The specific activity of the purified protein alone was expected to be

higher than that of the co-purified QbsC/E (2 μmol min^{-1} mg^{-1}) because the QbsC preparation only contained QbsC and not an approximately equal amount of QbsE as in the co-overexpression preparation. Again, the presence of reductants such as DTT and TCEP had no effect on the reaction.

4.3.2 Kinetics of sulfur transfer

In order to fully characterize the enzyme the kinetic parameters were determined, both for QbsC alone and for the co-purified QbsC/E. The initial rates were determined with UV-Vis spectroscopy by monitoring the formation of the iron(III)-thiocyanate complex. K_m and k_{cat} were determined by plotting the initial rates as monitored by UV spectroscopy versus the substrate concentrations in GraFit. The kinetic parameters for QbsC and QbsE co-purified were determined first (figure 4.10)

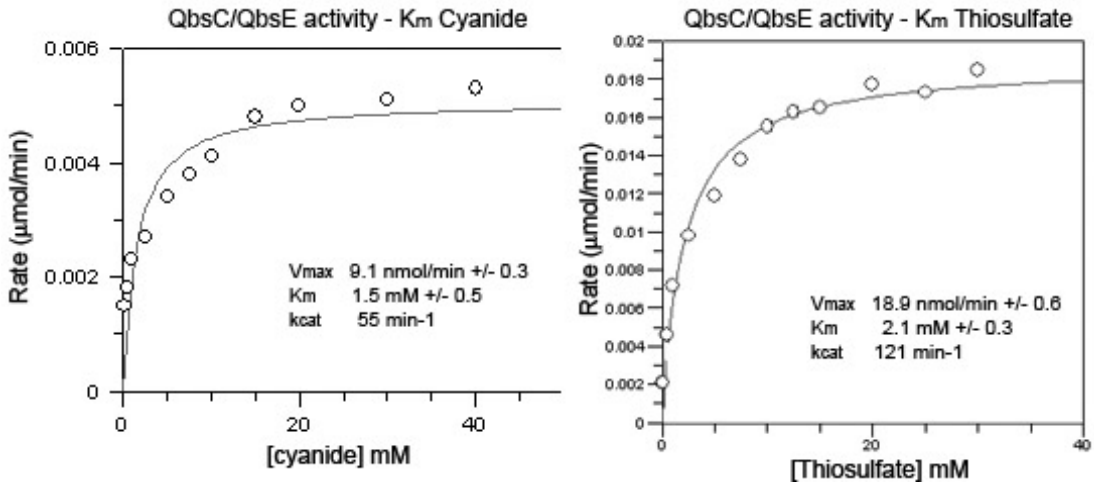

Figure 4.10 Plot of substrate concentrations versus initial rates for QbsC and QbsE. The amounts of enzymes (QbsC and QbsE) used in the reactions was 75μg. The concentration of thiosulfate was varied to determine its K_m, and likewise the concentration of cyanide was varied to determine its K_m. The concentration of the constant substrate was added to approximately five times its K_m. All data points were determined in triplicate.

The kinetic parameters for the thiosulfate sulfurtransferase activity of QbsC/QbsE were determined to be: K_m(thiosulfate) 2 mM +/- 0.3, K_m(cyanide) 1.5 mM +/- 0.5, k_{cat} 121 min^{-1}. The k_{cat} determined from the initial rates plot for cyanide is lower than it should be, probably due to the high concentrations of the cyanide (up to 40 mM).

The kinetic parameters for QbsC alone were determined next to see if the absence of QbsE had any effect (figure 4.11). The same total amount of protein was used in the assays of QbsC alone as was used with QbsC/E assays.

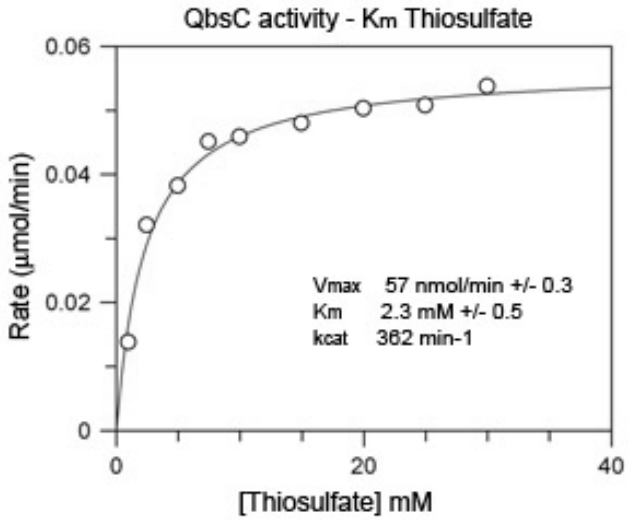

Figure 4.11 Plot of substrate concentrations versus initial rates for QbsC. The amounts of enzyme (QbsC) used in the reactions was 75µg. The concentration of thiosulfate was varied to determine its K_m. The concentration of cyanide was added to approximately five times its K_m. All data points were determined in triplicate.

The kinetic parameters for the thiosulfate sulfur-transferase activity of QbsC were determined to be: K_m(thiosulfate) 2.3 mM +/- 0.3, k_{cat} 362 min^{-1}. The K_m

for QbsC alone is the same within experimental error as for both QbsC and QbsE. In the case of k_{cat}, it is about three times higher when QbsC is alone when compared to QbsC/E. This is due to the higher 'purity' of QbsC when it is purified alone, without an approximately equal amount of QbsE.

4.4 Mutagenesis of the catalytic cysteine

In order to confirm that the catalytic mechanism did indeed involve the rhodanese domain the catalytic cysteine found in the C[R/K]XGXR domain was mutated and the activity of the protein was tested.

4.4.1 Cloning of the QbsC.C345S mutant

The *qbsC* gene was mutated using the Stratagene QuickChange II kit. The catalytic cysteine residue (Cys345) was mutated to a serine using the following primers: forward 5'- GAC GCC GAG ATC GTC GTG TAT TCC AAG GCC GGC AGC CGC TCC -3' and reverse 5'- GGA GCG GCT GCC GGC CTT GGC ATA CAC GAC GAT CTC GGC GTC -3'. The mutagenesis PCR was carried out with pPfQbsC.28a as the template. The plasmid PCR product was digested with DpnI to remove any template vector, and transformed into Top10 Cells. Plasmids were purified from the colonies and sequenced to verify the presence of the mutation. A clone with the correct sequence was identified and named pPfQbsC.C345S.28a.

4.4.2 Overexpression of QbsC.C345S with QbsE

Two plasmids, one containing QbsC.C345S and the other QbsE (see chapter 5 for cloning), were co-transformed into Tuner (DE3) cells and overexpressed at 15 °C with reduced amounts of IPTG (500 μM) and 0.1% sorbitol added to

the media. The cells were lysed with Triton X-100 and purified by Ni-NTA affinity chromatography. A typical purification yielded about 20 mg of total protein (QbsC.C345S and QbsE) per liter of cell culture.

4.4.3 Characterization of the activity of the mutant

It is interesting to note that the yield of soluble QbsC increased significantly both with and without co-overexpressed QbsE when the catalytic rhodanese cysteine was mutated, implying that the solubility issues were partly due to this residue. When this is coupled with the fact that the QbsC(wt) solubility increases with the presence of QbsE, it seems to indicate that QbsE may shield this reactive cysteine by interacting with it. Perhaps QbsE prevents aggregation and thus increases solubility.

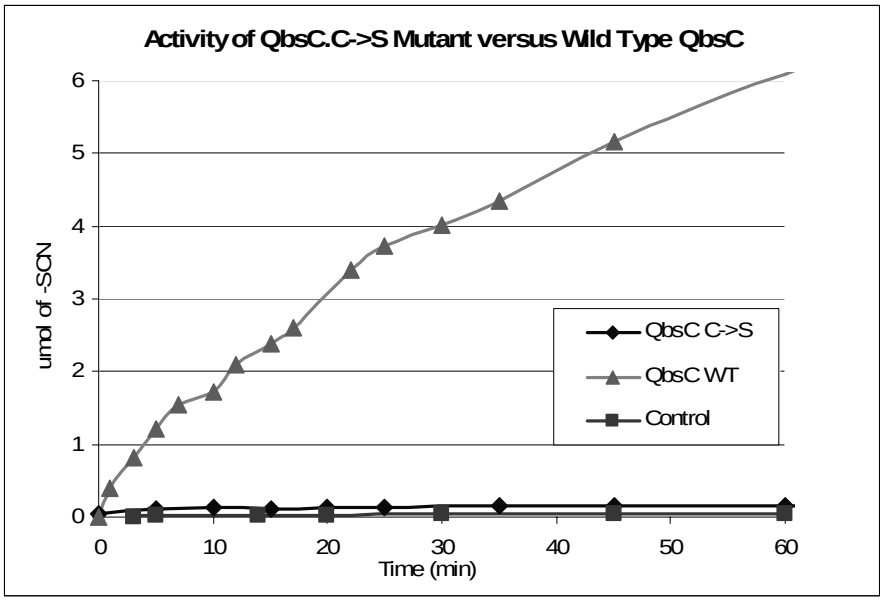

Figure 4.12 Rhodanese activity of QbsC.C345S/QbsE co-overexpressed and purified versus wild type QbsC/E. The control reaction contained an equal amount of BSA. The amount of thiosulfate used was 10μmol and about 75μg of protein was used. Diamonds – QbsC.C345S/QbsE; Squares – BSA; Triangles – QbsC(wt)/QbsE.

The activity of the C345S mutant was assayed as before by monitoring the formation of thiocyanate (figure 4.12). Assays were performed using co-overexpressed and purified QbsC.C345S and QbsE. The figure clearly shows that the cysteine mutant had no rhodanese activity above that of the background BSA reaction, confirming that Cys345 is the catalytic residue responsible for the rhodanese activity.

4.5 Conclusions

In this chapter, we showed that QbsC, which has a rhodanese domain, can activate sulfur from thiosulfate in the form of a persulfide. When the putative catalytic cysteine, Cys345, of the conserved rhodanese domain (C[R/K]XGXR) was mutated to a serine the protein lost all activity. Like the other proteins in the pathway, QbsC was not appreciably soluble by itself. When QbsC was co-overexpressed with its putative binding partner, QbsE, its solubility increased dramatically.

QbsC only accepted thiosulfate as a substrate and did not take cysteine or mercaptopyruvate. The kinetic parameters for the thiosulfate sulfurtransferase activity of QbsC with QbsE present were determined to be: K_m(thiosulfate) 2 mM +/- 0.3, K_m(cyanide) 1.5 mM +/- 0.5, k_{cat} 121 min^{-1}. With QbsC alone, the kinetic parameters were K_m(thiosulfate) 2.3 mM +/- 0.3, k_{cat} 362 min^{-1}. The catalytic efficiency (k_{cat}/K_m) of QbsC alone was 160 $mM^{-1}min^{-1}$, and for both QbsC and QbsE it was 60 $mM^{-1}\,min^{-1}$. The difference in k_{cat}/K_m can be accounted for by the different amount of QbsC used in each of the determinations. Although the same total amount of protein (QbsC or

QbsC+QbsE) was used the amount of QbsC was different, resulting in different k_{cat}'s. In the QbsC and QbsE protein preparation the ratio of QbsC to QbsE was about 1:1.5. QbsC had a specific activity of about 4.2 μmol min^{-1} mg^{-1}.

4.6 Materials and experimental procedures

All materials were obtained from Sigma-Aldrich unless otherwise noted.

4.6.1 Cloning of *qbsC*

Genomic DNA from *P. fluorescens ATCC 17400* was isolated using the Wizard™ Plus DNA prep kit. This was used to PCR amplify *qbsC* using the following primers: forward 5'- GGA ACA CAT ATG CAA CTT CCA CCC TTG GTA GAA GCC -3' and reverse 5'- GC AAC ATA AGC GAA TTC TCA GTA GGC CGG CAG -3' (IDT oligos). PCR reactions were carried out using Platinum Pfx Polymerase and dNTPs from Invitrogen according to the literature protocol, except using 100 pmol of each primer and 4 μL of enhancer per 10 μL reaction. The PCR product (~1.1 kb) was purified by agarose gel electrophoresis, excised and purified with the Qiagen Gel Extraction kit. PCR amplified *qbsC* was digested with NdeI and EcoRI obtained from New England Biolabs. The digested *qbsC* was purified directly from the reaction mixture with the QiaQuick MiniElute PCR purification kit. The cut insert was ligated into a similarly digested pET28a vector (Novagen) that had been purified by gel electrophoresis with T4 DNA ligase (New England Biolabs). Supercompetent *E. coli* Top 10 cells were used to transform the ligated pET28a and insert. Standard methods were used for DNA restriction endonuclease digestion, ligation and transformation of DNA. Colonies were

then screened for the *qbsC* insert. Those colonies that had insert were grown at 37 ºC in LB/Kan media for 8 hrs, and the plasmid harvested. The prepared plasmid was sequenced and a plasmid with the correct sequence was selected and named pPfQbsC.28a. Plasmid DNA was purified with the Qiagen Plasmid purification kit. Plasmid storage and propagation was performed using *E. coli* Mach1 $T1^R$ cells.

4.6.2 Overexpression and purification of QbsC

All cultures contained 50 mg/L kanamycin sulfate. 10 mL of LB/Kan were inoculated with a single colony of pPfQbsC.28a in *E. coli* tuner (DE3) cells and grown at 37ºC for 7 hours with agitation. The entire starter culture was used to inoculate 1L of LB/Kan media with 0.1% sorbitol. The culture was grown at 37ºC to an OD_{600} of 0.4, at which point the temperature was decreased to 15ºC. At an OD_{600} of 0.6, overexpression was induced by the addition of 500μM IPTG and growth is continued overnight. The cells were harvested by centrifugation at 7800xg for 12 min at 4ºC and then stored at -20ºC.

Purification of the protein was carried out by Ni-NTA affinity chromatography using His-trap columns (Amersham). The cell pellet was resuspended and lysed in 50 mM sodium phosphate buffer, pH 8, 300 mM NaCl, 10 mM imidazole and 0.1% Triton X-100 with sonicaiton on ice. The cellular debris was removed by centrifugation at 27000xg for 30 min at 4ºC and the supernatant was loaded onto a Ni-NTA column pre-equilibrated in lysis buffer. The column was washed with 20 column volumes of wash buffer, 50 mM sodium phosphate pH 8, 300 mM NaCl, and 100 mM imidazole. The protein was eluted with 50 mM sodium phosphate, 300 mM NaCl and 500 mM

imidazole. The protein was only stable under relatively high salt concentrations, a minimum of 50 mM NaCl, and was typically desalted into 75 mM Tris pH 7.8 with 150 mM NaCl. The protein was stable for about a week at 4 ºC.

4.6.3 Overexpression and purification of QbsC co-overexpressed with QbsE

All cultures contained 50 mg/L kanamycin sulfate and 45 mg/L chloramphenicol. *E. coli* Tuner (DE3) cells containing pPfQbsC.28a were made competent with $CaCl_2$ and transformed with pPfQbsE.ACYC. Colonies with both plasmids were selected for on LB/Kan/Chlr plates. Cultures were grown as described for QbsC alone except all media contained kanamycin and chlromaphenicol. Purification of the protein was carried out by Ni-NTA affinity chromatography using His-Trap columns as described for QbsC alone.

4.6.4 Activity assays for thiocyanate formation by UV-Vis

A typical reaction for determination of rhodanese activity was carried out with about 75 μg of total protein (either QbsC(wt/mut)/QbsE or just QbsC), between 5 mM and 25 mM ammonium thiosulfate, 25 mM cyanide, 75 mM Tris pH 7.8 and 150 mM NaCl. At specific time points, a 50 μL aliquot of the reaction was quenched with 25μL of 37% formaldehyde. Addition of 75 μL of ferric nitrate reagent (100g of $Fe(NO_3)_3$*$9H_2O$ in 200 mL of 65% HNO_3, diluted to 1.5 L with dH_2O) yielded the red thiocyanate-iron(III) complexes. The absorbance was read immediately at 460 nm.

A typical reaction for the K_m/k_{cat} determination with ammonium thiosulfate consisted of 75 μg of protein (either QbsC/QbsE or just QbsC), 25 mM cyanide, 75 mM Tris pH 7.8, and 150 mM NaCl. The concentration of thiosulfate was varied from 100 μM to 30 mM. A typical reaction for the K_m/k_{cat} determination with cyanide consisted of 75 μg of protein (either QbsC/QbsE), 25 mM thiosulfate, 75 mM Tris pH7.8, and 150 mM NaCl. The concentration of cyanide is varied from 100 μM to 40 mM. Initial rates were measured by quenching the reaction (500 μL volume) after 1.5 min with 250 μL of 37% aqueous formaldehyde. The red color was developed by the addition of 750 μL of ferric nitrate reagent. The absorbance was read immediately at 460 nm. All data points were obtained in triplicate and kinetic parameters were determined by fitting with GraFit.

4.6.5 Mutagenesis of Cys345 of QbsC

The *qbsC* gene was mutated using the Stratagene QuickChange II kit (Novagen). The catalytic cysteine residue (Cys345) was mutated to a serine using the following primers: forward 5'- GAC GCC GAG ATC GTC GTG TAT TCC AAG GCC GGC AGC CGC TCC -3' and reverse 5'- GGA GCG GCT GCC GGC CTT GGC ATA CAC GAC GAT CTC GGC GTC -3'. The mutagenesis PCR was carried out with 25ng of pPfQbsC.28a as the template as described in the published protocol. The plasmid PCR product was digested with DpnI at 37°C for 1 hour to remove any template vector, and transformed into Supercompetent Top10 Cells and plated out onto LB/Kan plates. Plasmids were purified from the colonies using the QiaQuick plasmid prep kit (Qiagen), and sequenced by the BioResource Center (Cornell

University) to verify the presence of the mutation. A clone with the correct sequence was identified and named pPfQbsC.C345S.28a.

4.6.6 Growth, overexpression and purification of QbsC.C345S with QbsE

All cultures contained 50 mg/L kanamycin sulfate and 45 mg/L chloramphenicol. *E. coli* Tuner (DE3) cells containing pPfQbsC.C345S.28a were made competent with $CaCl_2$ and transformed with pPfQbsE.ACYC. Colonies with both plasmids were selected for on LB/Kan/Chlr plates. Cultures were grown as described for QbsC alone except all media contained kanamycin and chlromaphenicol. Purification of the protein was carried out by Ni-NTA affinity chromatography using His-Trap columns as described for QbsC alone.

4.7 References

1. Budzikiewicz, H., *Heteroaromatic monothiocarboxylic acids from Pseudomonas spp.* Biodegradation, 2003. **14**(2): p. 65-72.

2. Park, J.-H., et al., *Biosynthesis of the Thiazole Moiety of Thiamin Pyrophosphate (Vitamin B1).* Biochemistry, 2003. **42**(42): p. 12430-12438.

3. Bordo, D. and P. Bork, *The rhodanese/Cdc25 phosphatase superfamily.* EMBO reports, 2002. **3**(8): p. 741-7461.

4. Saidu, Y., *Physiochemical features of rhodanese: A review.* African Journal of Biotechnology, 2004. **3**(4): p. 370-374.

5. Settembre, E.C., et al., *Thiamin biosynthesis in Bacillus subtilis: Structure of the thiazole synthase/sulfur carrier protein complex.* Biochemistry, 2004. **43**(37): p. 11647-11657.

6. Matthies, A., M. Nimtz, and S. Leimkuhler, *Molybdenum Cofactor Biosynthesis in Humans: Identification of a Persulfide Group in the Rhodanese-like Domain of MOCS3 by Mass Spectrometry.* Biochemistry, 2005. **44**: p. 7912-7920.

7. Sorbo, B.J., *Rhodanese.* Methods in Enzymology, 1955. **2**: p. 334-337.

CHAPTER 5:

INVESTIGATING SULFUR TRANSFER FROM QbsC TO THE SMALL SULFUR CARRIER PROTIEN, QbsE

5.1 Introduction

A number of naturally occurring molecules contain sulfur including thiamin, molybdopterin, 4-thiouridine, cysteine, biotin and lipoic acid. The biosyntheses of these molecules takes place without the use of free sulfide, as is often used in traditional organic synthesis. In the case of cysteine, however, it is important to note that there is more than one pathway known, and while one of them does not use free sulfide, it is not as common as the one that does. Nature has evolved routes for the transfer of sulfur that do not involve free sulfide, though the reasons for this are not completely known. In the previous chapter, we described that QbsC has homology to proteins in the biosynthesis of thiamin and molybdopterin. We also found that it is capable of activating sulfur from thiosulfate in the form of a persulfide. Now we are interested in exploring if sulfur is incorporated into quinolobactin via a similar mechanism as is found in thiamin, molybdopterin, and cysteine biosynthesis.

The biosynthetic schemes for the incorporation of sulfur into the thiazole portion of thiamin, molybdopterin, and cysteine are shown below (figure 5.1). There is more than one method used by nature to incorporate sulfur into cysteine. One involves the use of free sulfide and the other does not.

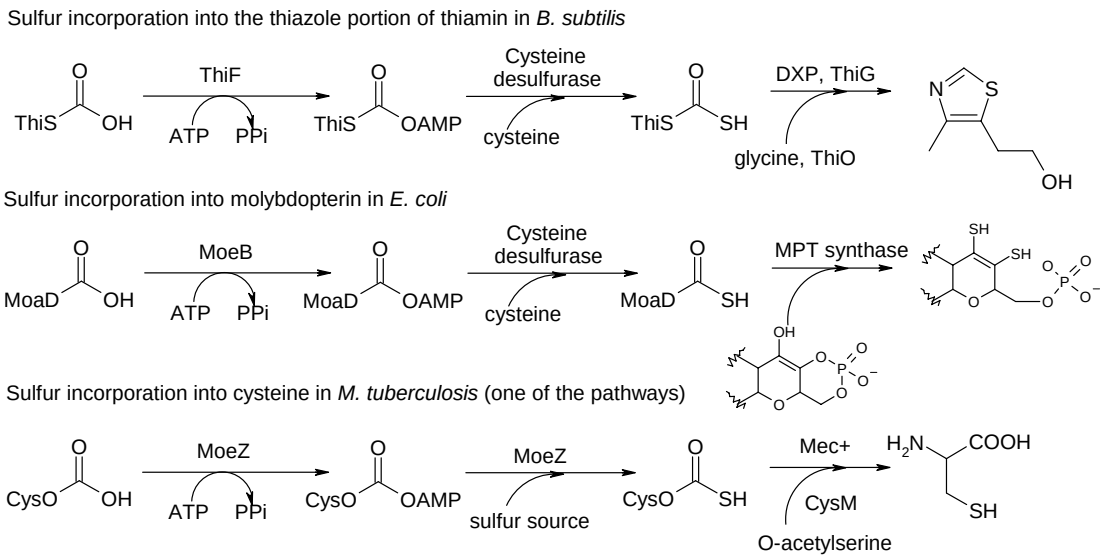

Figure 5.1 Comparison of the sulfur incorporation into thiazole, molybdopterin and cysteine. In all of the examples, a small sulfur carrier protein (ThiS, MoaD, or CysO) is used to deliver the sulfur to its target molecule.

In all of the cases given, the sulfur is incorporated into its target small molecule by a similar mechanism. In the thiamin and molybdopterin biosyntheses a small sulfur carrier protein (ThiS, MoaD) clusters with an adenylating protein (ThiF, MoeB) within the biosynthetic operon.[1-3] The sulfur carrier protein, usually about 10 kDa, is responsible for holding onto and delivering the sulfur to its target molecule. The C-terminus of each of the proteins is a highly conserved -GG-COOH. The diglycine at the C-terminus gives the protein a 'floppy tail,' onto which the sulfur can be placed and subsequently transferred. Before the sulfur is placed on the C-terminus of the sulfur-carrier protein the terminal carboxylate must be activated. For the examples given, the activation is done through the formation of a C-terminal acyl adenylate by the adenylating enzymes (ThiF, MoeB) that cluster with the sulfur carrier protein.

For both thiamin biosynthesis in *B. subtilis* and molybdopterin biosynthesis in *E. coli*, the sulfur is provided by a cysteine desulfurase. Cysteine desulfurases remove the sulfur from cysteine to generate alanine in a PLP-dependent mechanism.[4] A persulfide is generated on the cysteine desulfurase and the sulfane sulfur is then transferred to the sulfur-carrier protein acyl adenylate, forming a C-terminal thiocarboxylate. In other organisms, however, not only does the adenylating enzyme activate the C-terminus of the sulfur carrier protein but it can also act as an intermediate in sulfur transfer. This is seen in cysteine biosynthesis in *M. tuberculosis,* where the adenylating protein, MoeZ, mediates the transfer of sulfur to the sulfur carrier protein CysO. In the biosynthesis of molybdopterin in humans, the enzyme (MOCS3) that is responsible for the adenylation of the sulfur carrier protein (MOCS2A) can also transfer sulfur to the acyl adenylate.[5] MOCS3 has two domains, a MoeB-like adenylating domain and a rhodanese domain and has been shown to perform both the adenylation and sulfur transfer to the sulfur carrier protein.

The quinolobactin biosynthetic operon also has a small putative sulfur carrier protein, QbsE, clustering with an adenylating protein, QbsC. QbsC has homology to the adenylating proteins ThiF, MoeB, and MoeZ, and is likely to catalyze the activation of the C-terminus of QbsE. Like the human enzyme MOCS3, QbsC also possesses a rhodanese domain, which may catalyze the transfer of sulfur to QbsE as well. QbsC from *P. fluorescens* has high sequence homology with MOCS3 (figure 5.2). These two proteins align well and share almost 40% identity and 55% similarity (figure 5.3). This gives good insight into the possible functions of QbsC.

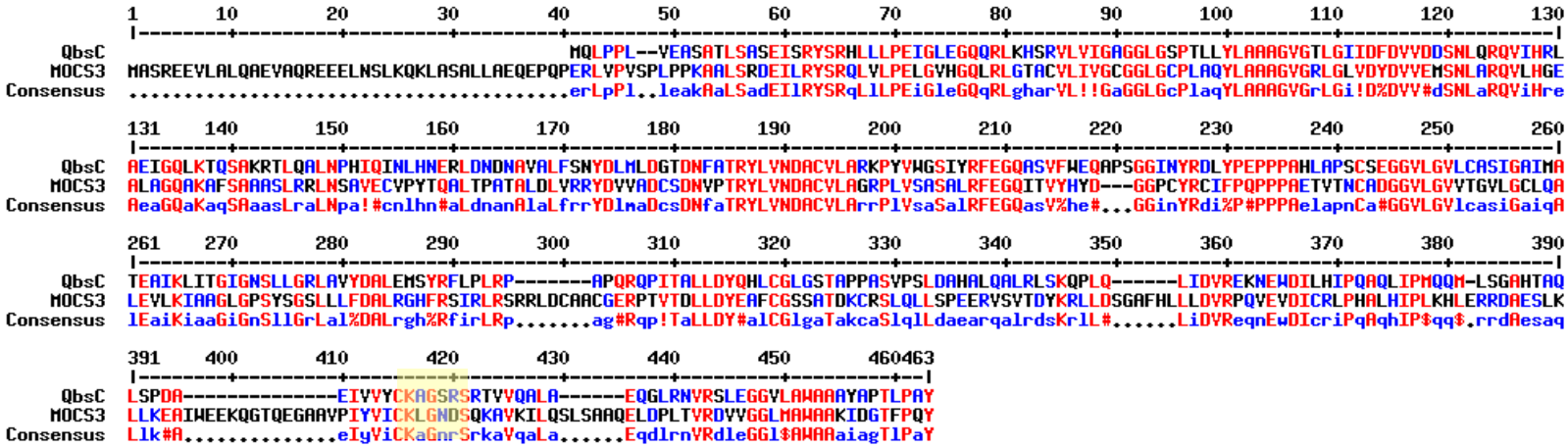

Figure 5.2 Sequence alignment of QbsC from *P. fluorescens* and MOCS3 from human. The ThiF/MoeB/HesA domain ranges approximately from residues 55-295 (as numbered), and the rhodanese domain is from residues 330-415. The conserved rhodanese motif C[R/K]XGXR is highlighted in yellow. Red residues are conserved and blue and black residues are not conserved between the two proteins.

Score = 244 bits (622), Expect = 1e-62
Identities = 161/405 (39%), Positives = 223/405 (55%),
Gaps = 41/405 (10%)

Figure 5.3 Sequence homology of QbsC and MOCS3 (created with BLAST 2 sequences, http://www.ncbi.nlm.nih.gov/blast/ bl2seq). Above the homology diagram are the two domains found in the proteins.

The small sulfur carrier proteins, ThiS, MoaD, and CysO, do not share significant sequence similarity. However, each of them is small (about 10 kDa), and each possess a diglycine at its C-terminus. QbsE is also small, about 10 kDa and possesses diglycine on its C-terminus. However, immediately following the diglycine are two other amino acids (cysteine and phenylalanine). Alignment of the small sulfur carrier proteins is seen in figure 5.4. While other MoaD/ThiS-like proteins in various organisms have amino acids after the diglycine, none have been tested for activity in a sulfur transfer system. Either the GGCF-COOH at the C-terminus of QbsE could still provide it with the 'floppy tail' needed for adenylation and sulfur transfer, or the cysteine and phenylalanine are cleaved from the C-terminus generating the QbsE-GG-COOH found in ThiS, MoaD, and CysO.

```
           1       10        20        30        40        50        60        70        80        90   95
           |--------+---------+---------+---------+---------+---------+---------+---------+---------+----|
ThiS                                    MLQLNGKDVKWKKDTGTIQDLLASYQLENKIVIVER---NKEIIGKERYHEVELCDRDVIEIVHFVGGG
MoaD     MIKVLFFAQVRELVGTDATEVAADFP---TVEALRQHMAAQSDRWALALEDGKLLAAVN--------QTLVSFDHPLTDGDEVAFFPPVTGG
CysO    MNVTVSIPTILRPHTGGQKSVSASGDTLGAVISDLEANYSGISERLMDPSSPGKLHRFVNIYVNDEDVRFSGGLATAIADGDSVTILPAVAGG
QbsE      MKITVPTLMRNLTANQKTVEAQGQTVRQVIDALEQQYPGIAARLVEGN---KVHKFINIYINDDDIRFLQSLDSAVAQHDQITILPAVAGGCF
Consensus  ..........r..........a....l......l......i.drla......K.....n...n.e.i.........l.#.D.!.i.p.V.GG..
```

Figure 5.4 Alignment of the small sulfur carrier proteins, ThiS (thiamin), MoaD (molybdopterin), and CysO (cysteine) with QbsE. The only amino acids that are conserved among the proteins are the two glycines at the C-terminus. QbsE has two extra amino acids after the diglycine.

The last protein that is clustered with the adenylating protein QbsC and the small sulfur carrier protein, QbsE, is QbsD. It does not have sequence similarity with any of the proteins involved in thiamin or molybdopterin biosynthesis but it does align with Mec+, found in cysteine biosynthesis.[1] Mec+ is a Zn^{2+} dependent hydrolase that is responsible for cleaving cysteine off of CysO after the sulfur is transferred. Homology searching with QbsD reveals that it has a JAB-MPN domain, like Mec+ (figure 5.5).

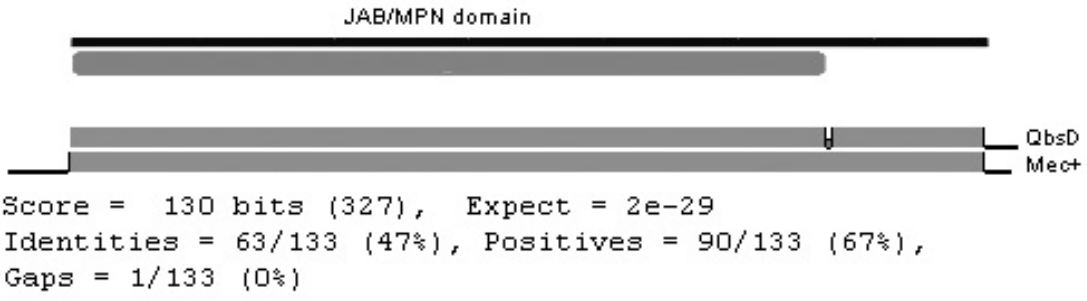

Figure 5.5 Sequence homology of QbsD and Mec+ (created with BLAST 2 sequences, http://www.ncbi.nlm.nih.gov/blast/ bl2seq). Above the homology diagram is the domain found in both proteins.

The putative function of QbsD in the biosynthesis of thio-quinolobactin is unknown. Based on the presence of the metal-dependent hydrolase domain, we first hypothesized that QbsD may be responsible for the cleaving QbsE from quinolobactin once the sulfur has been transferred. Another possible function would be the cleavage of the amino acids following the diglycine of QbsE (QbsE-GGCF-COOH → QbsE-GG-COOH). This would generate diglycine at the C-terminus of QbsE, which is found in ThiS (thiamin), MoaD (molybdopterin), and CysO (cysteine).

By looking at the sequence homologies and similarities with other proteins known to be involved in sulfur transfer in other sulfur transfer systems, the steps of sulfur activation and transfer in thio-quinolobactin can be proposed (figure 5.6). In order for the diglycine moiety to be freed at the C-terminus of QbsE, allowing it to be ready for activation and subsequent sulfur transfer, the last two residues are hydrolyzed by QbsD. Similar to the thiamin, molybdopterin, and cysteine sulfur transfer motifs, the small sulfur carrier protein, modified QbsE, can be activated at its C-terminus in the form of an acyl adenylate by an adenylating protein, QbsC. Like in cysteine biosynthesis in tuberculosis (MoeZ) and the biosynthesis of molybdopterin in humans (MOCS3), QbsC may also be able to transfer a sulfur atom to the activated QbsE to form a C-terminal thiocarboxylate. The sulfur on QbsE is then transferred to a quinolobactin acyl adenylate that is formed by QbsL, and this is potentially mediated by QbsL itself. The covalent intermediate between QbsE and quinolobactin can be hydrolyzed to form the free thio-quinolobactin.

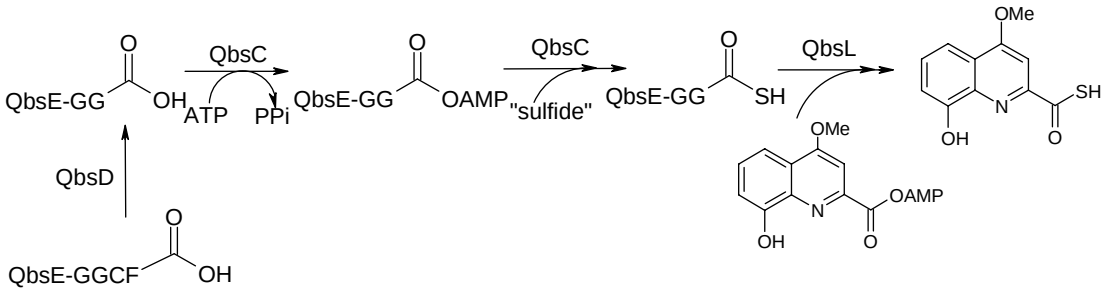

Figure 5.6 Proposed steps in the transfer of sulfur in thio-quinolobactin biosynthesis.

5.2 Cloning, overexpression, and purification of the small putative sulfur carrier protein, QbsE, in *E. coli*

5.2.1 Cloning of *qbsE*

The *qbsE* gene was PCR amplified from *P. fluorescens* ATCC 17400 genomic DNA using the following primers: forward 5'- TTC CAT CAT ATG AAG ATC ACT GTC CCC ACC -3' and reverse 5'- CAA GGG CAC ATG GAA TTC TTC CTC CCC GGG -3'. The PCR product was purified by agarose gel electrophoresis and restriction digested with NdeI and EcoRI. The cut PCR product was ligated into an NdeI/EcoRI digested pET28a vector and transformed into Top10 Cells. Colonies were screened for insert and the hits were sent for sequencing to verify the correct gene sequence. A clone with the correct sequence was identified and named pPfQbsE.28a.

5.2.2 Overexpression and purification of QbsE

Suitable conditions for overexpression of soluble QbsE needed to be identified so that its potential role in sulfur transfer could be studied. QbsE was overexpressed and found to be soluble without any media additives like sorbitol. In order to express the protein solubly it was expressed in *E. coli* tuner (DE3) cells with a lower amount of IPTG (500 μM) and at a reduced temperature (15ºC) for 12 hrs. The highest yield of soluble protein was achieved when the cells were lysed with 1% Triton X-100. The *qbsE* gene product could then be purified by Ni-NTA chromatography (Figure 5.7)

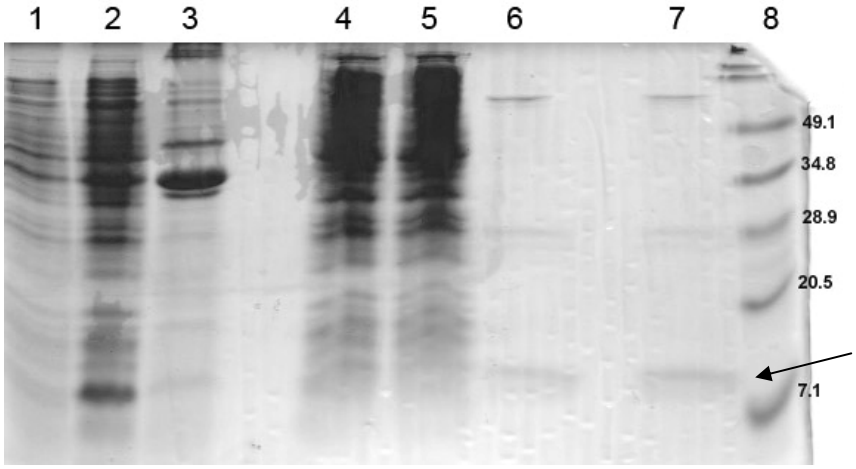

Figure 5.7 SDS gel electrophoresis (15%) analysis of the overexpression and purification of QbsE. Lane 1: Pre-induction Lane 2: Post-induction Lane 3: Insoluble pellet Lane 4: Soluble supernatant Lane 5: Column flowthrough Lane 6: Ni-NTA Column elution Lane 7: Buffer exchanged protein Lane 8: molecular weight markers (kDa).

QbsE was soluble and a typical preparation yielded about 5 mg/liter of cell culture. The purity of QbsE was greatly enhanced by the use of His-trap Ni-NTA columns (Amersham), which enabled a more stringent wash step to be used.

5.3 Cloning, overexpression, and purification of a hydrolase, QbsD, in *E. coli*

5.3.1 Cloning of *qbsD*

The *qbsD* gene was PCR amplified from *P. fluorescens* ATCC 17400 genomic DNA using the following primers: forward 5'- GAC CCG CAT ATG TTG CTG CTC AGC CAA GAC -3' and reverse 5'- GGG ATG GAA TTC CGT GGA GGG TTA ATA GGG -3'. The PCR product was purified by agarose gel electrophoresis and restriction digested with NdeI and EcoRI. The cut PCR product was ligated into an NdeI/EcoRI digested pET28a vector and

transformed into Top10 Cells. Colonies were screened for insert and the hits were sent for sequencing to verify the correct gene sequence. A clone with the correct sequence was identified and named pPfQbsD.28a.

5.3.2 Overexpression and purification of QbsD

Unlike the other proteins in this biosynthetic pathway, QbsD was not overexpressed exceptionally well. Like many of the other proteins, what did express was not very soluble. By overexpressing the protein in *E. coli* tuner (DE3) cells with a lower amount of IPTG (500μM) and at a reduced temperature (15ºC), a small amount of soluble protein was obtained. The highest yield of soluble protein was achieved when the cells were lysed with 1% Triton X-100 and when sorbitol was added to the growth media to 0.1% (figure 5.8).

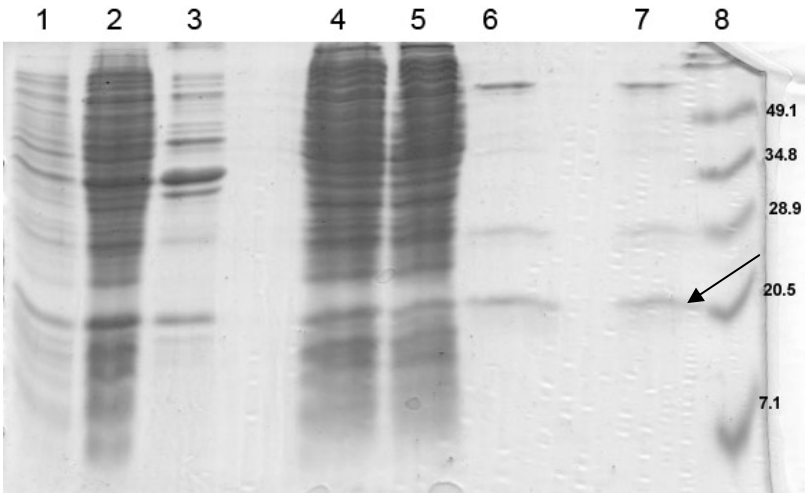

Figure 5.8 SDS gel electrophoresis (15%) analysis of the overexpression and purification of QbsD. Lane 1: Pre-induction Lane 2: Post-induction Lane 3: Insoluble pellet Lane 4: Soluble supernatant Lane 5: Column flowthrough Lane 6: Ni-NTA Column elution Lane 7: Buffer exchanged protein Lane 8: molecular weight markers (kDa). QbsD is indicated by an arrow.

Very little soluble QbsD was obtained that was not very pure. As with QbsE, a much higher purity was achieved when His-trap columns (Amersham) were utilized. A typical preparation yielded 1-2 mg/liter of cell culture.

5.4 Cloning and overexpression of the putative sulfur transfer genes *qbsCDE* in *E. coli*

Based on homology with other proteins involved in sulfur transfer, we believe that QbsC, QbsD, and QbsE are involved in sulfur activation, carrying, and transfer to quinolobactin. QbsC has already been shown to have the ability to activate sulfur for transfer via its rhodanese domain. The three putative sulfur transfer genes cluster with each other on the *P. fluorescens* genome (figure 5.9), and were cloned as a contiguous unit into a pET vector. By this method, only QbsC would have a 6x-his tag, while QbsD and QbsE would not.

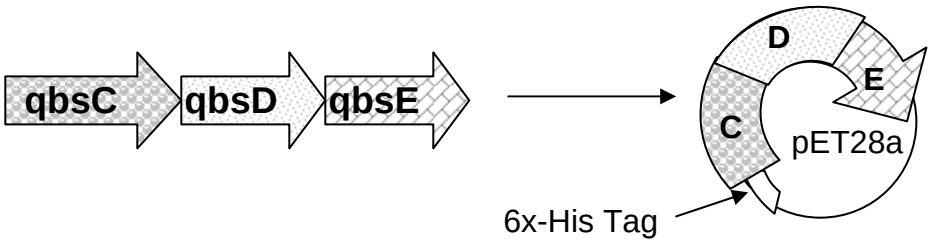

Figure 5.9 Clustering of the putative sulfur transfer genes and subsequent arrangement in a pET vector.

5.4.1 Cloning of *qbsCDE*

The *qbsCDE* gene cluster was PCR amplified from *P. fluorescens* ATCC 17400 genomic DNA using the following primers: forward 5'- GGA ACA CAT ATG CAA CTT CCA CCC TTG GTA GAA GCC -3' and reverse 5'- CAA GGG CAC ATG GAA TTC TTC CTC CCC GGG -3'. The PCR product was purified

by agarose gel electrophoresis and restriction digested with NdeI and EcoRI. The cut PCR product was ligated into a similarly digested pET28a vector and transformed into Top10 Cells. Colonies were screened for insert and the hits were sent for sequencing to verify the correct gene sequence. A clone with the correct sequence was identified and named pPfQbsCDE.28a.

5.4.2 Overexpression of QbsCDE

All of the proteins in the vector appeared to overexpress, but again, solubility was enhanced when *E. coli* Tuner (DE3) cells were used at reduced temperature (15 °C) and lower amounts of IPTG (500 μM) were added. Sorbitol was also added to the growth media at a concentration of 0.1%.

5.5 Purification of QbsCDE

Since only QbsC had a 6x-his tag, this overexpression clone was not intended to be used to purify all three of the proteins it encoded. What we intended to do with this clone was to see if we could get larger amounts of soluble QbsC and also to use the crude extracts, which would contain all three proteins, in assays.

5.5.1 Pull-down of QbsE with QbsC

Based on homology with other proteins, we predicted that QbsC and QbsE would interact with each other. We decided to try a pull down experiment with this clone to determine if either QbsD or QbsE interacts with QbsC. The pull-down assay is an *in vitro* method used to determine physical interaction between proteins. They are useful as an initial screening assay for identifying previously uncharacterized protein-protein interactions. Pull-down screens

require a tagged protein that can be immobilized on a column and be used to 'pull-down' a protein binding partner. In our pull down experiment, the 6x-his tagged QbsC would adhere to the resin in a Ni-NTA column and act as 'bait'. The other two proteins would not stick because they possess no 6x-his tags. However, if QbsD or QbsE interact strongly with QbsC they will stick to the QbsC that is bound to the column and elute off with QbsC.

The clarified lysates from QbsCDE were applied to a Ni-NTA column. The column was washed to remove any adventitiously bound proteins and then QbsC was eluted off. An SDS-PAGE gel was run to determine if either QbsD or QbsE co-eluted with QbsC (figure 5.10).

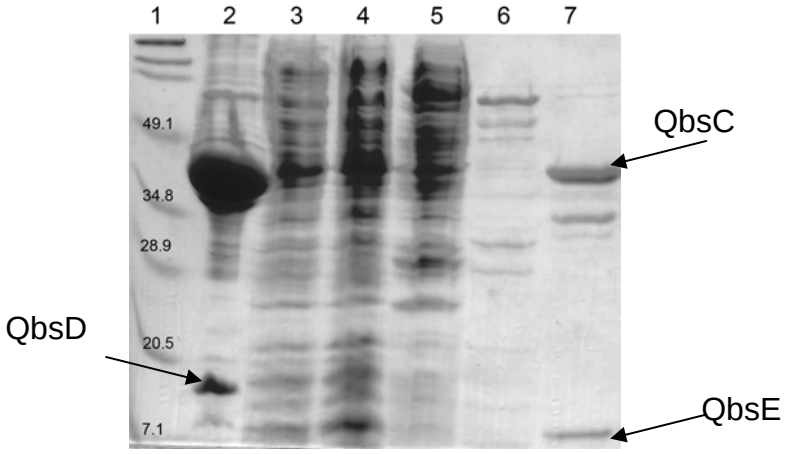

Figure 5.10 SDS PAGE (15%) analysis of the QbsCDE pull-down assay. Lane 1: molecular weight markers (kDa) Lane 2: Insoluble pellet Lane 3: Soluble supernatant Lane 4: Column flowthrough Lane 5: Ni-NTA Column wash 1 Lane 6: Ni-NTA Column wash 2 Lane 7: Elution.

As noted previously, when QbsCDE were co-overexpressed, QbsC becomes much more soluble than if it was expressed by itself. Interestingly, when QbsC, the bait protein, was eluted from the column, QbsE eluted with it.

Though this was indicative of some type of stable protein-protein interaction it did not confirm it. Further experiments will be described to confirm that QbsC and QbsE do indeed stably interact.

5.6 Evidence of an adduct formed between QbsC and QbsE

The confirmation for a stable protein-protein interaction between QbsC and QbsE came surreptitiously while we were attempting to look for the formation of a C-terminal thio-carboxylate on QbsE by ESI-FTMS.

5.6.1 ESI-FTMS detection of a covalent adduct

The two proteins, 6x-his-QbsC and 6x-his QbsE, were co-overexpressed and co-purified via Ni-NTA affinity chromatography. The proteins were then analyzed by ESI-FTMS to determine their initial molecular weights before any reactions were carried out with them. We were able to identify a molecular ion for the smaller protein QbsE at 11997.2 Da (figure 5.11 – panel A). To our surprise, however, we saw no molecular ion that corresponded to his-tagged QbsC (~43.9 kDa). Instead, we observed a molecular ion of about 55940 Da (+/- 20) (figure 5.11 – panel B).

The molecular weight of 55940 Da could correspond to a covalent adduct formed between QbsC (~44 kDa) and QbsE (~12 kDa). Fragmentation of the molecular ion gave rise to peaks that had molecular ions corresponding to those of QbsC and QbsE. Due to the conditions used to spray the proteins, it was likely that this adduct is covalent. When the protein complex was then treated with DTT the adduct disappeared and a molecular ion was observed for QbsC as well as QbsE.

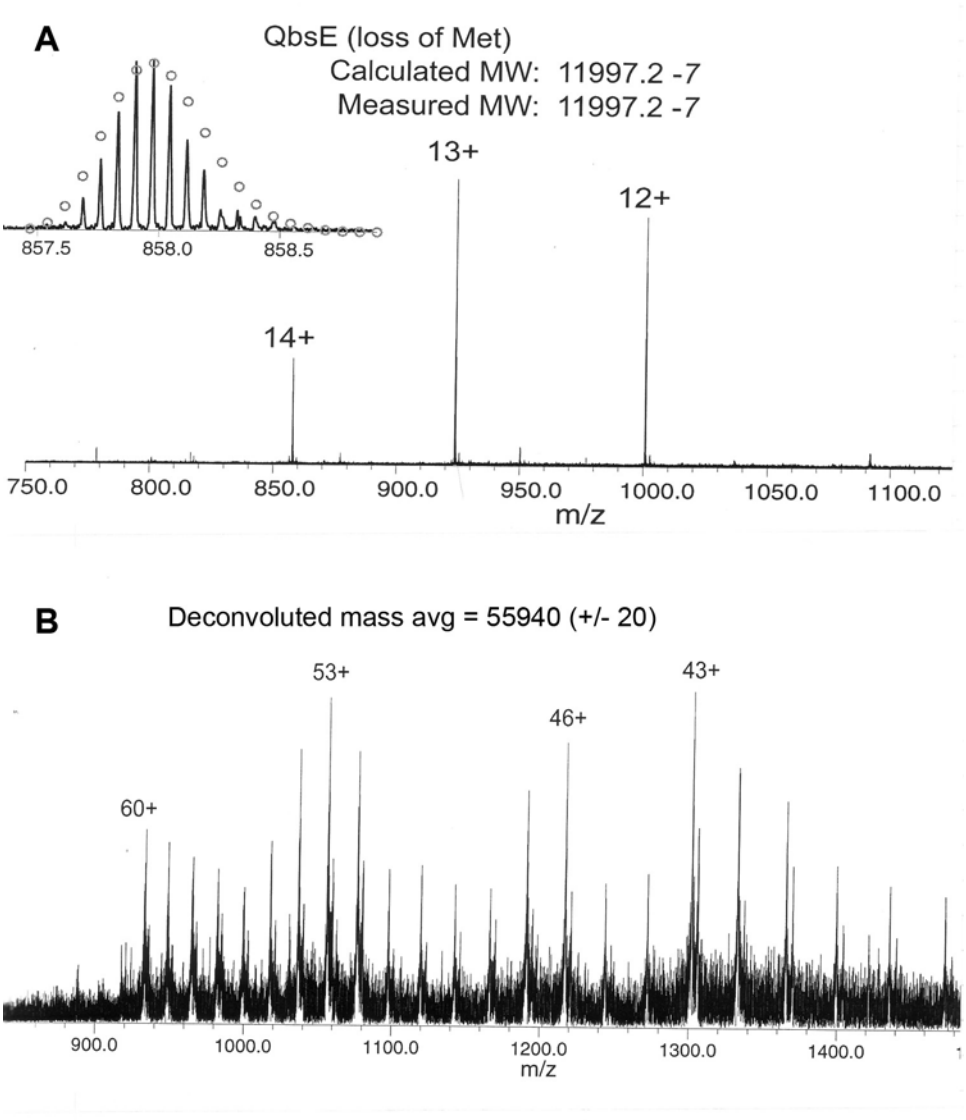

Figure 5.11 ESI-FTMS of QbsC and QbsE co-overexpressed and co-purified. Panel A shows the molecular ion for QbsE (11997.2 Da) and panel B shows the molecular ion for the potential QbsC-QbsE adduct (55940 Da +/- 20). Mass spectrum obtained by Jin Mi (McLafferty group).

This indicated that the linkage between the two proteins was a disulfide bond. It was not clear if this was an artifact of co-overexpression or if it is related to

the function of these two proteins. The fact that all of the QbsC that was observed by mass spectrometry when QbsC and QbsE were co-overexpressed came from an adduct with QbsE seemed to indicate that the only soluble QbsC produced was complexed with QbsE.

5.7 Co-overexpression of QbsD and QbsE

Given the increased solubility observed in the QbsCDE construct where QbsE co-purified with his-tagged QbsC, we attempted to improve the solubility of QbsD in the same manner. It was difficult to determine whether the solubility of QbsD improved in the QbsCDE construct since it did not co-purify with QbsC. When his-tagged QbsD was co-overexpressed with his-tagged QbsE, QbsD did become much more soluble (figure 5.12), yielding about 8-9 mg of total protein per liter of cell culture.

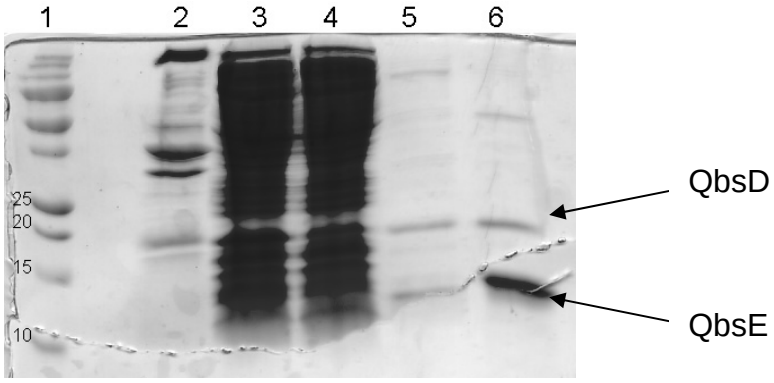

Figure 5.12 SDS PAGE (15%) analysis of the co-overexpression and co-purification of his-tagged QbsD and his-tagged QbsE. Lane 1: molecular weight markers (kDa) Lane 2: Insoluble pellet Lane 3: Soluble supernatant Lane 4: Column flowthrough Lane 5: Ni-NTA Column wash 1 Lane 6: Lane 7: Elution.

It appeared as though the wash was too stringent (100 mM imidazole), as a significant portion of QbsD and QbsE were removed from the column in the

wash. Subsequent purifications using only 50 mM imidazole improved the yield of protein in the elution. The solubility of many of the JAMM-motif proteins is poor, making identification of their function and crystallization difficult.[6]

5.7.1 Evidence of a role for QbsD in the formation of QbsE-GG-COOH

When his-tagged QbsD (JAMM-motif protein) was co-expressed with his-tagged QbsE (sulfur carrier protein) their solubility increased dramatically. When these two proteins were co-purified by Ni-NTA affinity chromatography a species was detected by ESI-FTMS that was 250 Da less than the expected molecular weight of unmodified QbsE (Figure 5.13). This difference corresponded to cleavage of the two C-terminal residues of QbsE, cysteine and phenylalanine. MS-MS analysis localized the modification to the C-terminus of QbsE.

The reaction catalyzed by QbsD resembles that of Rpn11, which is a proteasomal cap protein containing a JAMM motif that is responsible for the deubiquitination of doomed proteins.[7] Although the JAMM motif is found in prokaryotes, archaea, and eukaryotes, complete characterization of its activity and indeed even functional assignment remains elusive. Only one JAMM motif protein in prokaryotes has a functional assignment, the cysteine biosynthetic protein Mec+.[1] QbsD and Mec+ share significant sequence homology (47% identical, 67% similar), and although they catalyze similar hydrolysis reactions, their functions in the biosynthetic pathways are clearly different. Mec+ hydrolyzes the product from CysO after sulfur has been

transferred, while QbsD hydrolyzes the amino acid residues from the C-terminus of QbsE so it can be activated as the thiocarboxylate.

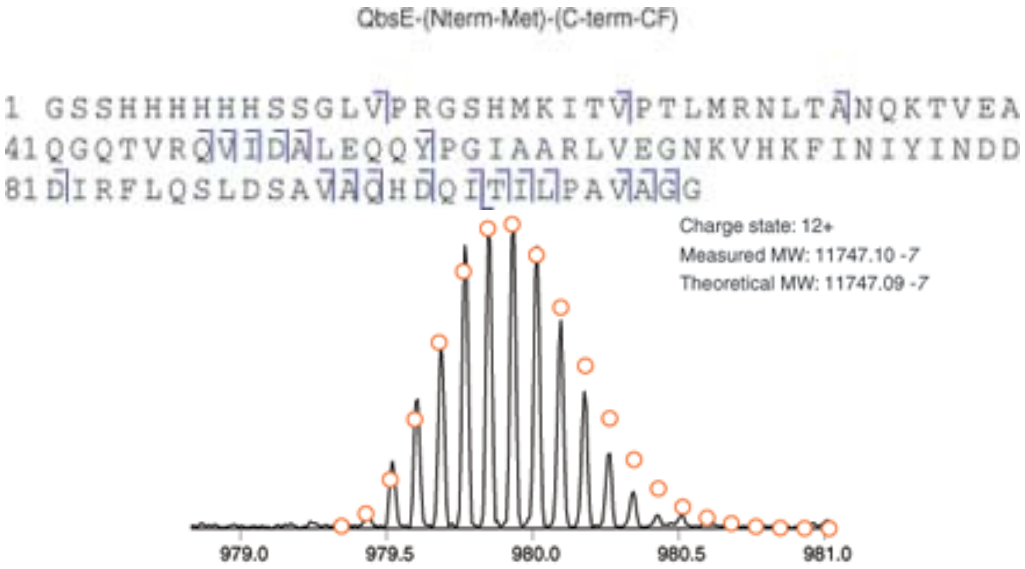

Figure 5.13 ESI-FTMS spectrum showing the molecular ion corresponding to the formation of his-tagged QbsE-GG-COOH (11747 Da). MS-MS analysis showed the modification of QbsE occurring on the C-terminus, verifying that the terminal cysteine and phenylalanine were indeed hydrolyzed.

5.8 Looking for acyl adenylate formation on QbsE

The sulfur transfer motif found in incorporation of sulfur into thiamin and molybdopterin shows activation of the C-terminus of a small-sulfur carrier protein (ThiS, MoaD) with AMP. Based on protein similarities, we believed that a similar motif might be used to activate the C-terminus of QbsE (figure 5.14). The C-terminus of QbsE is adenylated by QbsC with ATP. The adenylation activates QbsE so that it can accept a sulfur for subsequent transfer to the small molecule, quinolobactin. Like with QbsL adenylation activity, QbsC adenylation was monitored by the hydrolysis of AMP from the QbsE-adenylate.

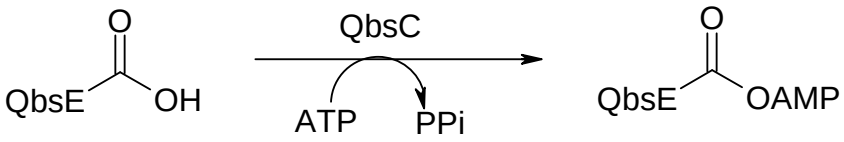

Figure 5.14 Possible activation of the C-terminus of QbsE with AMP by QbsC.

When QbsC was incubated with unmodified QbsE (QbsE-GGCF-COOH) the results were difficult to reproduce and we obtained only small amounts of AMP formation. However, We were able to observe the formation of AMP when we incubated QbsC and a QbsE mutant in which the terminal cysteine and phenylalanine were removed (QbsE-GG-COOH). The activity was not very high but reproducible and enzyme concentration dependent.

5.8.1 α-^{32}P-AMP formation with QbsC and QbsE-GG-COOH

Due to the instability of the C-terminal QbsE adenylate, if it was free in solution the AMP should be hydrolyzed off, and could be readily detected by TLC. In a purified system, we could directly detect any AMP that was released from the QbsE adenylate. When we attempted to reconstitute this reaction with QbsC and QbsE that still had the two extra amino acids on the C-terminus the results were difficult to reproduce and we obtained only small amounts of AMP formation. Since we believe that QbsD might play a role in processing the C-terminal end of QbsE, we decided to use a mutant where the cysteine and phenylalanine were remove from the C-terminus of QbsE. Purified QbsC and QbsE-GG-COOH were incubated with α-^{32}P-ATP and the formation of α-^{32}P-AMP was monitored (figure 5.15).

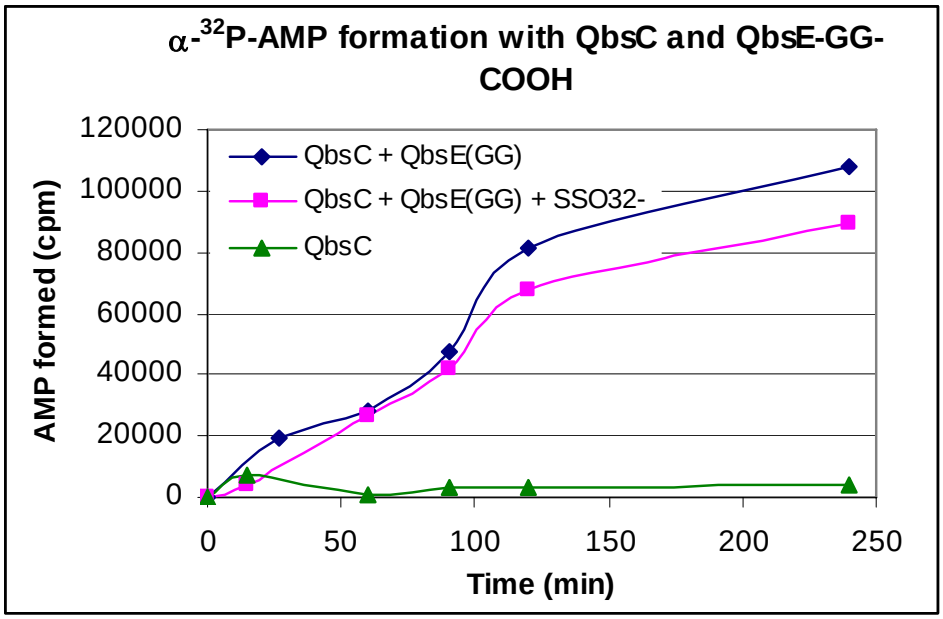

Figure 5.15 QbsC and QbsE dependent hydrolysis of α-^{32}P-ATP to α-^{32}P-AMP. Diamonds – QbsC + QbsE-GG-COOH + α-^{32}P-ATP; Squares - QbsC + QbsE-GG-COOH + α-^{32}P-ATP + thiosulfate; Triangles - QbsC + α-^{32}P-ATP. In each assay, 36nmol of QbsE and 26nmol of QbsC were added.

In this assay, when QbsC and QbsE-GG-COOH were incubated with α-^{32}P-ATP, α-^{32}P-AMP was clearly formed. Incubation of α-^{32}P-ATP with only QbsC yielded a significantly reduced ATP hydrolysis activity. However, when only QbsE was added no ATP hydrolysis was observed.

Only a small amount of AMP formation was observed, but it was well above background. The amount of AMP formed was approximately equal to the amount of QbsC and QbsE-GG-COOH added to reaction. The enzymes were only able to complete approximately one turnover, assuming that all soluble protein was active. One possible reason for this would be that QbsC and QbsE-GG-COOAMP formed a stable complex that did not dissociate readily in solution. Thus, any QbsE adenylate that was formed would be greatly

stabilized inside the active site of the enzyme complex and α-^{32}P-AMP would not be released until the sample was spotted onto a TLC plate and incubated in methanol, causing the proteins to denature. The addition of thiosulfate did not appear to affect the amount of α-^{32}P-AMP that was formed. Again, if sulfur transfer to the activated C-terminus of QbsE was occurring with thiosulfate and QbsC, it would be a dead end for the molecule. Once the AMP was hydrolyzed off and QbsE was sulfurylated, the QbsE-COSH could not be further activated as the acyl adenylate and no further turnovers would occur. Unfortunately, this does not provide conclusive evidence of the activation of the C-terminus of QbsE-GG-COOH but does indicate that it may occur.

5.9 Testing for thiocarboxylate formation on QbsE

Since there was some evidence that QbsC may be activating a carboxylic acid on QbsE as the acyl adenylate we decided to test for sulfur transfer to this activated species. Based on similarity with other sulfur transfer enzymes, after QbsE was activated as the acyl adenylate by QbsC, a sulfur from QbsC would displace the adenylate and form a thiocarboxylate on QbsE (figure 5.16).

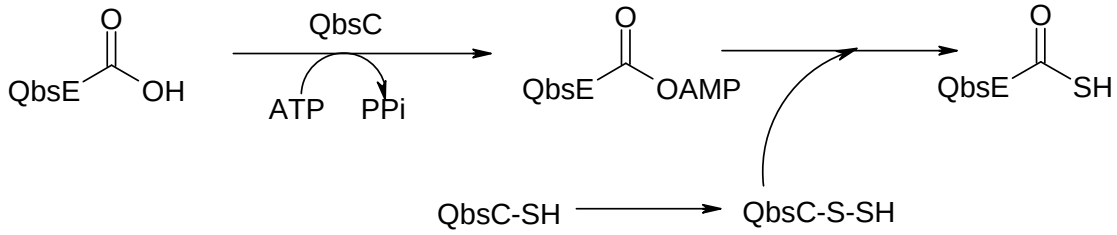

Figure 5.16 Proposed biosynthetic scheme for the formation of the QbsE-thiocarboxylate. The sulfur of the thio-carboxylate would then be transferred to the small molecule quinolobactin.

Ideally, we would have liked to use either radioactive ^{35}S-thiosulfate, which could be utilized by QbsC to transfer the sulfur, or ^{35}S-sulfide, which could displace the AMP for the QbsE acyl adenylate directly. Unfortunately, neither of these compounds were available radioactively. Therefore other indirect and less efficient methods were utilized to look for sulfur transfer to QbsE. Although it was shown in chapter 4 that QbsC can utilize thiosulfate as its source of sulfur, this may not be its substrate *in vivo*. *In vivo* concentrations of thiosulfate are in the mid micromolar range and the K_m of thiosulfate for QbsC is greater than 2 mM. Cysteine is a more likely sulfur donor, similar to thiamin and molybdopterin biosynthetic pathways. A cysteine desulfurase would remove the sulfur from cysteine, forming a protein bound persulfide.[4] The sulfane sulfur would then be transferred to the activated cysteine of the rhodanese domain on QbsC.

5.9.1 Using ^{35}S-cysteine and a cysteine desulfurase to generate sulfide

We attempted to use ^{35}S-cysteine, which is commercially available, in conjunction with know cysteine desulfurases from *B. subtilis*. There are two mechanisms that would result in sulfur transfer to the QbsE acyl adenylate in our *in vitro* assay: 1) formation of sulfide and 2) transfer of the sulfane sulfur from the cysteine desulfurase to QbsC and subsequent transfer to QbsE (figure 5.17). In route (1), the persulfide is formed on the cysteine desulfurase via ^{35}S-cysteine and a reductant, such as DTT, is added to the reaction to generate a small amount of free sulfide. The free sulfide then displaces the AMP from QbsE, thus forming the thiocarboxylate. In route (2), the persulfide is again formed on the cysteine desulfurase with ^{35}S-cysteine and the sulfane sulfur of the persulfide is transferred to the activated cysteine of the rhodanese

domain of QbsC. The sulfane sulfur of the QbsC persulfide is then transferred to the QbsE acyl adenylate. This route would be very inefficient for an *in vitro* experiment since the cysteine desulfurase from *B. subtilis* is certainly not the one utilized in *P. fluorescens*.

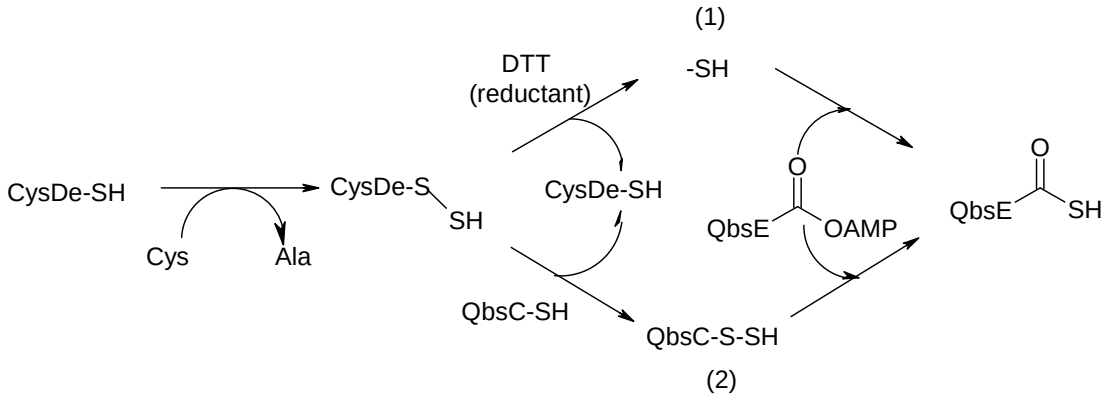

Figure 5.17 Possible methods of sulfur transfer utilizing ^{35}S-cysteine and a cysteine desulfurase (CysDe) in our *in vitro* assay. Route (1) first forms sulfide while route (2) transfers the sulfane sulfur from the cysteine desulfurase to QbsC. The sulfur in either form is subsequently transferred to QbsE.

We evaluated a number of cysteine desulfurases including, YrvO, NifS, and NifZ. While all of the cysteine desulfurases were active, the most active and the enzyme that produced the best results was YrvO. YrvO is a PLP dependent cysteine desulfurase from *B. subtilis* whose *in vivo* function is not well characterized. The sulfur transfer proteins QbsC and QbsE were incubated with ATP, ^{35}S-cysteine, YrvO, PLP, and, in some cases, DTT (figure 5.18). These were purified from the QbsCDE overexpression construct, meaning that only QbsC had a 6x-his tag and that QbsE co-purified with it.

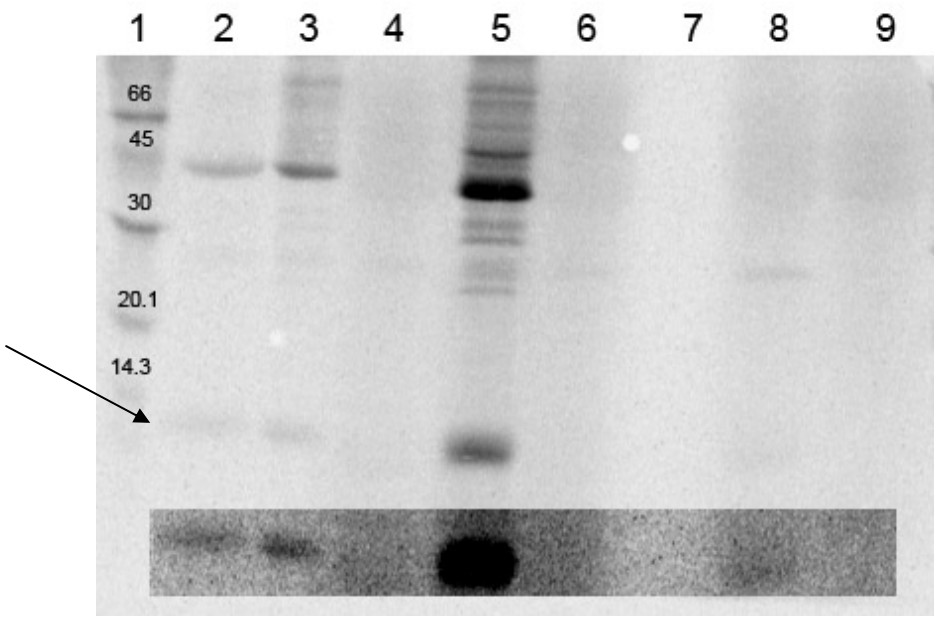

Figure 5.18 Transfer of sulfur from ^{35}S-cysteine to QbsE (black arrow) under two different conditions (with and without DTT). The band at about 45kDA could be either YrvO or QbsC, which have similar molecular weights. All lanes contain the following and were run for 3hrs prior to analysis unless otherwise noted: QbsC, QbsE, YrvO, ATP, PLP, ^{35}S-cysteine, and DTT. Lane 1 – molecular weight markers (kDa); Lane 2 – Exp; Lane 3 – Exp no DTT; Lane 4 – Exp 13 hr; Lane 5 – Exp 13 hr no DTT; Lane 6 – Cont no ATP; Lane 7 – Cont no cys; Lane 8 – Cont no YrvO; Lane 9 – Cont no QbsC no QbsE. No reductant was added to the SDS-PAGE sample buffer.

The gel shows that there was a low-level of sulfur transfer to QbsE (black arrow) after 3 hours both with and without DTT present. Though the amount of labeling was low, it was still at least six times higher than the highest background reading. When the reaction was run overnight no ^{35}S-incorportation was seen in the sample with DTT but, in the sample without DTT, there was a considerable amount of labeling. Most likely this was an artifact of disulfide bond formation between the ^{35}S-cysteine and cysteines on the proteins. Since DTT was added neither to these reactions, nor to the SDS-PAGE sample buffer, the disulfide would remain intact. This non-specific

labeling could occur in any of the samples without DTT if there was a cysteine in the protein. The controls without ATP, ^{35}S-cysteine, YrvO, and QbsC and QbsE showed very low to undetectable levels of ^{35}S-incorporation into the proteins.

This experiment was repeated with the addition of crude extracts from *P. fluorescens* ATCC 17400 that were grown under iron-limiting conditions to the reactions. Since the organism was forced to produce siderophores in order to survive, a low level of the quinolobactin biosynthetic proteins would be present. This would include any other proteins that may be involved in sulfur transfer to QbsE, such as cysteine desulfurases. If the cysteine desulfurase from *P. fluorescens* was present it would be able to much more efficiently catalyze the transfer of the radiolabel from ^{35}S-cyteine onto QbsE. In these experiments, YrvO, the cysteine desulfurase from *B. subtilis,* was omitted from the reactions.

The sulfur transfer proteins, QbsC and QbsE, were incubated with ATP, ^{35}S-cysteine, crude extracts from *P. fluorescens*, and DTT (figure 5.19). Like before, these were purified from the QbsCDE overexpression construct, meaning that only QbsC had a 6x-his tag and that QbsE co-purified with it.

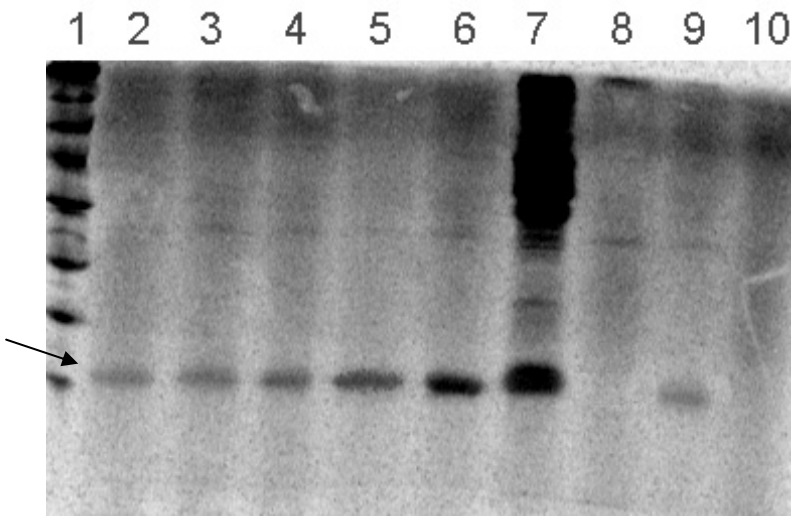

Figure 5.19 Transfer of sulfur from ^{35}S-cysteine to QbsE (black arrow) in an experiment with crude extracts from *P. fluorescens* added. The following were used in a reaction unless otherwise noted: QbsC, QbsE, ATP, PLP, ^{35}S-cysteine, crude extracts from *P. fluorescens* and DTT. Controls were incubated for 420 min. Lane 1 – molecular weight markers (kDa); Lane 2 – 15 min; Lane 3 – 60 min; Lane 4 – 120 min; Lane 5 – 240 min; Lane 6 – 420 min; Lane 7 – Cont no DTT; Lane 8 – Cont no ATP; Lane 9 – Cont no *P. fluorescens* crude extract; Lane 10 – Cont no QbsC/E. No reductant was added to the SDS-PAGE sample buffer.

The gel shows that there was a low-level of sulfur transfer to QbsE (black arrow) that increased with time. Again the amount of QbsE labeling was lower than expected but was still clearly visible. Based on the amount of protein seen in the stained gel, only a low percentage of QbsE was actually labeled. When DTT was omitted a large amount of non-specific labeling due to disulfide formation between the radio-labeled cysteine and the cysteines of the proteins was observed. The controls without ATP and without crude extract showed very low to undetectable levels of ^{35}S-incorporation into the proteins. However, the control where crude extracts from *P. fluorescens* were omitted still showed some labeling of QbsE.

5.9.2 Identification of QbsE-GG-COSH by ESI-FTMS

The most direct way to identify a thiocarboxylate on QbsE is by mass spectrometry. ESI-FTMS would clearly show a shift in mass of +16Da if a thiocarboxylate was present. Additionally, if the residues after the diglycine of QbsE are cleaved off, this would also be seen in the mass spectrum.

Since all of the proteins (QbsC, QbsD, and QbsE) were only sparingly soluble when expressed alone, we decided to use the QbsCDE overexpression construct, where all of the proteins were overexpressed together *in vivo*. Unmodifed QbsE (QbsE-GGCF-COOH) has a mass of 9965 Da. Even though QbsD did not co-purify with QbsC and QbsE, if it was at all active, it could hydrolyze the C-terminal residues of QbsE off *in vivo*, generating QbsE-GG-COOH with a mass of 9715 Da. The substitution of a thiocarboxylate for a carboxylate would increase the mass by 16 Da, yielding either a mass of 9981 Da for QbsE-GGCF-COSH or 9731 Da for QbsE-GG-COSH. This functionalization of the C-terminal end of QbsE could potentially happen *in vivo* since the adenylating and sulfurylating protein QbsC would be present.

In the experiment, the QbsCDE overexpression construct was grown in *E. coli* Tuner(DE3) and the proteins, his-tagged QbsC and QbsE (without a his-tag), were purified as described in section 5.5.1. The purified proteins were analyzed by ESI-FTMS, as seen in figure 5.20.

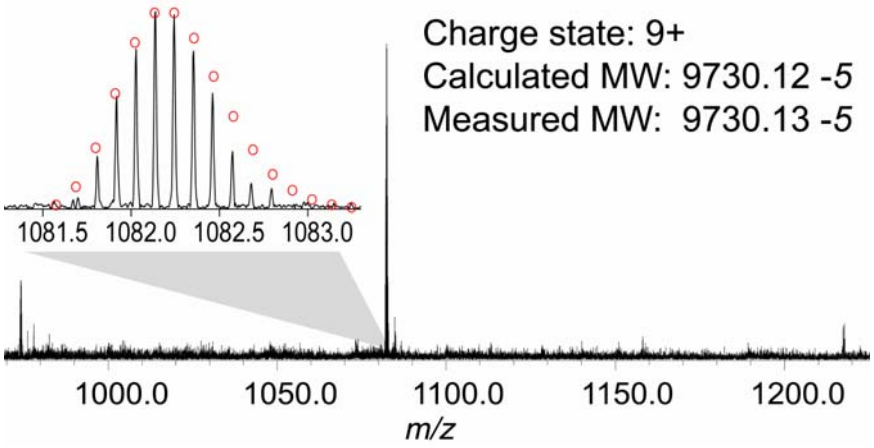

Figure 5.20 ESI-FTMS spectrum showing the molecular ion (monoisotopic peak of 9730 Da) corresponding to the formation of QbsE-GG-COSH (average isotopic mass of 9731Da).

The mass that was observed was clearly much lower than the expected mass of unmodified QbsE, implying that the two C-terminal residues of the protein was indeed removed. However, the measured average mass of 9731 also indicated that not only was the cysteine-phenylalanine removed from the C-terminus but also that a sulfur has been added in place of an oxygen on the protein, probably as the thiocarboxylate on the C-terminus. When QbsC and QbsE were co-overexpressed without QbsD, no modification of the C-terminus of QbsE was observed.

5.10 Conclusions

This chapter described experiments towards understanding if and how sulfur transfer to QbsE, a small putative sulfur-carrier protein, could occur. The proteins were first cloned into pET vectors and then overexpressed. Like all of the other proteins in this cluster, these proved to be difficult to work with due to their very low solubilities in all of the growth conditions tested. Despite

the low yields and solubilities, the proteins were tested for their proposed activities (figure 5.19).

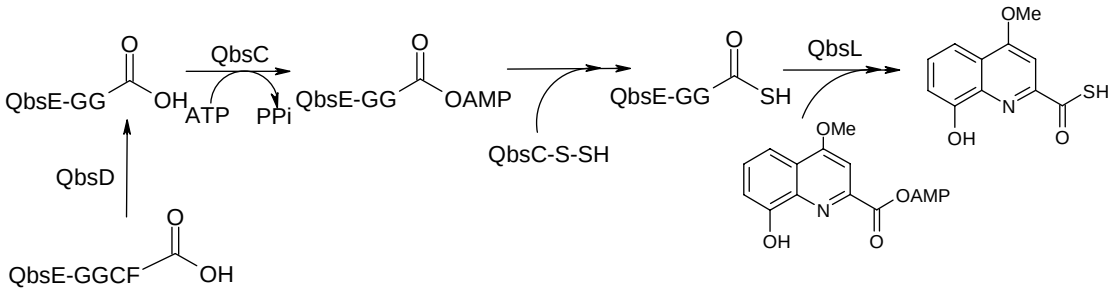

Figure 5.21 Proposed steps in the transfer of sulfur to form thio-quinolobactin.

When QbsC and QbsE, which had the cysteine-phenylalanine removed from the C-terminus, were incubated together with ATP, some AMP was released. Although this was not direct evidence that QbsC was able to activate the C-terminus of QbsE as the acyl adenylate, it did support it. The AMP formation when both enzymes were incubated was much higher than the background when the individual enzymes capacity to generate AMP was tested.

Modification of the C-terminus of QbsE and sulfur incorporation were much less enigmatic. Co-overexpression of QbsD and QbsE resulted in purification of modified QbsE as with its C-terminal cysteine and phenylalanine removed. The formation of QbsE-GG-COOH was confirmed by MS-MS. We were able to see a small amount of sulfur transfer to QbsE when a non-native cysteine desulfurase, YrvO, was used in conjunction with ^{35}S-cysteine. This showed that ^{35}S was incorporated into QbsE but did not definitively show that it was incorporated as a thiocarboxylate. The same incorportation of ^{35}S was observed when YrvO was omitted and crude extracts from *P. fluorescens* was

added instead. Mass spectrometry clearly showed that the cysteine and phenylalanine at the C-terminus of QbsE were hydrolyzed. It also showed the incorporation of sulfur into QbsE as the C-terminal thiocarboxylate, QbsE-GG-COSH.

5.11 Materials and experimental procedures

All materials were obtained from Sigma-Aldrich unless otherwise noted.

5.11.1 Cloning of *qbsE* into pET28a

Genomic DNA from *P. fluorescens* ATCC 17400 was isolated using the Wizard^{TM} Plus DNA prep kit. This was used to PCR amplify *qbsE* using the following primers: forward 5'- TTC CAT CAT ATG AAG ATC ACT GTC CCC ACC -3' and reverse 5'- CAA GGG CAC ATG GAA TTC TTC CTC CCC GGG -3'. PCR reactions were carried out using Platinum Pfx Polymerase and dNTPs according to the literature protocol, except using 100 pmol of each primer and 4 μL of enhancer per 10 μL reaction. The PCR product (~0.4 kb) was purified by agarose gel electrophoresis, excised and purified with the Qiagen Gel Extraction kit. PCR amplified *qbsE* was digested with NdeI and EcoRI obtained from New England Biolabs. The digested *qbsE* was purified directly from the reaction mixture with the QiaQuick MiniElute PCR purification kit. The cut insert was ligated into a similarly digested pET28a vector (Novagen) that had been purified by gel electrophoresis with T4 DNA ligase (New England Biolabs). Supercompetent *E. coli* Top 10 cells were used to transform the ligated pET28a and insert. Standard methods were used for DNA restriction endonuclease digestion, ligation and transformation of DNA. Colonies were then screened for the *qbsE* insert and those colonies that had

insert were grown at 37 ºC in LB/Kan media for 8 hrs, and the plasmid was harvested. The prepared plasmid was sequenced and a plasmid with the correct sequence was selected and named pPfQbsE.28a. Plasmid DNA was purified with the Qiagen Plasmid purification kit. Plasmid storage and propagation was performed using *E. coli* Mach1 $T1^R$ cells.

5.11.2 Overexpression and purification of QbsE

All cultures contained 50 mg/L kanamycin sulfate. 10 mL of LB/Kan were inoculated with a single colony of pPfQbsE.28a in *E. coli* tuner (DE3) cells and grown at 37 ºC for 7 hrs with agitation. The entire starter culture was used to inoculate 1 L of LB/Kan media with 0.1% sorbitol. The culture was grown at 37 ºC to an OD_{600} of 0.4, at which point the temperature was decreased to 15ºC. At an OD_{600} of 0.6, overexpression was induced by the addition of 500 μM IPTG and growth was continued overnight. The cells were harvested by centrifugation at 7800xg for 12 min at 4 ºC and then stored at -20 ºC.

Purification of the protein was carried out by His-trap Ni-NTA chromatography (Amersham). The cell pellet was resuspended and lysed in 50 mM sodium phosphate buffer, pH 8, 300 mM NaCl, 10 mM imidazole, and 0.1% triton X-100 with sonicaiton on ice. The cellular debris was removed by centrifugation at 27000xg for 30 min at 4 ºC and the supernatant was loaded onto a Ni-NTA column pre-equilibrated in lysis buffer. The column was washed with 20 column volumes of wash buffer, 50 mM sodium phosphate pH 8, 300 mM NaCl, and 100 mM imidazole, and the protein was eluted with 50 mM sodium phosphate, 300 mM NaCl and 500 mM imidazole. The protein was only stable in the presence of salt, and was typically desalted with

EconoPac DG-10 columns (BioRad) into 50 mM Tris pH 7.8 with 50 mM NaCl.

5.11.3 Cloning of *qbsD* into pET28a

Genomic DNA from *P. fluorescens* ATCC 17400 was used to PCR amplify *qbsD* using the following primers: forward 5'- GAC CCG CAT ATG TTG CTG CTC AGC CAA GAC -3' and reverse 5'- GGG ATG GAA TTC CGT GGA GGG TTA ATA GGG -3'. Cloning was carried out as described for *qbsE* except for the use of 4 μL of enhancer per 10 μL reaction. A plasmid with the correct sequence was selected and named pPfQbsD.28a.

5.11.4 Overexpression and purification of QbsD

All cultures contained 50 mg/L kanamycin sulfate. *E. coli* Tuner (DE3) cells containing pPfQbsD.28a were grown as described for QbsE alone. Purification of the protein was carried out by Ni-NTA affinity chromatography using His-Trap columns as described for QbsE alone. The protein was only stable under relatively high salt concentrations, a minimum of 50mM NaCl, and was typically desalted into 50mM Tris pH 7.8 with 50mM NaCl with EconoPac DG10 columns.

5.11.5 Cloning of *qbsCDE* into pET28a

Genomic DNA from *P. fluorescens* ATCC 17400 was used to PCR amplify *qbsCDE* as a contiguous unit using the following primers: forward 5'- GGA ACA CAT ATG CAA CTT CCA CCC TTG GTA GAA GCC -3' and reverse 5'- CAA GGG CAC ATG GAA TTC TTC CTC CCC GGG -3'. Cloning was carried out as described for *qbsE* except for the use of 3 μL of enhancer per

10 μL reaction. A plasmid with the correct sequence was selected and named pPfQbsCDE.28a.

5.11.6 Overexpression and preparation of QbsCDE

All cultures contained 50 mg/L kanamycin sulfat. *E. coli* Tuner (DE3) cells containing pPfQbsCDE.28a were grown as described for QbsE alone. The frozen cell pellet was resuspended and lysed in 50 mM tris buffer, pH 8 and 150 mM NaCl with sonicaiton on ice. The cellular debris was removed by centrifugation at 27000xg for 30min at 4ºC. The supernatant was desalted into 50 mM Tris pH 7.8, 50 mM NaCl using EconoPac DG10 columns (BioRad).

5.11.7 Pull-down experiment with QbsCDE overexpression construct

Since only QbsC possessed a 6x-his tag in this construct, this was not a purification. The pull-down experiment was carried out by Ni-NTA chromatography. The cell pellet was resuspended and lysed in 50 mM sodium phosphate buffer, pH 8, 300 mM NaCl, 10 mM imidazole, and 0.1% triton X-100 with sonicaiton on ice. The cellular debris was removed by centrifugation at 27000xg for 30min at 4ºC and the supernatant was loaded onto a Ni-NTA column pre-equilibrated in lysis buffer. In this step the 6x-his QbsC was bound to the Ni-NTA resin (Qiagen) and all proteins that did not bind strongly to it were removed in the flow-through. The column was washed with 100 mL of wash buffer, 50 mM sodium phosphate pH 8, 300 mM NaCl, 25 mM imidazole, to remove any non-specifically bound proteins. QbsC and any protein associated with it were eluted with 50 mM sodium phosphate,

300 mM NaCl and 250 mM imidazole. Analysis of the eluted proteins was performed by SDS PAGE using a 15% gel.

5.11.8 Detection of α-^{32}P-AMP from the hydrolysis of the QbsE acyl adenylate

A typical reaction contained 8.5 μM QbsC, 11 μM QbsE, 100 μM ATP, 1 mM $MgCl_2$, 50 mM Tris pH7.8, and 100 mM NaCl. All reagents except for the ATP were mixed, and the reaction was started by the addition of 100 μM ATP and 1.16 μCi of α-^{32}P-ATP in a stock of cold ATP. Aliquots of the reaction were taken at various intervals and quenched by direct spotting on a 20x20 cm silica TLC plate. The plates were run in 4:1:1 n-BuOH:water:acetic acid mixture. After drying the plates were wrapped in plastic wrap and then exposed to a phosphorimaging screen from Amersham. The screen was developed using the Storm 860 Phosphorimager and quantitated using ImageQuant. In some cases the amount of QbsE added to the reaction was changed such that the concentrations were 5.5 μM or 3 μM.

5.11.9 Growth and lysis of *Pseudomonas fluorescens* ATCC 17400

A 5 mL starter culture was inoculated with a single colony of *P. fluorescens* and grown at 27 ºC overnight in casamino acid media (CAA). No exogenous iron was added. The cultures were used to inoculate a 1 L culture of CAA media and the cells were grown at 27 ºC for 40 hrs. Cells were harvested by centrifugation, 7800 rpm for 15 min. *P. fluorescens* was lysed by sonication and the cellular debris was removed by centrifugation at 17,000 rpm for 60 min. The clarified crude extracts were desalted into 50 mM Tris pH 7.8 and 150 mM NaCl. The lysate was stored in 35% glycerol at -70 ºC.

5.11.10 Detection of ^{35}S-sulfur incorporation into QbsE by SDS PAGE

A typical reaction contained 7 μM QbsC, 10 μM QbsE, 1 mM ATP, 5 mM $MgCl_2$, 2.5 μM YrvO, 1 mM cysteine, 4 mM DTT, 50 mM Tris pH 7.8, and 100 mM NaCl. In some reactions the DTT was omitted. All reagents except for the cysteine were mixed and the reaction was started by the addition of 1 mM cold cysteine and 0.3 μCi of ^{35}S-cysteine. Aliquots of the reaction were taken at either 3 hrs or after overnight incubation (about 13 hrs), and quenched by the addition of SDS PAGE sample buffer without reductant. The samples were subsequently frozen on dry ice and stored. Frozen samples were thawed and heated at 100ºC for 5 min. A 15% gel was used to separate the proteins. The gels were dried on a gel dryer between pieces of cellophane and, after drying the gels were exposed to a phosphorimaging screen from Amersham. The screen was developed using the Storm 860 Phosphorimager and quantitated using ImageQuant.

5.11.11 Overexpression and purification of QbsD and QbsE

All cultures contained 50mg/L kanamycin sulfate and 35mg/L chloramphenicol. 10mL of LB/Kan/Chlr was inoculated with a single colony of pPfQbsD.28a and pPfQbsE.ACYC (co-transformed) in *E. coli* tuner (DE3) cells and grown at 37ºC for 7 hours with agitation. The entire starter culture was used to inoculate 1L of LB/Kan/Chlr media with 0.1% sorbitol. The culture was grown at 37ºC to an OD of 0.4, at which point the temperature was decreased to 15ºC. At an OD of 0.6, overexpression was induced by the addition of 500μM IPTG and growth was continued overnight. The cells were harvested by centrifugation at 7800xg for 12 min at 4ºC and then stored at -20ºC.

Purification of the protein was carried out by His-trap Ni-NTA chromatography. The cell pellet was resuspended and lysed in 50mM sodium phosphate buffer, pH8, 300mM NaCl, 10mM imidazole, and 0.1% triton X-100 with sonicaiton on ice. The cellular debris was removed by centrifugation at 27000xg for 30min at 4ºC and the supernatant was loaded onto a Ni-NTA column pre-equilibrated in lysis buffer. The column was washed with 20 column volumes of wash buffer, 50mM sodium phosphate pH 8, 300mM NaCl, 50mM imidazole, and the protein was eluted with 50mM sodium phosphate, 300 mM NaCl and 500mM imidazole. The protein was only stable under relatively high salt concentrations and at low protein concentrationsl, and was typically desalted into 50mM Tris pH 7.8 with 50mM NaCl. To improve yield, the proteins were eluted into elution buffer to ensure appropriate dilution and prevent precipitation.

5.11 References

1. Burns, K.E., et al., *Reconstitution of a new cysteine biosynthetic pathway in Mycobacterium tuberculosis.* Journal of the American Chemical Society, 2005. **127**(33): p. 11602-11603.

2. Park, J.-H., et al., *Biosynthesis of the Thiazole Moiety of Thiamin Pyrophosphate (Vitamin B1).* Biochemistry, 2003. **42**(42): p. 12430-12438.

3. Wuebbens, M.M. and K.V. Rajagopalan, *Mechanistic and Mutational Studies of Escherichia coli Molybdopterin Synthase Clarify the Final Step of Molybdopterin Biosynthesis.* Journal of Biological Chemistry, 2003. **278**(16): p. 14523-14532.

4. Behshad, E., S.E. Parkin, and J.M.J. Bollinger, *Mechanism of Cysteine Desulfurase Slr0387 from Synechocystis sp. PCC 6803: Kinetic Analysis of Cleavage of the Persulfide Intermediate by Chemical Reductants.* Biochemistry, 2004. **43**: p. 12220-12226.

5. Matthies, A., M. Nimtz, and S. Leimkuhler, *Molybdenum Cofactor Biosynthesis in Humans: Identification of a Persulfide Group in the Rhodanese-like Domain of MOCS3 by Mass Spectrometry.* Biochemistry, 2005. **44**: p. 7912-7920.

6. Ambroggio, X.I., D.C. Rees, and R.J. Deshales, *JAMM: A Metalloprotease-Like Zinc Site in the Proteasome and Signalosome.* PLOS Biology, 2004. **2**(1): p. 113-119.

7. Verma, R., et al., *Role of Rpn11 Metalloproteases in Deubiquitination and Degredation by the 26S Proteasome.* Science, 2002. **298**: p. 611-615.

CHAPTER 6:

SUMMARY AND FUTURE DIRECTIONS WITH THIO-QUINOLOBACTIN BIOSYNTHESIS

6.1 Thio-quinolobactin biosynthesis

The biosynthesis of thio-quinolobactin was an interesting system for us to study given its similarity to other biosynthetic pathways that we have studied in the lab. The proposed biosynthetic scheme is given in figure 6.1.

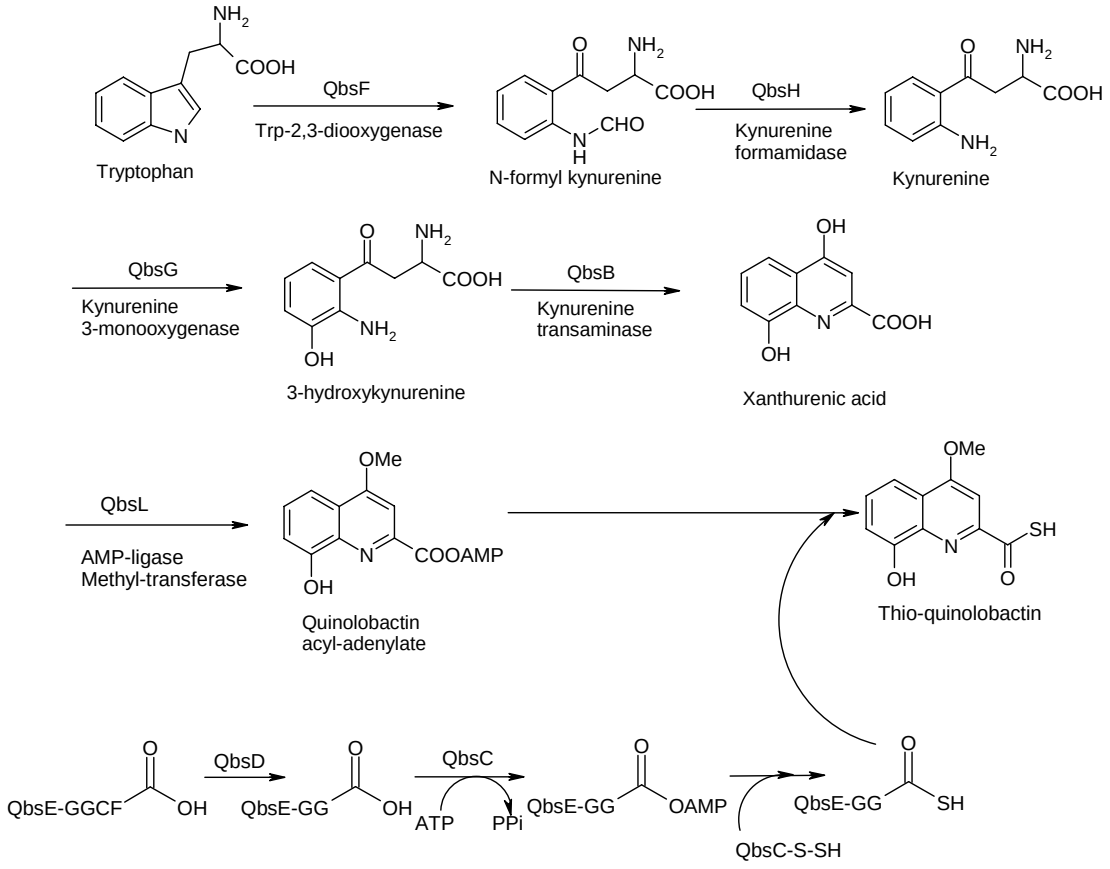

Figure 6.1 Scheme of the thio-quinolobactin biosynthetic pathway. We were interested in studying the pathway starting with 3-hydroxykynurenine and QbsB.

Based on sequence homology of gene products from the thio-quinolobactin biosynthetic gene cluster with known proteins, it appeared as though the biosynthesis combined two pathways that have been studied in the Begley lab previously. The first half of the pathway (QbsF, QbsH, QbsG) appeared similar to that found in the biosynthesis of nicotinamide, where tryptophan is catabolized to 3-hydroxykynurenine before going on to NAD.[1] 3-Hydroxykynurenine is a common metabolite along both the biosynthetic pathway to both nicotinamide and thio-quinolobactin. The latter part of the pathway (QbsC, QbsD, and QbsE) is the sulfurylation of quinolobactin to form the thiocarboxylate. The genes putatively responsible for this sulfur transfer are similar to those found in the sulfur transfer systems found in thiamin, molybdopterin, and one of the cysteine biosynthetic pathways. [2-5]

We were interested in studying the gene products responsible for the conversion of 3-hydroxykynurenine, the divergence point between thio-quinolobactin and nicotinamide biosynthesis, to thio-quinolobactin. The catabolism of tryptophan to 3-hydroxykynurenine has already been well characterized in this lab, so this was not investigated, although we did clone one of the genes, *qsbF*, and found the gene product (a tryptophan dioxygenase) to be completely insoluble. The proposed biosynthetic pathway based on putative gene functions from 3-hydroxykynurenine to thio-quinolobactin is seen in figure 6.2.

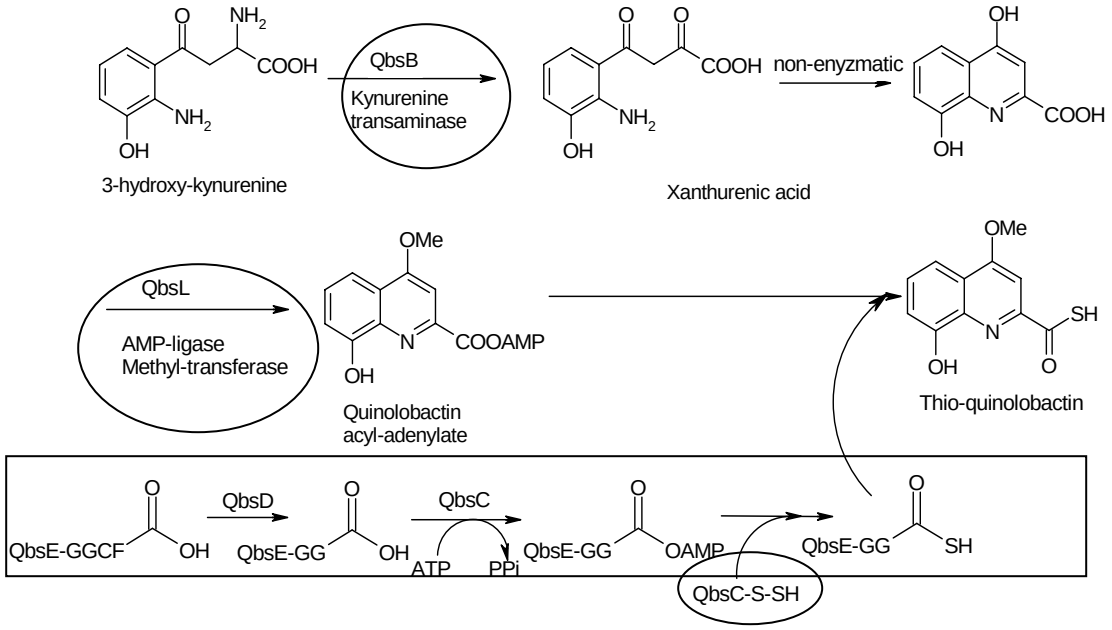

Figure 6.2 Portion of the thio-quinolobactin pathway that we have investigated. Proteins that are in circles have had at least one of their activities characterized, proteins in boxes have been studied and we have some evidence of their roles/existence.

The biosynthetic pathway begins with the PLP-dependent deamination of 3-hydroxykynurenine by QbsB to form the α-ketoacid, which can cyclize to xanthurenic acid. This is methylated by QbsL in a SAM-dependent reaction to form quinolobactin. QbsL also activates the quinaldic acid as the acyl adenylate, readying it for sulfur transfer. Sulfur transfer putatively involves two proteins, QbsC and QbsE. These proteins are sulfur activating and carrying proteins, used by nature to transfer a sulfide equivalent without using free sulfide. Another protein, QbsD, is involved in cleaving the two C-terminal amino acid residues (cysteine, phenylalanine) off of QbsE, generating the C-terminal diglycine.

The biosynthesis of thio-quinolobactin involves some interesting transformations. We were interested in verifying the putative functions of each

of the enzymes and then characterizing their activities. Although kynurenine-aminotransferases have been studied in eukaryotic systems, they are not as prevalent in prokaryotes, and very few have been characterized. The dual functionality that QbsL appears to possess is unique in the two reactions that it combines. There are relatively few examples of well-characterized examples of sulfur transfer, and no sulfur transfer systems in psuedomonads have been thoroughly investigated.

6.2 Summary of results

We began our studies with the putative aminotransferase, QbsB, which appeared to be responsible for the deamination and subsequent cyclization of 3-hydroxykynurenine to xanthurenic acid. When the enzyme was heterologously overexpressed in *E. coli*, it was completely intractable due to insolubility. When a NusA tag was added to the protein to improve solubility, we were able to obtain soluble protein that was able to catalyze the conversion of 3-hydroxykynurenine to xanthurenic acid in a PLP-dependent fashion. The protein with the tag purifies with pyridoxamine phosphate bound, and has a specific activity of 700 nmol min^{-1} mg^{-1}. The enzyme was able to take L-histidine as a substrate in addition to L-3-hydroxykynurenine. D-histidine, L-phenylalanine, and L-tyrosine were not substrates. The kinetic parameters were determined to be K_m(L-3-hydroxykynurenine) 125μM +/- 30, K_m(α-ketoglutarate) 420μM +/- 60, k_{cat} 60 min^{-1}.

The next enzyme in the pathway, QbsL, appeared to have two functions: one as a methyltransferase and another as an AMP ligase. We believed that QbsL was responsible for the methylation of the 4-hydroxy position on xanthurenic

acid to generate quinolobactin, and that it could also activate the carboxylic acid to an acyl adenylate readying the molecule for sulfurylation. Like QbsB, this enzyme also had low solubility, but appropriate growth conditions were found where we were able to obtain soluble protein. We have shown that QbsL was able to catalyze the SAM dependent transfer of a methyl group to xanthurenic acid. The activity was detectable by HPLC in crude extracts, but no quinolobactin was detected with purified QbsL. In order for activity to be seen in crude extracts, the putative sulfur transfer proteins were added. A minute but detectable amount of methyl transfer was seen with purified QbsL alone when ^{14}C-methyl-SAM was used.

In addition, we have evidence that QbsL may also catalyze the formation of the quinolobactin acyl adenylate in an ATP dependent reaction. We have observed QbsL dependent formation of α-^{32}P-AMP with quinolobactin, which implies that QbsL may be activating the carboxylic acid of quinolobactin with AMP. In addition, when dansyl hydrazine was added to QbsL crude extracts in the presence of the putative sulfur transfer proteins, quinolobactin, and ATP, we saw a new species by HPLC that migrated with a dansyl-quinolobactin conjugate standard. This provided evidence that QbsL could indeed activate the carboxylic acid of quinolobactin as the acyl adenylate.

We were able to fully characterize the rhodanese activity of QbsC, which has a rhodanese domain and can activate sulfur from thiosulfate in the form of a persulfide. When the putative catalytic cysteine, Cys345, of the conserved rhodanese domain (C[R/K]XGXR) was mutated to a serine, the protein lost all activity. Like the other proteins in the pathway, QbsC was not appreciably

soluble by itself. When QbsC was co-overexpressed with its putative binding partner, QbsE, its solubility increased dramatically. Though QbsE increased the solubility of QbsC, its presence did not seem to affect the rate of sulfur transferase activity. QbsC only accepted thiosulfate as a substrate and did not take cysteine or mercaptopyruvate. QbsC had a specific activity of about 4.2μmol min^{-1} mg^{-1}. The kinetic parameters for the thiosulfate sulfurtransferase activity of QbsC with QbsE present were determined to be: K_m(thiosulfate) 2mM +/- 0.3, K_m(cyanide) 1.5mM +/- 0.5, k_{cat} 121 min^{-1}. With QbsC alone, the kinetic parameters were K_m(thiosulfate) 2.3mM +/- 0.3, k_{cat} 362 min^{-1}. The efficiency for the reactions where both QbsC and QbsE were present was about half that for that of QbsC alone, but this was to be expected because of the relative amounts of pure QbsC present. In the QbsC and QbsE protein preparation the ratio of QbsC to QbsE was about 1:1.5.

We verified that sulfur transfer to QbsE does occur, and that it probably follows the motifs seen in thiamin and molybdopterin biosynthesis, as well as cysteine biosynthesis in tuberculosis. All three sulfur transfer proteins had minimal solubility when they were overexpressed heterologously in *E. coli*. We have evidence both from pull-downs and mass-spectrometry that QbsC and QbsE, two proteins believed to be involved in sulfur transfer, interacted with each other, something that was observed in thiamin biosynthesis.[6] Additionally, when the proteins (QbsC and QbsE) were co-overexpressed, we observed a marked increase in solubility. We were able to conclusively show that QbsC can activate sulfur in the form of a persulfide, a key step in the hypothesized sulfur transfer mechanism.

Modfication of the C-terminus of QbsE and sulfur incorporation was much less enigmatic. When QbsD and QbsE were co-overexpressed and co-purified, QbsE purified out with its two C-terminal amino acids hydrolyzed. This was confirmed by ESI-MS as QbsE-GG-COOH. We were able to see a small amount of sulfur transfer to QbsE when a non-native cysteine desulfurase, YrvO, was used in conjunction with ^{35}S-cysteine. This showed that ^{35}S was incorporated into QbsE, but does not definitively show that it was incorporated as a thiocarboxylate. The same incorportation of ^{35}S was observed when YrvO was omitted, and crude extracts from *P. fluorescens* was added instead. Mass spectrometry clearly showed that the cysteine and phenylalanine at the C-terminus of QbsE were hydrolyzed. It also showed the incorporation of sulfur into QbsE as the thiocarboxylate.

6.3 Future directions

A major hurdle in fully characterizing the activities of these proteins has been their lack of solubility. Very little soluble protein is obtained when the genes were heterologously over-expressed in *E. coli*. Where possible, we have identified activities and characterized the proteins and have had success with a few of the proteins. We have certainly shown that QbsB can catalyze the formation of xanthurenic acid, and that QbsL can methylate it and form quinolobactin. There is also conclusive evidence of the rhodanese activity of QbsC, implicating its involvement in sulfur-transfer. It is also apparent that QbsC and QbsE form a complex, and when these two proteins are co-overexpressed there is a large increase in solubility of the otherwise insoluble QbsC. We have evidence of the modification of the C-terminus of QbsE by cleavage of the cysteine and phenylalanine residues by QbsD. Mass

spectrometry also indicates that QbsE is further modified by the addition of a sulfur, probably in the form of a thiocarboxylate.

There is still a lot of work to be done with this system as we were unable to fully reconstitute and characterize the sulfur transfer system. The ability to obtain soluble protein is essential to elucidating the details involved in sulfur transfer. Heterologous overexpression of these *Pseudomonas* proteins in *E. coli* does not work well, and gives primarily insoluble proteins. A caveat to this is that co-overexpression of certain proteins (QbsC and QbsE) results in much higher protein solubilities. Something that could be done is to clone each of the operons (seen in figure 1.2) into separate vectors and then co-overexpress all of the proteins in the cluster in an *E. coli* overexpression strain together. The lysate can then be tested for the ability to make thio-quinolobactin from 3-hydroxy kynurenine or even tryptophan. Co-overexpression may increase the solubility of the proteins, and may aid in the formation of any complexes that may need to form for the proteins to work. It would seem, given the instability of a number of species along the pathway, that the biosynthetic proteins need to interact with each other in order to function properly.

Future work includes growing *P. fluorescens* ATCC 17400 under iron-limiting conditions, which induces expression of genes involved in siderophore biosynthesis. Clarified crude cell-lysates can then be tested for their ability to make quinolobactin or thio-quinolobactin from 3-hydroxy kynurenine. Sulfur incorporation and methyl transfer can be done by using radioactive ^{35}S-cysteine or ^{14}C-methyl-SAM as described previously for the over-expression system. Although these proteins will not be over-expressed and will not have

an affinity tag for purification, expression in their native organism should at least yield soluble protein. The cell lysate will also contain any auxiliary proteins that may be necessary for thio-quinolobactin biosynthesis, such as a cysteine desulfurase that may be responsible for sulfur transfer to QbsC.

An exciting possibility for future work is to overexpress the proteins in *Pseudomonas* itself. A system of overexpression in *Pseudomonas aeruginosa* is available, using the vector pUCP19 and an engineered *Pseudomonas aeruginosa* strain PAO1-LAC. This system employs the shuttle vector pUCP19, which is a plasmid constructed such that it can replicate in at least two types of host organisms. In this case it is *E. coli* and *P. aeruginosa*. By utilizing this system, we may be able to obtain soluble protein in much larger quantities since the proteins will be expressed in an organism much more similar to its true host than *E. coli*.

6.4 Conclusions

Although we have made significant steps towards elucidating the biosynthetic pathway to thio-quinolobactin from 3-hydroxykynurenine, there is still work to be done on the system. We have cloned all of the genes putatively involved in the transformation of 3-hydroxykynurenine to thio-quinolobactin, and characterized their activities when possible. We have also cloned some of the other genes found in the biosynthetic operon, including QbsF, QbsK, and QbsJ, and found them to be intractable due to insolubility. The ability to overexpress these proteins solubly will greatly aid in the determination of the mechanism of sulfur transfer.

6.5 References

1. Kurnasov, O., et al., *NAD biosynthesis: Identification of the tryptophan to quinolinate pathway in bacteria.* Chemistry & Biology, 2003. **10**(12): p. 1195-1204.

2. Dorrestein, P.C., et al., *The biosynthesis of the thiazole phosphate moiety of thiamin: the sulfur transfer mediated by the sulfur carrier protein ThiS.* Chemistry & Biology, 2004. **11**(10): p. 1373-1381.

3. Burns, K.E., et al., *Reconstitution of a new cysteine biosynthetic pathway in Mycobacterium tuberculosis.* Journal of the American Chemical Society, 2005. **127**(33): p. 11602-11603.

4. Park, J.-H., et al., *Biosynthesis of the Thiazole Moiety of Thiamin Pyrophosphate (Vitamin B1).* Biochemistry, 2003. **42**(42): p. 12430-12438.

5. Wuebbens, M.M. and K.V. Rajagopalan, *Mechanistic and Mutational Studies of Escherichia coli Molybdopterin Synthase Clarify the Final Step of Molybdopterin Biosynthesis.* Journal of Biological Chemistry, 2003. **278**(16): p. 14523-14532.

6. Taylor, S.V., et al., *Thiamin biosynthesis in Escherichia coli. Identification of the thiocarboxylate as the immediate sulfur donor in the thiazole formation.* Journal of Biological Chemistry, 1998. **273**(26): p. 16555-16560.

CHAPTER 7:

THIAMIN PYROPHOSPHATE PROTEOMICS: AN INTRODUCTION

7.1 Introduction

Thiamin pyrophosphate (TPP) is an essential cofactor utilized by proteins in key prokaryotic and eukaryotic metabolic pathways. The ability to observe and compare relative amounts of these vital proteins when cells are grown under different conditions can give valuable insight into how cells respond to stressors such as starvation, disease, or drugs. Thiamin pyrophosphate analogs incorporating a photolabile substituent that generates a reactive species upon irradiation were synthesized and tested as proteome probes. The selective, irreversible incorporation of the photoprobes into thiamin pyrophosphate utilizing enzymes should allow for the detection and relative quantitation of these key proteins among all other cellular proteins. Only certain diagnostic proteins are being detected, therefore analysis of cellular response to varying growth conditions is simplified.

7.2 The metabolic importance of vitamin B_1

Thiamin pyrophosphate (TPP), vitamin B_1, is an essential cofactor used to stabilize acyl-carbanions. The substituted thiazole portion of thiamin creates an electron sink capable of stabilizing the carbanion through resonance. Thiamin pyrophosphate containing enzymes commonly catalyze the decarboxylation of α-keto acids. This motif is illustrated in the conversion of

two molecules of pyruvate to acetolactate catalyzed by acetolactate synthase, seen in figure 7.1.[1]

TPP is activated by removal of the C_2 proton on the thiazolium ring to create an ylide that can attack the carbonyl group of pyruvate. The carbanion generated in the decarboxylation is stabilized by the thiazolium ring. A second molecule of pyruvate is added and elimination of the regenerated thiamin pyrophosphate ylide produces acetolactate.

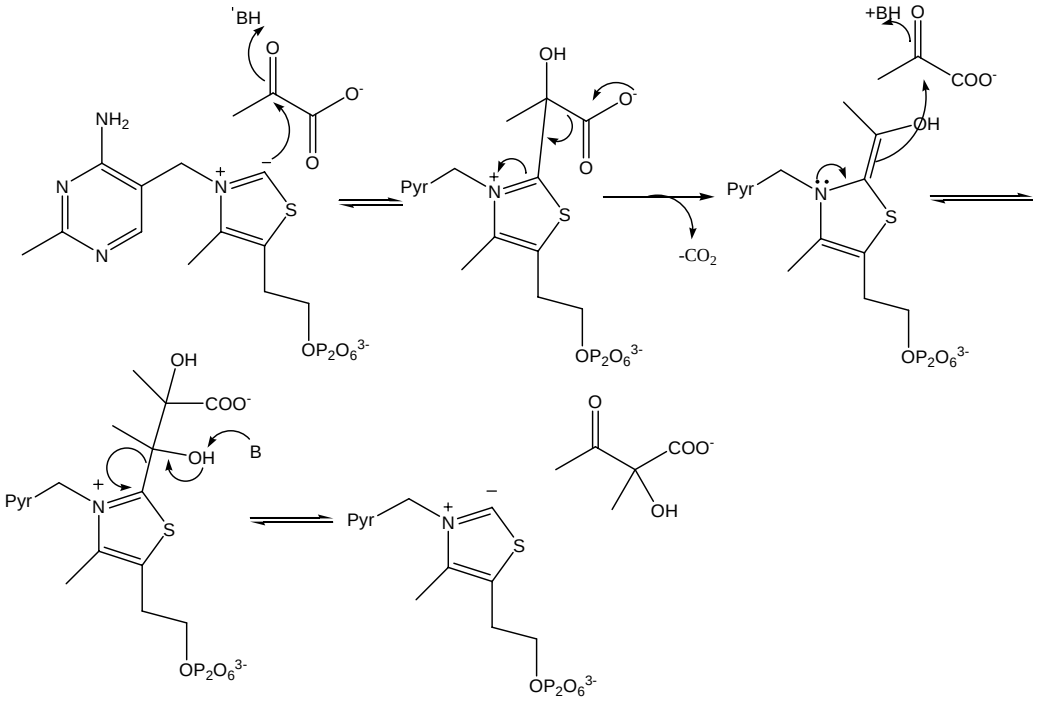

Figure 7.1 Proposed mechanism for the reaction catalyzed by acetolactate synthase, a thiamin pyrophosphate utilizing enzyme.

Though the number of thiamin pyrophosphate utilizing enzymes in the cell is relatively small, it is used to catalyze enzymatic reactions in some of the most important metabolic pathways in cells, ranging from glycolysis to the biosynthesis of thiamin itself. A schematic overview of the pathways

employing the thiamin pyrophosphate requiring enzymes in *E. coli* is shown in figure 7.2.

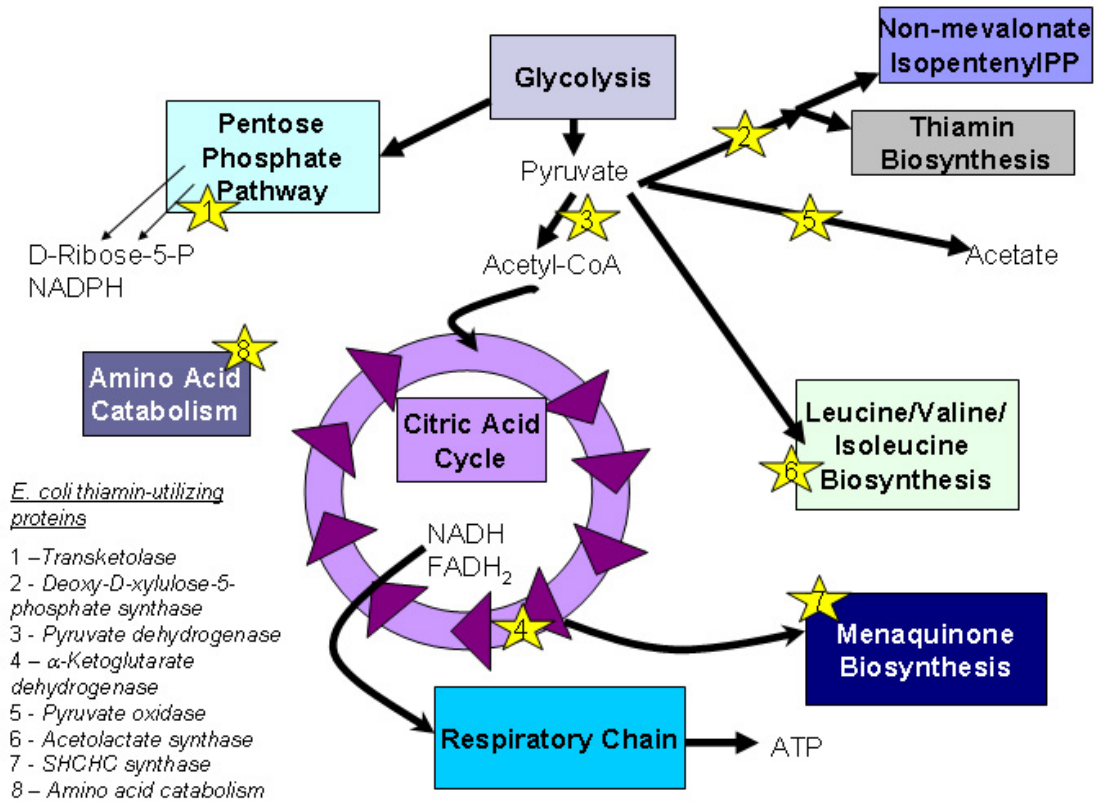

Figure 7.2 Metabolic pathway chart highlighting the presence of thiamin pyrophosphate utilizing enzymes in important pathways.

In the cell, glucose is shuttled from glycolysis into the pentose phosphate pathway, which contains transketolase (figure 7.2, (1)). Transketolase is a key enzyme in the reversible link between glycolysis and the pentose phosphate pathway, and is responsible for the production of NADPH, a reducing agent, and D-ribose-5-phosphate, the sugar used in nucleic acid biosynthesis. The biosynthesis of steroids through the non-mevalonate pathway requires deoxy-D-xylulose-5-phosphate (DXP), produced by DXP synthase (figure 7.2, (2)). Pyruvate oxidase catalyzes the conversion of pyruvate to acetate under

anaerobic conditions (figure 7.2, (5)). Similarly, pyruvate dehydrogenase catalyzes the oxidation of pyruvate to acetyl-CoA under aerobic conditions (figure7.2, (3)). The acetyl-CoA is shuttled into the citric acid cycle, often referred to as the “hub of metabolism” due its tight regulation and various anabolic pathways branching out. The citric acid cycle, which contains the thiamin pyrophosphate utilizing enzyme α-ketoglutarate dehydrogenase, generates energy containing molecules such as NADH and $FADH_2$ that are transferred to the respiratory chain ultimately generating ATP (figure 7.2, (4)). Acetolactate synthase is present in the shared biosynthetic pathways of leucine, isoleucine, and valine biosynthesis (figure 7.2, (6)). Lastly, the first committed step in menaquinone biosynthesis involves SHCHC synthase (figure 7.2, (7)).[2]

7.3 Proteomics

Proteomics allows for the direct comparison of protein levels in a cell, information that transcriptomics, the study of mRNA levels, cannot do accurately. Work done by Aebersold found that there was insufficient correlation between mRNA and protein levels to use mRNA as an accurate predictor of protein expression.[3] In order to get an accurate representation of protein levels in a cell, the actual proteins, not mRNA or DNA, must be used. The response of the proteome to different growth conditions is simplified by fractionating the proteome into families of proteins based on mechanistic functioning, referred to as activity based proteomics.[4]

Activity based proteomics typically uses a chemical approach to profile changes in enzyme activity in complex proteomes.[5] Small molecule probes

are designed that will label the enzyme active site based on the activity or mechanism of the protein. Many of the chemical probes that have been developed are mechanism based inhibitors. An illustrative proof of concept experiment involves the profiling of protein expression of the family of serine hydrolases. An active site directed probe was chemically synthesized such that it could be used to tag proteins for detection. Design considerations mandated that the probe be both general enough to label all serine hydrolases and specific enough that it does not non-specifically label non-serine hydrolases. The probe, a biotinylated fluorophosphonate, was incubated with crude tissue extracts, and was able to label, with high sensitivity, a large number of serine hydrolases. These were isolated for profiling by the biotin tag, and as expected different tissues gave different profiles of serine hydrolases.[6]

7.4 Thiamin proteomics

We intend to design photoaffinity probes that allow for the direct comparison of relative amounts of all thiamin pyrophosphate utilizing proteins in the cell proteome when the cells are exposed to different biological stimuli. These probes were designed to selectively label the active sites of the thiamin utilizing proteins in the cell proteome. The proteome is extremely complex, being made up of thousands of different proteins, and protein content in a cell can vary depending on the health of the cell, the phase of the life cycle, the environment, and myriad other factors. Since these photoreactive reagents will label only a subset of diagnostic proteins of the proteome, analysis of cell response to external stimuli is greatly simplified.

Thiamin pyrophosphate utilizing proteins share the common mechanistic function of stabilizing an acyl carbanion generated upon decarboxylation of an α-keto-acid. By detecting only these enzymes, analysis of cellular responses to different conditions is simplified. Due to the presence of thiamin pyrophosphate utilizing enzymes in key metabolic pathways, the development of a probe that can irreversibly label these proteins provides a straightforward way to observe cellular response to stressors or stimulants. By detecting only thiamin pyrophosphate utilizing proteins through the attachment of a probe, information about diverse cellular events such as energy production, cofactor biosynthesis, DNA biosynthesis, and amino acid biosynthesis can be acquired. For example, in bacterial cells grown in the presence of the amino acids, it is expected that the level of acetolactate synthase would be decreased, while in cells grown without the amino acids present, the level of acetolactate synthase would increase. In another more medically relevant example, the amount of transketolase present in a cell gives insight into the relative amount of DNA production. In rapidly dividing tumor cells, there is a large need for DNA replication and hence an increased presence of transketolase when compared to normally dividing cells.

Ideal probes would be able to identify any protein that binds thiamin pyrophosphate as a cofactor, a substrate, or an allosteric regulator. Since thiamin pyrophosphate is never covalently attached to the protein, the design of an electrophilic functional group that can be attacked by an active site nucleophile becomes difficult. Electrophiles are generally incorporated into probes where an “activated” active site nucleophile is present, such as the serine residue in serine hydrolases. Photolabile functional groups offer the

advantage of using light to generate a reactive species that is capable of covalent modification of both small molecules and proteins. These functional groups offer distinct advantages over electrophilic groups: they are inert until they are irradiated with light, the species generated is generally highly reactive, and most photolabile groups are small.

When developing photoaffinity probes to covalently modify proteins, wavelengths needed for generation of the reactive species should be greater than 300nm. Aromatic amino acids such as tryptophan, tyrosine, and phenylalanine absorb in the region of 250-280nm, so irradiation with light less than 300nm can excite these residues and cause photodamage to the protein. The probes should be stable to both storage and experimental conditions, and should closely resemble the original molecule to ensure binding specificity.[7]

Two functional groups, the azido and thio-carbonyl, were chosen for construction of thiamin analogs due to their ease of incorporation, stability in the absence of light, and absorbance characteristics. Both are relatively small functionalities and can be introduced into the thiamin skeleton with little perturbation, thereby producing photoaffinity labels that can gain access to the enzyme active site and bind. Some possible photoaffinity labels that have been synthesized for this study are shown in figure 7.3.

Generation 1 Photoaffinity Labels

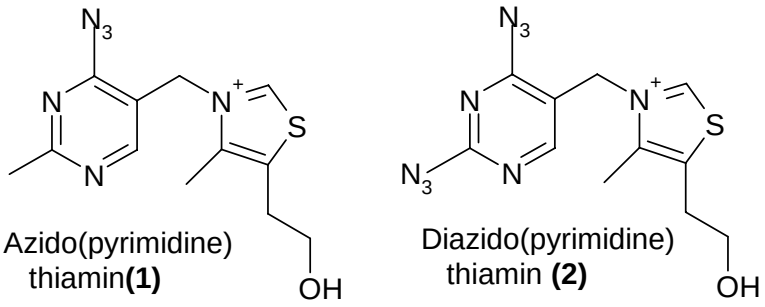

Generation 2 Photoaffinity Labels

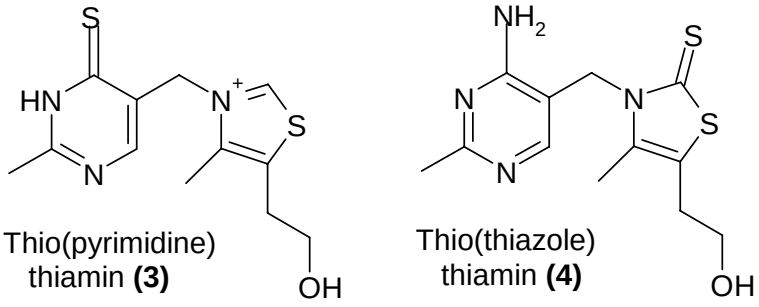

Generation 3 Photoaffinity Labels

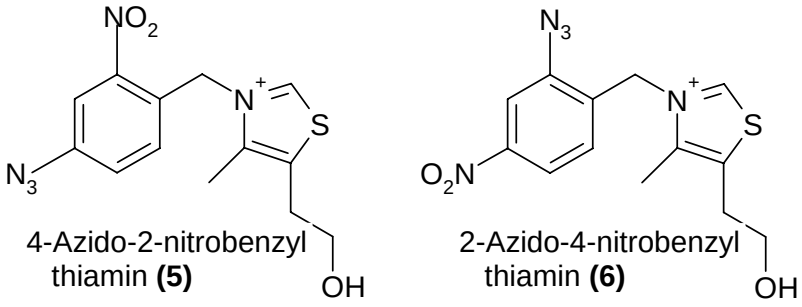

Figure 7.3 Proposed thiamin analogs with photolabile functionality incorporated that will be tested for their ability to covalently modify thiamin pyrophosphate utilizing proteins. A pyrophosphate group can be added to make the pyrophosphate analogs.

Generations 1 and 3 probes incorporate the azide group as the photolabile functionality. Azides are inert until activated, but must be handled under reduced light to prevent their premature photo-activation. Simple aryl azides absorb in the range of 250-280 nm, but the addition of an electron withdrawing

group, such as nitro, can shift the absorbance well above 300 nm. An important feature of azides is the extreme reactivity of the activated species. Azides will lose nitrogen gas upon irradiation to generate an extremely electrophilic singlet nitrene. The singlet nitrene species undergoes a variety of reactions ranging from interstate conversion to the diradical-like triplet, to insertion into bonds, to intramolecular rearrangement followed by nucleophilic attack.

The thio-carbonyl group incorporated into generation 2 probes is activated with wavelengths of light between 300 and 400nm, causing a π to π^* transition. The chemistry of the activated thio-carbonyl is not as diverse as the nitrene, but it is capable of inserting itself into various bonds, though insertion into alkenes is most efficient. Upon irradiation, a singlet is generated, which rapidly undergoes interstate conversion to the diradical-like triplet.

7.5 Usefulness of thiamin pyrophosphate photolabile analogs as proteomics probes

Generation 1 and 2 analogs were not amenable for use as probes to detect thiamin pyrophosphate utilizing enzymes. In the case of generation 1 probes, the molecules were unstable and could not be pyrophosphorylated, and degraded quickly in solution. Although the generation 2 probes were stable, inhibitors of α-ketoglutarate dehydrogenase, and could be pyrophosphorylated, they were not photo-labile enough to be used as proteomics probes.

Both of the generation 3 probes were pyrophosphorylated by thiamin pyrophosphate kinase, and in both cases were better substrates than thiamin itself. 4-azido-2-nitrobenzylthiamin pyrophosphate (5pp) was found to have an IC_{50} for α-ketoglutarate dehydrogenase of about 200 μM. However, 2-azido-4-nitrobenzylthiamin pyrophosphate (6pp) was not able to decrease product turnover. When we investigated 4-azido-2-nitrobenzyl thiamin pyrophosphate as a possible proteomics probe, we found that it labeled non-TPP utilizing enzymes in addition to TPP utilizing enzymes. This non-specific labeling was alleviated by the addition of a scavenger, although this drastically decreased the amount of labeling of the TPP-utilizing protein. Because TPP was able to remove the labeling that did occur when a scavenger was added, it implied that the photolabile analog was labeling at the enzyme active site.

The most promising of the probes that was designed and synthesized was 4-azido-2-nitrobenzyl thiamin pyrophosphate (5pp). Although it was an inhibitor of TPP-utilizing enzymes, it had a high amount of non-specific labeling. When scavengers were added to trap the reactive intermediate that formed upon photolysis, the amount of labeling of the TPP utilizing enzyme decreased to an amount that precluded this probe from further investigation.

7.6 References

1. Silverman, R.B., *The Organic Chemistry of Enzyme Catalyzed Reaction*. 2nd ed. 2002: Academic Press. 800.

2. Nelson, D.L. and M.M. Cox, *Lehninger Principles of Biochemistry*. 3rd ed. 2000, New York: W.H. Freeman & Company. 1200.

3. Gygi, S.P., et al., *Correlation between protein and mRNA abundance in yeast.* Molecular Cell Biology, 1999. **19**: p. 1720-1730.

4. Kozarich, J.W., *Activity-based proteomics: enzyme chemistry redux.* Current Opinion in Chemical Biology, 2003. **7**: p. 78-83.

5. Speers, A.E. and B.F. Cravatt, *Chemical Strategies for Activity-Based Proteomics.* ChemBioChem, 2003. **5**(1): p. 41-47.

6. Liu, Y., M.P. Patricelli, and B.F. Cravatt, *Activity-based protien profiling: The serine hydrolases.* Proceedings of the National Academy of Sciences of the United States of America, 1999. **96**(26): p. 14694-14699.

7. Work, T.S. and R.H. Burdon, eds. *Photogenerated reagents in biochemistry and molecular biology*. Laboratory Techniques in Biochemistry and Molecular Biology. Vol. 12. 1983, Elsevier: Amsterdam.

8. Walsh, D.A., et al., *The elementary reactions of the pig heart pyruvate dehydrogenase complex. A study of the inhibition by phosphorylation.* Biochemical Journal, 1976. **157**(1): p. 41-67.

CHAPTER 8:

DESIGN, SYNTHESIS, AND TESTING OF GENERATION 1 AND 2 PROBES

8.1 Introduction

The generation 1 probes incorporate an azide group into the pyrimidine ring of the thiamin, while the generation 2 probes incorporate a thione into either the pyrimidine or thiazole ring (figure 8.1).

Generation 1 Photoaffinity Labels

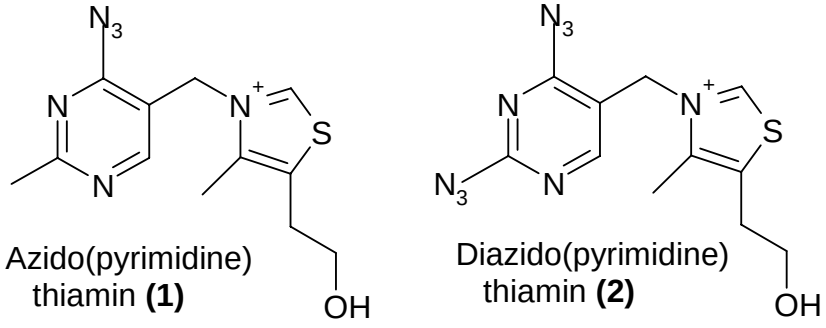

Generation 2 Photoaffinity Labels

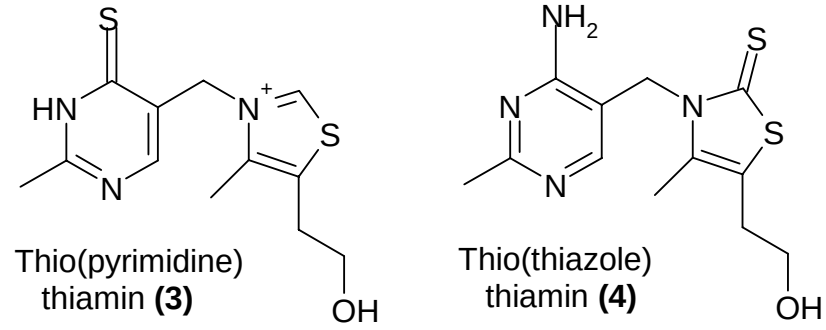

Figure 8.1 Structures of the generation 1 probes, azido(pyrimidine) thiamin and diazido(pyrimidine) thiamin, and generation 2 probes, thio(pyrimidine) thiamin and thio(thiazole) thiamin.

These probes are structurally very similar to thiamin and incorporate only small changes in order to introduce a photo-labile functionality.

8.2 Design of generation 1 probes

The first generation of probes was based on the photoaffinity label 2-azido-adenosine-triphosphate (2-azido-ATP), a close structural analog of ATP (figure 8.2). Theses probes have been used to detect proteins in a variety of systems, including the detection of a nucleotide binding site on chloroplast coupling factor I in the thylakoid membrane of spinach chloroplasts, where ~20% labeling of the protein was achieved.[1] 2-Azido-ATP has also been utilized in the detection of potential catalytic and regulatory subunits of protein kinases.[2] Like the generation 1 photoaffinity probes, 2-azido-ATP contains a pyrimidine ring with the azido group substituted at the 2-postion between the two ring nitrogens.

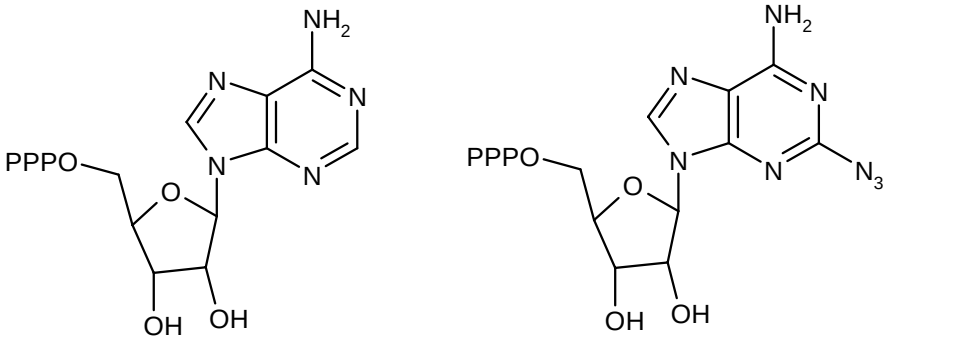

Adenosine triphosphate 2-Azido-adenosine triphosphate

Figure 8.2 Structures of ATP and the photoaffinity probe 2-azido-ATP.

8.3 Synthesis of generation 1 probes

The initial proposed synthetic route to azido(pyrimidine)thiamin (1), proceeded through chloro(pyrimidine)thiamin (12). This provided access to thiamin analogs with various substitutions on the 4-position of the pyrimidine ring, including azido(pyrimidine)thiamin (1) and thio(pyrimidine)thiamin (3). The overall synthetic route is shown in figure 8.2 below.

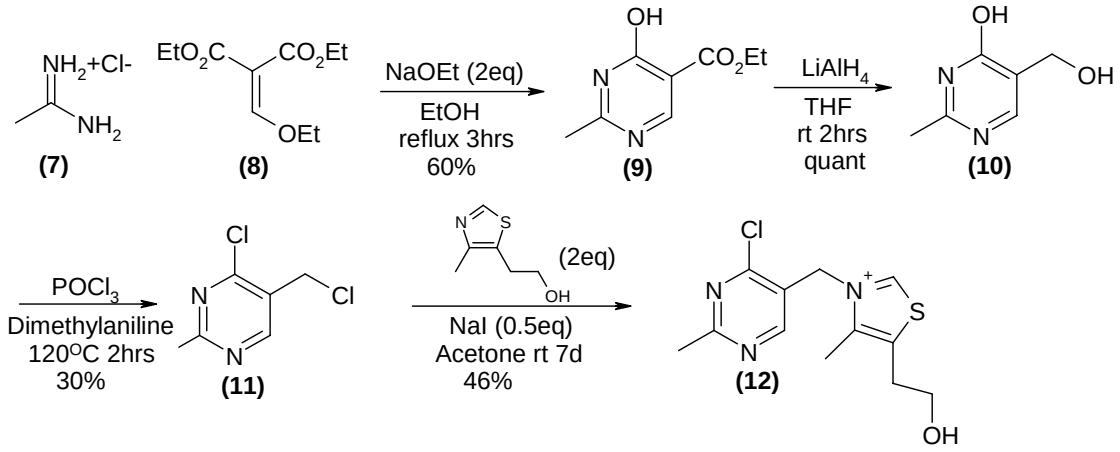

Figure 8.3 Synthesis of chloro(pyrimidine)thiamin (12).

The pyrimidine (9) was formed via the condensation of acetamidine hydrochloride (7) and diethylmalonylmalonate (8) in 60% yield. The ester functionality was then quantitatively reduced with lithium aluminum hydride to the alcohol, and the diol (10) that was produced was converted to 4-chloro-5-chloromethyl-2-methyl-pyrimidine (11) with phosphoryl chloride in 30% yield. Chloro(pyrimidine)thiamin (12) was produced by stirring 4-chloro-5-chloromethyl-2-methylpyrimidine, (11), with thiazole alcohol and sodium iodide, 45% yield.

Unfortunately, nucleophilic aromatic substitution could not be carried out on chloro(pyrimidine)thiamin due to the expulsion of thiazolium ring after

formation of the Meisenheimer complex, seen in figure 8.4. The release of the thiazolium ring and a substituted pyrimidine, where Nuc- was azide, was confirmed by mass spectrometry.

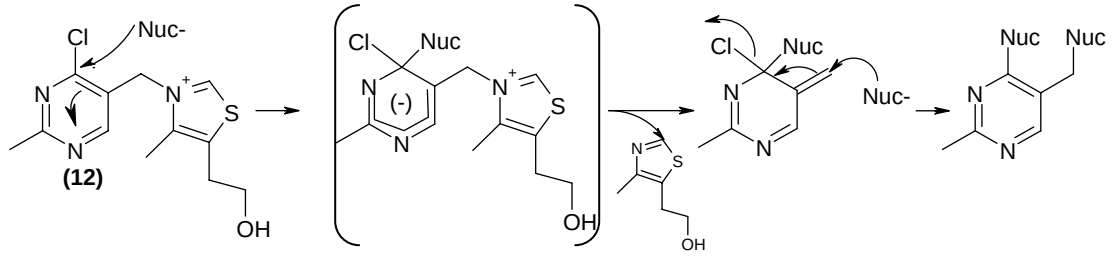

Figure 8.4 Attempted substitution on chloro(pyrimidine)thiamin with a nucleophile results in the formation of the Meisenheimer complex. When this collapses, the thiazolium ring is expelled.

This dictated carrying out the nucleophilic substitution on the pyrimidine ring prior to coupling it with the thiazolium ring, leading to the synthesis of diazido(pyrimidine)thiamin (2) as a possible photoaffinity probe incorporating the photolabile azido groups. The synthetic route to (2), seen in figure 8.5, provided a relatively short and appealing method to a pyrimidine ring that had been substituted with the azide functionality prior to coupling with the thiazolium ring.

Thymine (13) was treated with phosphoryl chloride to give the 2,4-dichloro-5-methyl pyrimidine (14) in 81% yield, which was subsequently treated with sodium azide to provide (15) in 46% yield. The methyl group of (15) was converted to bromomethyl via radical bromination using N-bromosuccinimde and benzoyl peroxide with a 30% yield. Diazido(pyrimidine)thiamin (2) was produced by nucleophilic substitution with thiazolium ring, 50% yield.

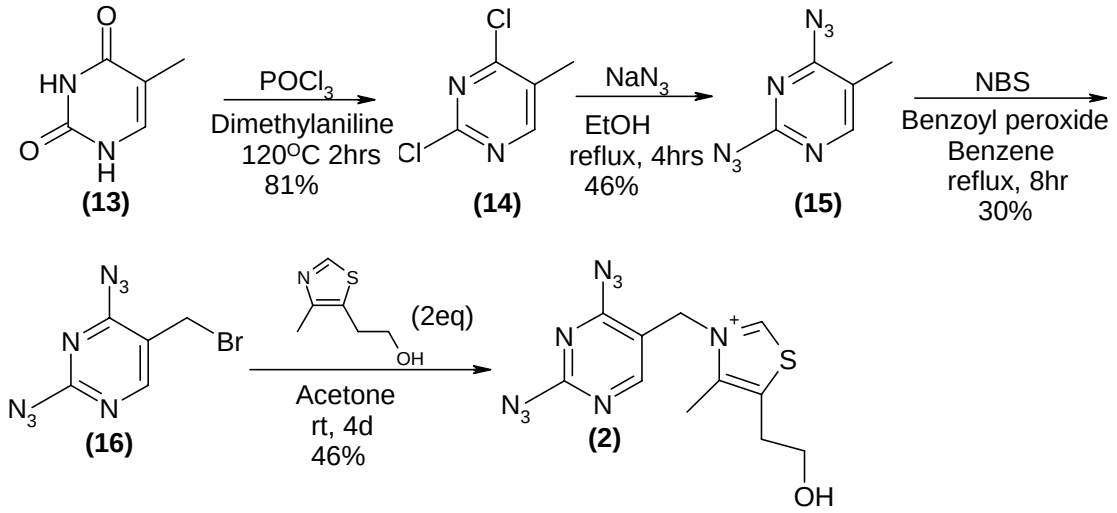

Figure 8.5 Synthesis of diazido(pyrimidine)thiamin (2).

The absorbance spectrum of (2) is shown below in figure 8.6. The diazido(pyrimidine)thiamin (2) had slight absorbance at wavelengths greater than 300 nm. This implies that the probe could be activated without causing significant photodamage to the protein.

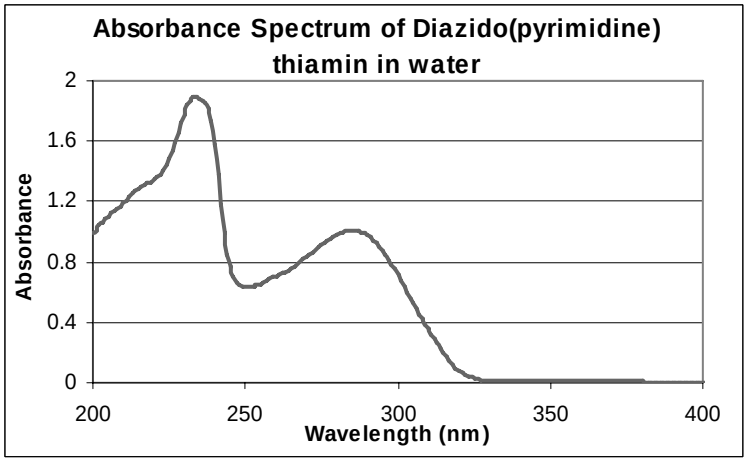

Figure 8.6 Absorbance spectrum of diazido(pyrimidine) thiamin (2).

An unanticipated effect of placing the azido group in the two and four positions of the pyrimidine ring that was found while synthesizing diazido(pyrimidine)thiamin was the tautomerization of the linear azide into the cyclic tetrazole. The NMR of 2,4-diazidopyrimidine (15) clearly showed the presence of two distinct species in an approximately one to one ratio. Previous work done by Wentrup confirms that in nitrogen containing heteroaromatic ring systems, such as pyrimidines, that have an azido group adjacent to the ring nitrogen, the azide substituent tautomerizes into a tetrazole ring, as seen in figure 8.7.[3]

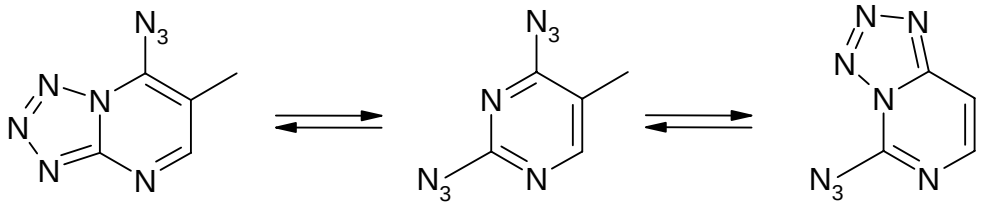

(15)

Figure 8.7 Two of the possible tautomerizations of the linear azide into the cyclic tetrazole.

This tautomerization is problematic for photoaffinity probes such as (1) and (2) due to the additional tetrazole ring that is formed. The tetrazole could prevent the photoaffinity probe from gaining access to the active site of enzymes. An additional problem presented by this tautomerization is the stability of the tetrazole to irradiation, though in diazido(pyrimidine)thiamin, it was suspected that one of the azido groups was in the tetrazole form and the other was in the linear, photoactive, form.

Diazido(pyrimidine)thiamine (2) did exist in two tautomeric forms, as demonstrated by NMR. It also proved to be highly unstable, and degraded in

a matter of days resulting in almost a complete loss of relevant proton signals. Despite the inherent instability of (2), it was produced in sufficient quantities to attempt the synthesis of the pyrophosphorylated compound, shown in figure 8.8.

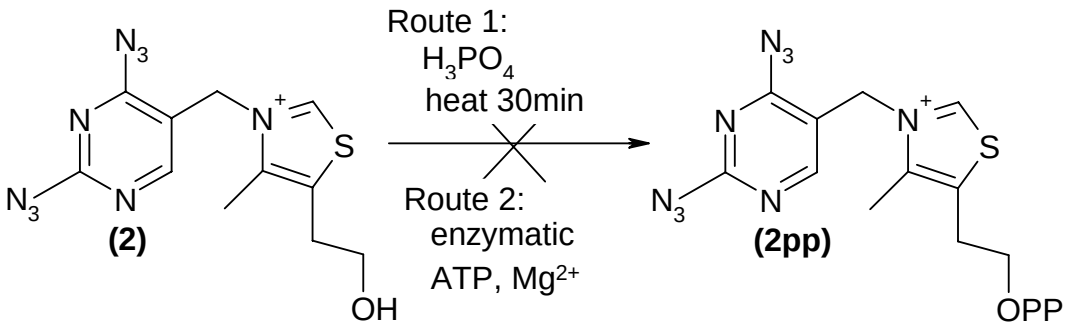

Figure 8.8 Two possible methods for the pyrophosphorylation of diazido(pyrimidine)thiamin. Route 1) chemical pyrophosphorylation with phosphoric acid and heat and route 2) enzymatic pyrophosphorylation with thiamin pyrophosphokinase and ATP.

The first method was chemical phosphorylation using phosphoric acid. Unfortunately, the conditions were too harsh, resulting in no product formation and decomposition of starting material. Additional pyrophosphorylation methods were attempted with no success. The second route employed the milder enzymatic pyrophosphorylation utilizing thiamin pyrophosphokinase. In this case, no product turnover was observed, presumably due to tautomerization into the cyclic tetrazole, which appended an additional ring that may have prevented access to the active site.

Although diazido(pyrimidine)thiamin (2) possesses a small amount of absorbance at wavelengths longer than 300 nm, the presence of the inactive

tetrazole tautomer, the failure to pyrophosphorylate, and the instability of the molecule deterred any further work with this compound. In addition, the synthesis of (1), though it could be accomplished, was not attempted due to the tetrazole tautomer that dominates in solution and the instability of the related diazido(pyrimidine)thiamin (2). Thus, the first generation of thiamin photoaffinity probes was shown to be poor candidates for use as proteome probes.

8.4 Design of generation 2 probes

The second generation of probes is based on the reaction of adamantanethione with cyclohexane. The excited thio-carbonyl group inserts into the carbon-hydrogen bond of cyclohexane, seen in figure 8.9.[4, 5] A number of other insertion reactions, both intermolecular and intramolecular, have been reported with thio-carbonyls activated by irradiation.[6]

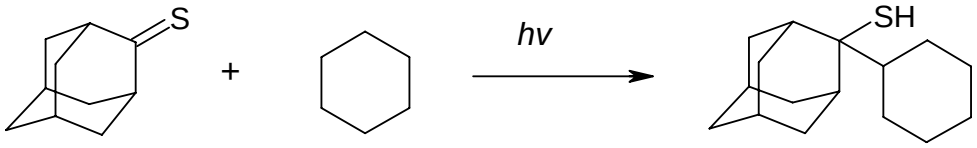

Figure 8.9 Insertion of an excited thio-carbonyl, adamantanethione, into the carbon-hydrogen bond of cyclohexane.

8.5 Synthesis of generation 2 probes

8.5.1 Synthesis of thio(pyrimidine)thiamin pyrophosphate

Thio(pyrimidine)thiamin pyrophosphate (3pp), is a close structural analog of oxythiamin pyrophosphate, which is a known thiamin antagonist (figure 8.10).[7] Given that oxythiamin pyrophosphate is able to penetrate the active site and act as an inhibitor of a variety of thiamin pyrophosphate utilizing

enzymes, thio(pyrimidine) thiamin pyrophosphate should also bind at the enzyme active site considering its structural similarity. The pyrophosphorylated form of thio(thiazole)thiamin (4) has previously been shown by Spencer to inhibit certain thiamin pyrophosphate utilizing enzymes, making the pyrophosphorylated versions of (3) and (4) good candidates as photoaffinity probes.[8]

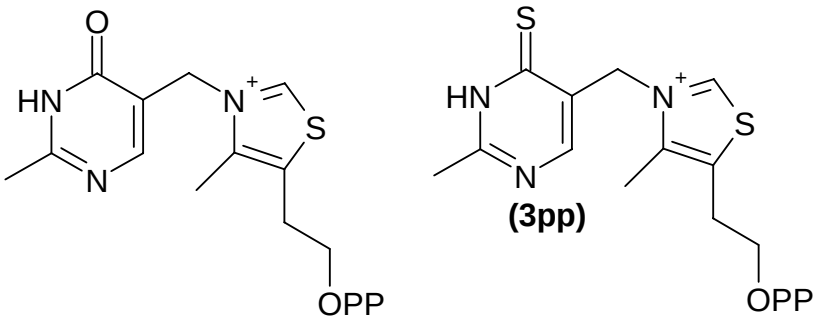

Figure 8.10 Structural similarity between oxythiamin and thio(pyrimidine) thiamin pyrophosphate.

The synthetic route to pyrophosphorylated thio(pyrimidine)thiamin (3pp) is outlined in figure 8.11.[9] The pyrimidine (9) is treated with excess phosphoryl chloride at refluxing temperatures to give the chloro-substituted pyrimidine (17) in 60% yield. The ester group is reduced to the alcohol with two equivalents of lithium aluminum hydride in 50% yield. 4-chloro-5-hydroxymethyl-2-methyl pyrimidine (18) can then be substituted with a nucleophilic species, allowing access to a variety of thiamin analogs substituted in the 4-position of the pyrimidine ring. In this case, sodium hydrogen sulfide is used as the nucleophile, and microwaves are used to promote the nucleophilic aromatic substitution, yielding (19) in 86% yield. The thio-pyrimidine (19) is subsequently treated with 33% hydrogen bromide in

acetic acid to give (20). Due to the lability of the methylbromide, no purification is performed and the compound is treated directly with the substituted thiazole to give thio(pyrimidine)thiamin (3) in 30% yield. The pyrophosphorylated analog (3pp) is made by treatment of thio(pyrimidine)thiamin with phosphoric acid.

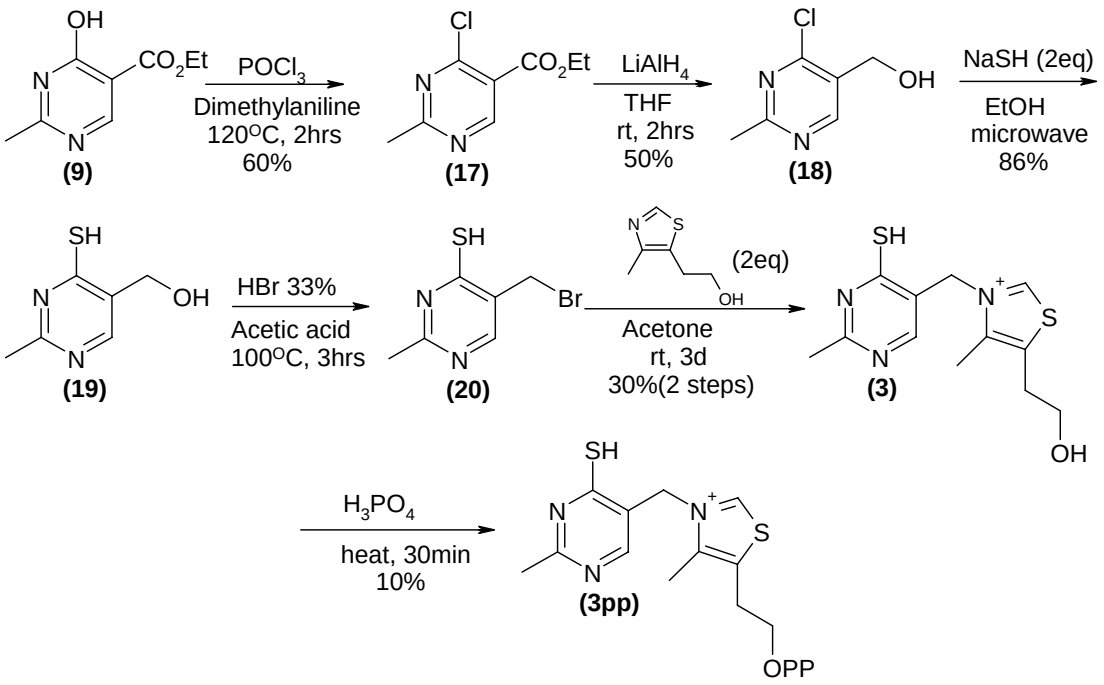

Figure 8.11 Synthesis of thio(pyrimidine)thiamin pyrophosphate (3pp).

The thio(pyrimidine)thiamin (3) tautomerizes between the thiol and thione species. The thiol form was the predominant in aqueous media, but when the dielectric constant of the solvent was lowered, the relative amount of thione tautomer present increased. This was demonstrated by the absorbance spectrum of thio(pyrimidine)thiamin (3) in water (ε =78.5), methanol (ε =32.6), and isopropanol (ε =18.3), figure 8.12.

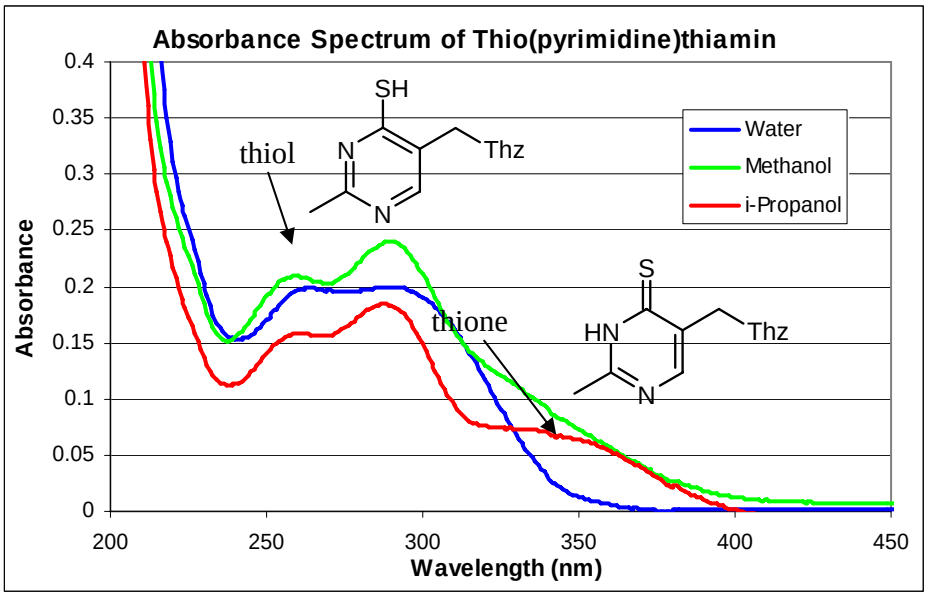

Figure 8.12 Absorbance spectrum of thio(pyrimidine)thiamin (3) in solvents of varying dielectric constant. The thiamin analog has some absorbance above 300 nm in water, but in isopropanol, there is significantly larger absorbance above 300 nm.

The spectra clearly showed that in solvents with lower polarity than water, the absorbance of the compound in the region of 350 nm increased. In water the compound existed primarily as the thiol tautomer, but clearly had significant absorbance at wavelengths greater than 300 nm.

Although it would have been ideal to incubate the photoaffinity label in isopropanol, where there was a large amount of absorbance greater than 300 nm, a protein would likely precipitate under these conditions. However, the enzyme active site could provide a micro-environment that is non-polar. It has been hypothesized that thiamin pyrophosphate exists in the active site of enzymes as the 1,4-iminopyrimidine tautomer.[10] This same mechanism could force the thiol/thione equilibrium to lie more in the direction of the thione tautomer for thio(pyrimidine)thiamin pyrophosphate.

The synthesized thio(pyrimidine)thiamin pyrophosphate acts as an inhibitor of the thiamin pyrophosphate utilizing enzyme α-ketoglutarate dehydrogenase. α-ketoglutarate dehydrogenase, a three subunit enzyme requiring five cofactors, converts α-ketoglutarate to the coenzyme A ester via decarboxylation of α-ketoglutarate, seen in figure 8.13.

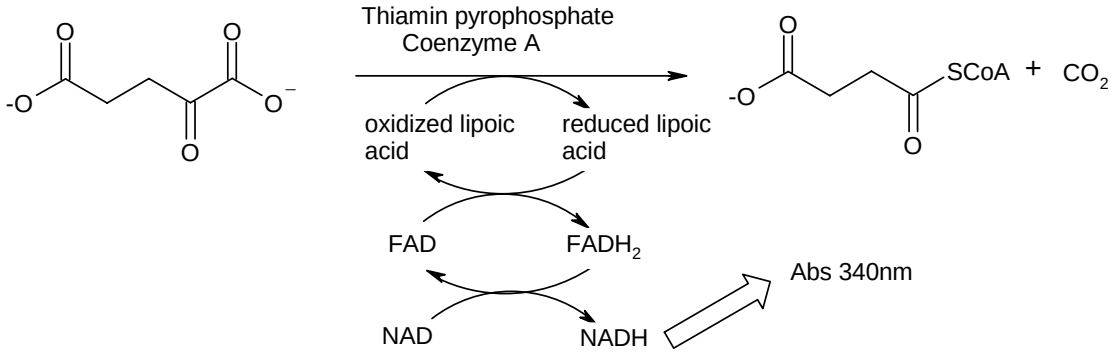

Figure 8.13 Reaction catalyzed by α-ketoglutarate dehydrogenase. α-ketoglutarate is decarboxylated with thiamin pyrophosphate, and in the presence of coenzyme A, lipoic acid is reduced. The lipoic acid is oxidized by FAD, generating $FADH_2$. This is oxidized by NAD, forming NADH, which absorbs at 340 nm.

Enzyme activity can be monitored by following the reduction of NAD to NADH, which absorbs at 340 nm. Figure 8.14 shows that when the enzyme was incubated with only thiamin pyrophosphate, the rate of conversion was approximately two and a half times faster than that of when the enzyme was incubated with thio(pyrimidine)thiamin pyrophosphate and thiamin pyrophosphate. It is likely that the thio(pyrimidine)thiamin pyrophosphate, a close structural analog of oxythiamin pyrophosphate, binds to the enzyme active site thereby decreasing its activity.

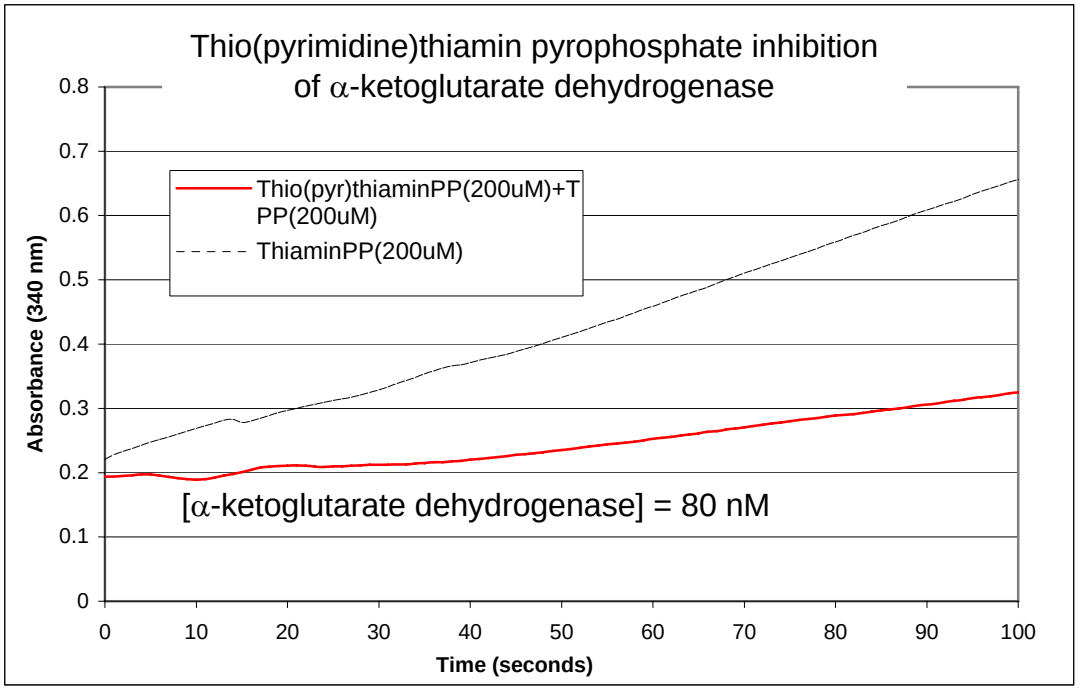

Figure 8.14 Activity assay of a-ketoglutarate dehydrogenase. The dotted line is the control, where α-ketoglutarate was incubated with thiamin pyrophosphate. The solid line is α-ketoglutarate incubated with both thiamin pyrophosphate and thio(pyrimidine)pyrophosphate. The rate of conversion in the control was about 2.5 times faster than when the analog was added.

8.5.2 Synthesis of thio(thiazole)thiamin pyrophosphate

Figure 8.15 shows the synthesis of pyrophosphorylated thio(thiazole)thiamin (4), established by Matsukawa in 1950.[5] Grewe diamine (21) was dissolved in ethanolic potassium hydroxide and then treated with 3-chloro-4-oxopentylacetate and carbon disulfide to yield (22) in 60% yield. Subsequent dehydration of (22) in 10% hydrochloric acid gave thio(thiazole)thiamin (4) in 70% yield. Pyrophosphorylation was carried out by heating (4) in phosphoric acid with 12% yield.

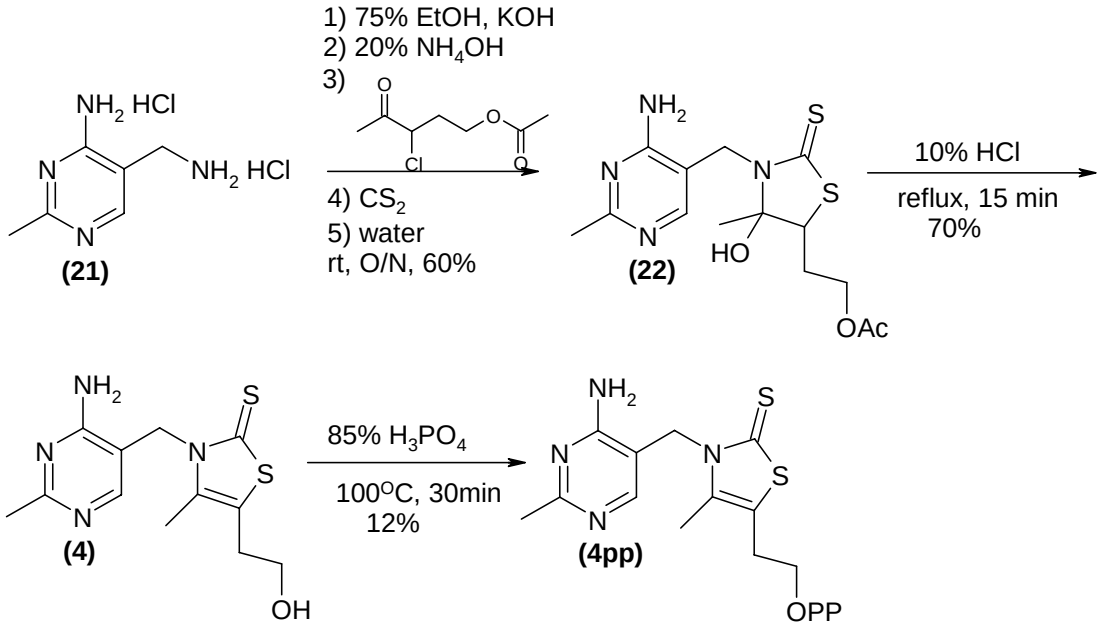

Figure 8.15 Synthesis of thio(thiazole)thiamin pyrophosphate.

Thio(thiazole)thiamin existed in the thione form and did not tautomerize. The absorbance spectrum, seen in figure 8.16, of the compound confirms this. There is a major peak with λ_{max} of 325 nm corresponding to the thione. If thio(pyrimidine)thiamin pyrophosphate (3^{PP}) or thio(thiazole)thiamin pyrophosphate (4^{PP}) was capable of labeling α-ketoglutarate dehydrogenase, it was expected that samples treated with the photoaffinity label and light would show a decreased rate of product turnover. The decreased activity would presumably result from the photoaffinity label forming a covalent adduct with the enzyme at the site where thiamin pyrophosphate would bind. In the case of covalent attachment, thiamin pyrophosphate would be prevented from entering the enzyme active site, and activity would not be restored by the addition of excess thiamin pyrophosphate.

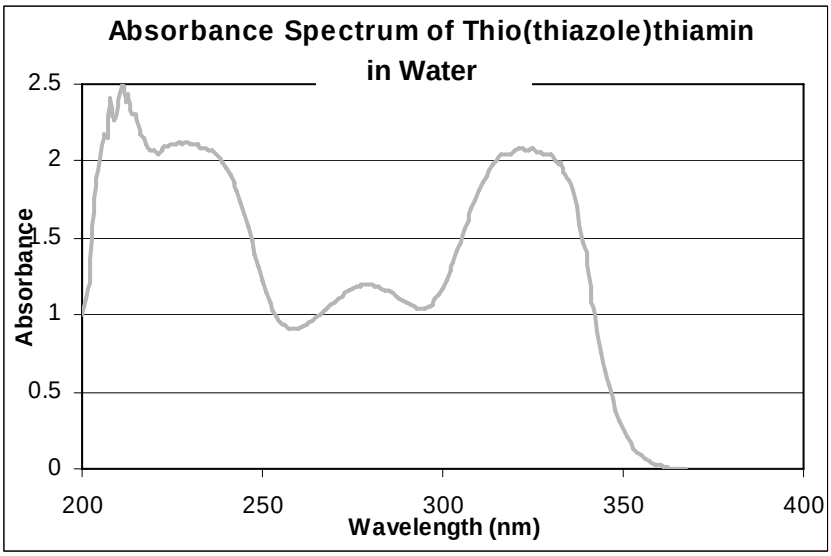

Figure 8.16 Absorbance spectrum of thio(thiazole) thiamin in water.

8.6 Testing of generation 2 probes

In order to determine if the photoaffinity probes could label α-ketoglutarate dehydrogenase, the activity assay described previously is used. The enzyme is incubated with the photoprobe thio(pyrimidine)thiamin pyrophosphate (3^{PP}) or thio(thiazole)thiamin pyrophosphate (4^{PP}) and irradiated with wavelengths of light greater than 300 nm in degassed buffer for varying amounts of time. It was determined experimentally, using 4-thio-pyrimidone as a model compound, that at least thirty to sixty minutes of irradiation was needed to observe measurable loss of the thione functionality. When α-ketoglutarate dehydrogenase was irradiated for thirty minutes, the rate of product formation was lowered to only 32% that of the control, which was α-ketoglutarate dehydrogenase that was not irradiated. Within sixty minutes of irradiation, the protein loses virtually all activity, with conversion rates less than 1% that of the control. This result indicates that the protein was inactivated without the

presence of the photoaffinity label. The inactivation by light alone could arise from the presence of the flavin cofactor in the protein, which also absorbed at wavelengths greater than 300 nm.

Another thiamin pyrophosphate utilizing enzyme that was more amenable to irradiation with near UV light, and preferably without any other cofactors, was needed in order to use activity assays to determine if the photoprobes could covalently label a protein. An alternative enzyme requiring only thiamin pyrophosphate as a cofactor is deoxy-D-xylulose-5-phosphate (DXP) synthase, which converts pyruvate and glyceraldehyde-3-phosphate to DXP via decarboxylation of pyruvate, seen in figure 8.17.

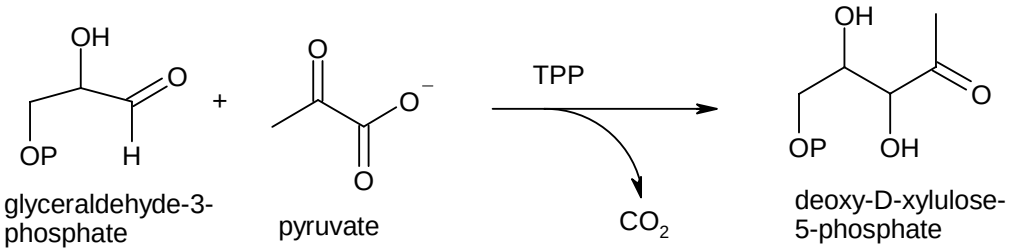

Figure 8.17 Conversion of glyceraldehydes-3-phosphate and pyruvate to deoxy-D-xyulose-5-phosphate (DXP) catalyzed by DXP synthase.

The activity of this enzyme cannot be monitored with UV-Vis spectrophotometrically, but product formation can be measured by NMR. DXP synthase loses about 60% of its activity after thirty minutes of irradiation with light greater than 300 nm without the presence of the photoaffinity probe. There is complete loss of activity within ninety minutes. Due to the loss of

activity in the proteins tested, an alternative approach to determine if the photoaffinity probes are labeling the protein was used.

ESI-FTMS, electrospray ionization – Fourier transform mass spectrometry, can be used to detect one dalton shifts in the molecular weight of proteins, so covalent attachment of thio(pyrimidine/thiazole)thiamin or their pyrophosphate analogs should be readily identified. A major limitation with this technique arises with analysis of high molecular weight proteins. Large molecular weight proteins, greater than 45 kDa, cannot be sprayed efficiently and therefore it is extremely difficult to get a signal with larger proteins. A characteristic that unites thiamin pyrophosphate utilizing proteins aside from the use of the same cofactor is their high molecular weight, with the smallest *E. coli* TPP-utilizing protein being ~60 kDa, too large for use with ESI-FTMS.

In order to avoid using high molecular weight proteins mouse thiamin pyrophosphokinase was utilized, which is a 29kDa protein. Thiamin pyrophosphokinase uses adenosine triphosphate to pyrophosphorylate the substrate thiamin, figure 8.18.

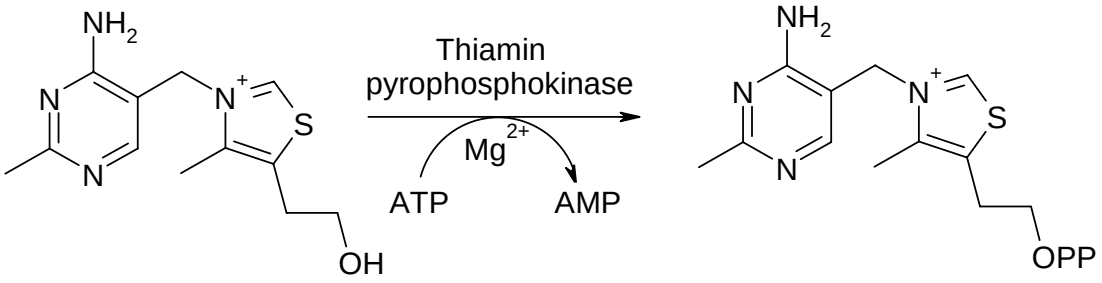

Figure 8.18 The ATP dependent pyrophosphorylation of thiamin to thiamin pyrophosphate by mouse thiamin pyrophosphokinse.

Due to its smaller size, thiamin pyrophosphokinase can be easily sprayed and analyzed by ESI-FTMS. In addition to its small size, the protein can also take thiamin analogs as substrates, making it an ideal candidate to determine if the synthesized probes can indeed covalently modify a protein. Thiamin pyrophosphokinase was subjected to ninety minutes of irradiation with wavelengths of light greater than 300 nm in the presence of either thio(pyrimidine)thiamin (3) or thio(thiazole)thiamin (4). Controls were run where the protein was not irradiated and no label was present, and where the protein was irradiated with light in the absence of any label. The results, indicated that no labeling occurred, are shown in figure 8.19. The charge state of the protein is given, either +28 or +27, and the pyrophosphate adducts of each of the charge states are indicated. The arrows in the figure specify where peaks corresponding to the labeled protein should appear.

The ESI-FTMS data clearly shows that irradiation of the enzyme in the presence of either of the two synthesized photoaffinity probes gave the same spectrum as the control, in which the enzyme was irradiated without any probe. No peak is present corresponding to the mass where a covalent adduct would occur. Thio(pyrimidine)thiamin (3) and thio(thiazole)thiamin (4) were ineffective photoaffinity probes since they did not covalently modify thiamin pyrophosphokinase.

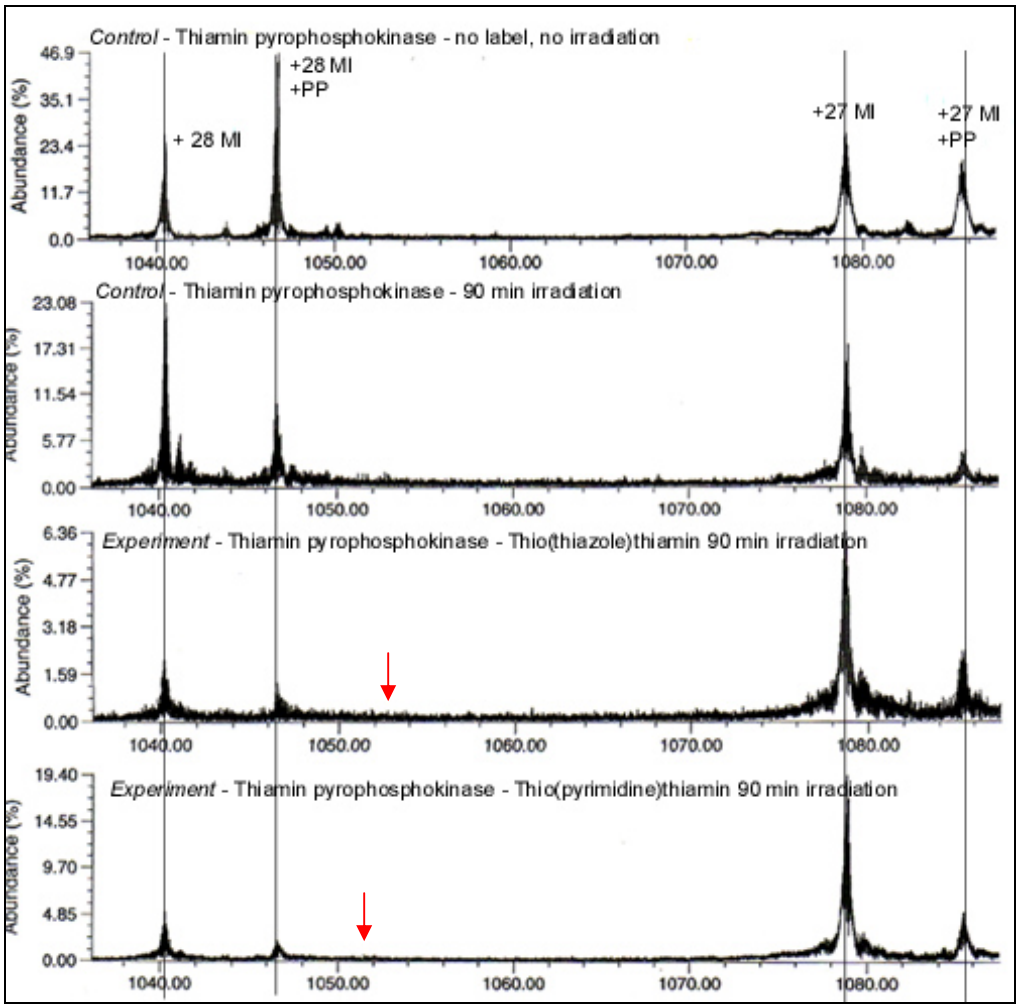

Figure 8.19 ESI-FTMS of thiamin pyrophosphokinase when irradiated in the presence of photoaffinity label. There is no peak shift as would be expected if the probes were covalently modifying the protein. Arrows indicate the site where the labeled protein peaks should occur (obtained by Huili Zhai).

8.7 Conclusions

Generation 1 and 2 analogs were not amenable for use as probes to detect thiamin pyrophosphate utilizing enzymes. In the case of generation 1 probes, the molecules were too unstable to be pyrophosphorylated, and would degraded quickly in solution. Although the generation 2 probes were stable

and could be pyrophosphorylated, they were not photo-labile enough to be used as proteomics probes.

8.8 Materials and procedures

All materials were obtained from Sigma-Aldrich unless otherwise noted. NMR spectra were obtained on a Mercury BB 300MHz NMR.

8.8.1 Synthesis of 5-carboxylic acid ethyl ester-4-hydroxyl-2-methyl-pyrimidine (9)

Into a round bottom flask is weighed 240 mg of sodium. 10.1 mL of absolute ethanol is added and stirred until all of the sodium has reacted. To the freshly prepared ethoxide/ethanol solution is added 1 g of acetamidine. This is stirred for 30 min, then filtered to remove precipitated NaCl. To the clear filtrate is added 2.14mL of diethyl ethoxymethylene malonoate. The mixture is refluxed for 3 hours then allowed to sit overnight at room temperature. The product is filtered and the solid is collected and dried *in vacuo*. Final product is yellow-white solid (note that this can be purified by flash in 70:30 chloroform:methanol to yield a white solid). NMR 300MHz in $CDCl_3$ δ(8.701, s, 1H) δ(4.397-4.327, quar, 2H) δ(2.579, s, 3H) δ(1.394-1.348, s, 3H). Yield: 60%

8.8.2 Synthesis of 4-hydroxy-5-hydroxymethyl-2-methyl-pyrimidine (10)

Into round bottom flask is placed 80 mg of lithium aluminum hydride (~3x molar excess of hydride). The round bottom is then purged with argon and 5 mL of anhydrous tetrahydrofuran is added. In a separate vial, 250 mg of 5-carboxylic acid ethyl ester-4-hydroxyl-2-methyl-pyrimidine is dissolved in ~20 mL of dry tetrahydrofuran. Under the positive pressure of argon, the

solution of pyrimidine is added by syringe slowly to the lithium aluminum hydride/tetrahydrofuran solution. The reaction is allowed to stir for 2 hrs. The resulting suspension is quenched with water and filtered through a small plug of fluorisil. The fluorisil is then washed with methanol and the solvent removed *in vacuo* to yield a white powder. NMR 300MHz in D_2O δ(7.860, s, 1H) δ(4.413, s, 2H) δ(2.339, s, 3H) δ(1.394-1.348, s, 3H). Yield: quantitative

8.8.3 Synthesis of 4-chloro-5-chloromethyl-2-methyl-pyrimidine (11)

310mg of 4-hydroxy-5-hydroxymethyl-2-methyl-pyrimidine is weighed into a round bottom flask equipped with a stir bar. To this 620 μL of dimethylaniline is added. (All subsequent steps are carried out under argon). With stirring, 2.5 mL of distilled phosphoryl chloride is slowly added. The mixture is heated at 120-130 °C for 2 hrs. After the reaction has cooled to room temperature, excess phosphoryl chloride is distilled off under aspirator pressure. To the remaining residue, ice is slowly added. This is then extracted 7-10x with 5 mL of ether. The ether layer is washed with 5% $NaHCO_3$ and dried over $MgSO_4$, filtered, and solvent removed *in vacuo*. The product is purified by flash chromatography using 3:1 hexanes:ethyl acetate as the solvent to yield a yellow oil. NMR 300MHz in $CDCl_3$ δ(8.628, s, 1H) δ(4.621, s, 2H) δ(2.718, s, 3H) Yield: 106 mg (30%)

8.8.4 Synthesis of 4-chloro(pyrimidine)thiamin (12)

325 mg of 4-chloro-5-chloromethyl-2-methyl pyrimidine is dissolved in 1.5 mL of dry acetone. To the solution is added 221 μL of thiazole and 32.5 mg of sodium iodide. The reaction is stirred at room temperature for seven days. The acetone is then removed *in vacuo* and the remaining solid is dissolved in

distilled water. The product is purified on an amberlite CG-50 cation exchange column. The column is washed first with 1 M NaOH, then distilled water, and finally with 1 M HCl. The column is washed again with distilled water until the eluate is neutral. After loading the crude sample onto the column, the starting materials are eluted with 0.001 M HCl. The product is eluted with 0.1 M HCl, and the fractions with product are pooled and lyophilized to give a light yellow solid. ESI mw = 284.8; NMR 300MHz in D_2O δ(9.593, s, 1H) δ(8.016, s, 1H) δ(5.259, s, 2H) δ(3.675-3.636, t, 2H) δ(2.965-2.927, t, 2H) δ(2.343, s, 3H) δ(2.327, s, 3H) Yield: 253mg (43%)

8.8.5 Synthesis of 2,4-dichloro-5-methyl pyrimidine (14)

Into a round bottom flask is weighed 2.5 g thymine. The round bottom is equipped with a stir bar and 2 mL of dimethylaniline is added. The vessel is purged with argon and 12 mL of phosphoryl chloride (distilled) is added with stirring. The flask is then equipped with a reflux condenser and the reaction refluxed at 120 – 130 °C for 2 hrs. After cooling to room temperature, excess phosphoryl chloride is removed under aspirator pressure. Ice is slowly added to quench the remaining phosphoryl chloride. This is extracted with ether, and the combined organic layers are washed with 5% $NaHCO_3$, dried over $MgSO_4$, filtered, and the solvent removed *in vacuo*. The residue is purified by flash chromatography with 3:1 hexanes:ethyl acetate to give a yellow oil. NMR 300MHz in $CDCl_3$ δ(8.400, s, 1H) δ(2.341, s, 3H) Yield: 2.6mg (81%)

8.8.6 Synthesis of 2,4-diazido-5-methyl pyrimidine (15)

1 g of 2,4-dichloro-5-methyl pyrimidine is weighed into a round bottom flask. To this is added 1.6 g of sodium azide and 40 mL of absolute ethanol. With

stirring, the reaction is refluxed for 4 hrs. The mixture is cooled to room temperature and the solvent removed *in vacuo*. The solid residue is dissolved in water and the product extracted into chloroform. The combined organic layers are dried with $MgSO_4$ and filtered. The chloroform is removed *in vacuo* to yield a light yellow solid. NMR 300MHz in $CDCl_3$ δ(8.666, s, 0.76H) δ(8.191, s, 1H) δ(2.293-2.297, d, 2.4H) δ(2.081, s, 3H) Note: two species are present, arising from the tautomers Yield: 500 mg (46%)

8.8.7 Synthesis of 5-bromomethyl-2,4-diazido pyrimidine (16)

Into an oven dried round bottom flask is weighed 54 mg of 2,4-diazido-5-methyl pyrimidine. The reaction is carried out under reduced light. Under the positive pressure of argon, 2.5 mL of anhydrous benzene is added. The mixture is refluxed for 30 min. To the hot solution, 54 mg of N-bromosuccinimide and 18 mg of benzoyl peroxide is added, and refluxing is continued for 8 hrs. The solvent is removed *in vacuo*, and the residue is dissolved in water and extracted with chloroform. The combined organic layers are dried with $MgSO_4$, filtered, and the solvent is removed *in vacuo*. The product is purified via flash chromatography with 4:1 hexanes:ethyl acetate to give a light yellow solid. NMR 300MHz in $CDCl_3$ δ(8.405, s, 1H) δ(4.330, s, 2H) Yield: 23 mg (30%)

8.8.8 Synthesis of 2,4-diazido(pyrimidine)thiamin (2)

Note: the reaction and purification are carried out with reduced light. To 6 mg of 2,4-diazido-5-chloromethyl pyrimidine is added 500uL of dry acetone. 7.1 uL of the substituted thiazole is added. The reaction is stirred 4 days at room temperature. The acetone is removed *in vacuo* and the residue is dissolved in

water and the starting materials are extracted exhaustively into ethyl acetate. The water is removed *in vacuo* to yield a light yellow solid. ESI mw = 318.4; NMR 300MHz in D_2O δ(8.550, s, 1H) δ(8.346, s, 1H) δ(5.565, s, 2H) δ(5.338, s, 2H) δ(3.650-3.571, m, 2H) δ(2.950-2.921, t, 2.1H) δ(2.353, s, 3H) δ(2.298, s, 1H) Note: two species are present, arising from the tautomers and there is some contaminating substituted thiazole. Yield: 6.6 mg (50%)

8.8.9 Synthesis of 5-carboxylic acid ethyl ester-4-chloro-2-methyl-pyrimidine (17)

Into an oven dry round bottom flask is weighed 500 mg of 4-hydroxy-5-carboxylic acid ethyl ester-2-methyl pyrimidine. To this is added 312 μL of dimethylaniline and 7 mL of distilled phosphoryl chloride under argon. The reaction is heated at 120 ºC for 55 min and then cooled to room temperature. Excess phosphoryl chloride is distilled under aspirator pressure and ice water is added to the remaining residue to react with any remaining phosphoryl chloride. The product is extracted with ether. The combined organic layers are washed with 5% $NaHCO_3$ and dried with $MgSO_4$. After filtering, the solvent is removed *in vacuo*. The product is purified by flash chromatography with chloroform to give a yellow oil. NMR 300MHz in $CDCl_3$ δ(9.005, s, 1H) δ(4.440-4.369, q, 2H) δ(2.740, s, 3H) δ(1.412-1.365, t, 3H) Yield: 332mg (60%)

8.8.10 Synthesis of 4-chloro-5-hydroxymethyl-2-methyl-pyrimidine (18)

100 mg of 5-carboxylic acid ethyl ester-4-chloro-2-methyl-pyrimidine is dissolved in 7 mL of dry ether and the solution is cooled to 0 ºC in an ice bath. Slowly, 58mg of lithium aluminum hydride is added and the reaction is stirred

an additional 15 min, keeping the temperature at 0 ºC. The reaction is quenched with 10% NH_4Cl and the solid precipitate is filtered and washed with water. The solvent is removed *in vacuo*. The product is purified by flash chromatography with 95:5 chloroform:methanol to yield a light yellow solid. NMR 300MHz in $CDCl_3$ δ(8.687, s, 1H) δ(4.791, s, 2H) δ(2.721, s, 3H) δ(2.2, br s, 1H) Yield: 40mg (51%)

8.8.11 Synthesis of 5-hydroxymethyl-2-methyl-4-thio-pyrimidine (19)

310 mg of 4-chloro-5-hydroxymethyl-2-methyl-pyrimidine is dissolved in 6 mL of ethanol. To this is added 400 mg of sodium hydrogen sulfide (56% pure). The reaction is carried out in the microwave (10% power) for 55 min. The solvent is removed *in vacuo* and the product is purified by flash chromatography with 90:10 chloroform:methanol to yield a light yellow solid. NMR 300MHz in $CDCl_3$ δ(7.841, s, 1H) δ(4.476, s, 2H) δ(2.374, s, 3H) Yield: 250mg (83%)

8.8.12 Synthesis of 5-bromomethyl-2-methyl-4-thio-pyrimidine (20)

4.3 mg of 5-hydroxymethyl-2-methyl-4-thio-pyrimidine is placed into a 1 mL reaction vial. This is dissolved in 150 μL of 33% HBr in acetic acid. The reaction vial is sealed and heated at 100 ºC for 3 hrs. The reaction is cooled and stirred over night at room temperature. The acetic acid is removed *in vacuo*. The crude residue is not purified further due to the labiality of the bromide.

8.8.13 Synthesis of thio(pyrimidine)thiamin (3)

The crude 5-bromomethyl-2-methyl-4-thio-pyrimidine is dissolved in 500 μL dry acetone and 2 μL of 4-methyl-5-thiazole ethanol is added. The reaction is stirred at room temperature for 3 days. The acetone is removed and the residue is dissolved in water. The starting materials are extracted exhaustively into ethyl acetate. The water layer is lyophilized to give a light yellow solid. ESI mw = 283.1; NMR 300MHz in D_2O δ(9.493, s, 1H) δ(7.950, s, 1H) δ(5.392, s, 2H) δ(3.671 t, 2H) δ(2.970, t, 2H) δ(2.384, s, 3H) δ(2.368, s, 3H) Yield: 2 mg (30%) – for 2 steps

8.8.14 Synthesis of thio(thiazole)thiamin (4)

Note that the order of addition of reagents is critical. 1.045 g of grewe diamine and 560 mg of KOH are dissolved in 13.2 mL of 75% ethanol. To the solution is added 1.13 mL of 20% NH_4OH and then 1.37 mL of 3-chloro-4-oxopentylacetate. 78.5 μL of carbon disulfide is added and stirred until completely dispersed. 2.8 mL of water is then added and the solution is stirred overnight at room temperature. The precipitate is filtered off and washed with water. The solid is then dissolved in 30 mL of 10% HCl and refluxed for 15 min. The solution is cooled to room temperature and neutralized with 10% NaOH. The resulting precipitate is filtered and washed with water to give a light yellow solid. NMR 300MHz in D_2O δ(7.299, s, 1H) δ(5.170, s, 2H) δ(3.608-3.569 t, 2H) δ(2.703-2.723, t, 2H) δ(2.381, s, 3H) δ(2.042, s, 3H) Yield: 956 mg (58%)

8.8.15 General method for chemical pyrophosphorylation

Into a vial is placed 1 mL of 85% *o*-phosphoric acid. This is heated with an open flame until the solution is slightly cloudy (on the sides of the flask) and a faint smoke is observed. The solution is cooled to room temperature to give a clear syrupy liquid. 200 mg of thiamin(analog) is added with stirring (glass rod) and heated to 100 ºC. The suspension is stirred continuously for 15-30 min, then cooled to room temperature. 800 μL water mixed with 200 μL phosphoric acid is added to the cooled solution and stirred for 2 hrs. The solution was then neutralized with 6 M NaOH and applied to a Dowex 1x4 200-400 anion exchange column. Products were eluted with 0.001 M HCl. Fractions containing thiamin pyrophosphate analogs are then pooled and lyophilized.

8.9 References

1. Czarnecki, J.J., M.S. Abbott, and B.R. Selman, *Photoaffinity Labeling with 2-azidoadenosine diphosphate of a Tight Nucleotide Binding Site on Chloroplast Coupling Factor 1.* Proceedings of the National Academy of Sciences of the United States of America, 1982. **79**(24): p. 7744-7748.

2. Haley, B.E., *Development and utilization of 8-azidopurine nucleotide photoaffinity probes.* Federation Proceedings, 1983. **42**: p. 2831-2936.

3. Wentrup, C., *Hetarylnitrenes—II : Azido/tetrazoloazine tautomerisation, and evidence for nitrene formation in the gas-phase.* Tetrahedron, 1970. **26**(21): p. 4969-4983.

4. Schonberg, A. and M. Mamluk, *Photo-dimerisierung des diphenylcyclopropenthions zu einem thiophenderivat.* Tetrahedron Letters, 1971. **12**(52): p. 4993-1994.

5. de Mayo, P., *Photochemical synthesis. 62. Thione photochemistry, and the chemistry of the S2 state.* Accounts of Chemical Research, 1976. **9**(2): p. 52-59.

6. Favre, A., *4-Thiouridine as an Intrinsic Photoaffinity Probe of Nucleic Acid Structure and Interactions*, in *Bioorganic Photochemistry: Photochemistry and the Nucleic Acids*, H. Morrison, Editor. 1990, John Wiley & Sons, Inc.: New York.

7. McCormick, D.B. and L.D. Wright, *Vitamins and Coenzymes Part A*. Methods in Enzymology. Vol. XVIII. 1970, New York: Academic Press.

8. Nemeria, N., et al., *Systematic study of the six cysteines of the E1 subunit of the pyruvate dehydrogenase multienzyme complex from Escherichia coli: none is essential for activity.* Biochemistry, 1998. **37**(3): p. 911-922.

9. Schellenberger, A. and K. Winter, *On the toxic properties of N-methyltoxopyrimidine.* Hoppe Seylers Z Physiol Chem, 1960. **322**: p. 173-176.

10. Jordan, F., et al., *Dual Catalytic Apparatus of the Thiamin Diphosphate Coenzyme: Acid-Base via the 1',4'-Iminopyrimidine Tautomer along with Its Electrophilic Role.* Journal of the American Chemical Society, 2003. **125**(42): p. 12732-12738.

CHAPTER 9:

DESIGN, SYNTHESIS, AND TESTING OF GENERATION 3 PROBES

9.1 Introduction

Like the generation 1 probes, the generation 3 probes incorporate an azide group, but the pyrimidine ring is replaced by a benzene ring. Lack of nitrogen in the ring prevents the azido-tetrazole tautomerization that was found in generation 1 probes. In order to shift the UV-absorbance of the compound above 300 nm, a nitro group was added (figure 9.1).

Generation 3 Photoaffinity Labels

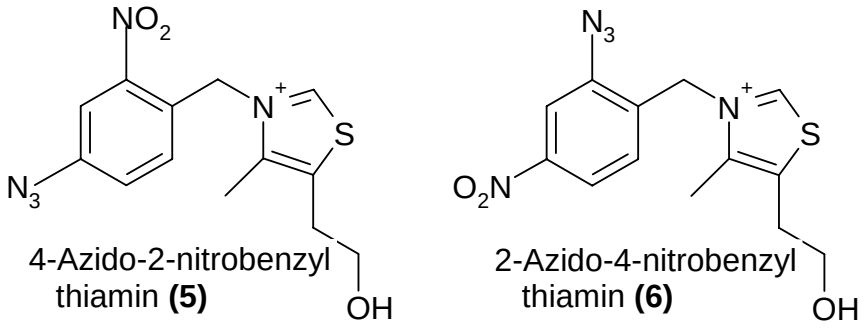

Figure 9.1 Structures of the generation 3 probes, 4-azido-2-nitrobenzyl thiamin and 2-azido-4-nitrobenzyl thiamin.

9.2 Design of generation 3 probes

Generation 3 photoaffinity probes are based loosely on the previously developed thiamin photoaffinity probe 4-azido-2-nitrobenzoylthiamin, figure 9.2. The probe was used to identify a thiamin-binding component in yeast plasma membrane responsible for thiamin transport into the cell.[1]

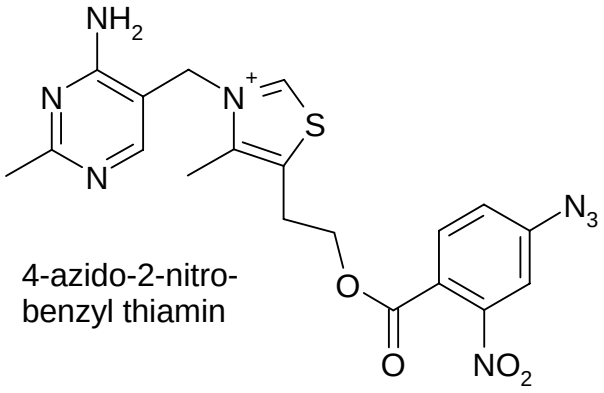

4-azido-2-nitro-
benzyl thiamin

Figure 9.2 Structure of 4-azido-2-nitrobenzylthiamin, which was used as a photoaffinity probe to detect thiamin binding component in yeast plasma membrane.

Although this probe was successful, it would not be amenable to studying thiamin pyrophosphate utilizing enzymes since the photoactive moiety of the molecule replaces the pyrophosphate group. The presence of the pyrophosphate group is essential for binding in thiamin pyrophosphate utilizing enzymes.

A significant difference in generation 3 probes is the replacement of the substituted pyrimidine ring found in generations 1 and 2, with a substituted benzene ring. Generations 1 and 2 photoaffinity probes were designed to closely mimic the structure of thiamin itself with the hope that the photoaffinity probes could easily gain access to the enzyme active site. Although generation 3 probes lack the pyrimidine nitrogens, it has been shown that when the pyrimidine ring of thiamin pyrophosphate is replaced by a benzene ring, it can act as a competitive binder in the thiamin pyrophosphate utilizing enzyme pyruvate decarboxylase.[2]

This major perturbation is expected to have an effect on the binding efficiency of the photoprobe. However, the majority of the binding specificity of thiamin comes from the positive charge on the nitrogen and the pyrophosphate group on the thiazolium ring.[3] The pyrophosphate analogs of photoprobes (5) and (6) should offer a suitable handle for binding, provided that the nitro and azido groups on the benzene ring can fit into the enzyme active site. Both of the substituents are required for the probe; the azido group is the photolabile functionality and the nitro group shifts the absorbance of the probe to useful wavelengths and decreases the likelihood of intramolecular rearrangement.

9.3 Synthesis of generation 3 probes

The synthesis of both 4-azido-2-nitrobenzyl thiamin (5) and 2-azido-4-nitrobenzyl thiamin (6) were carried out identically, as seen in figure 9.3 below.

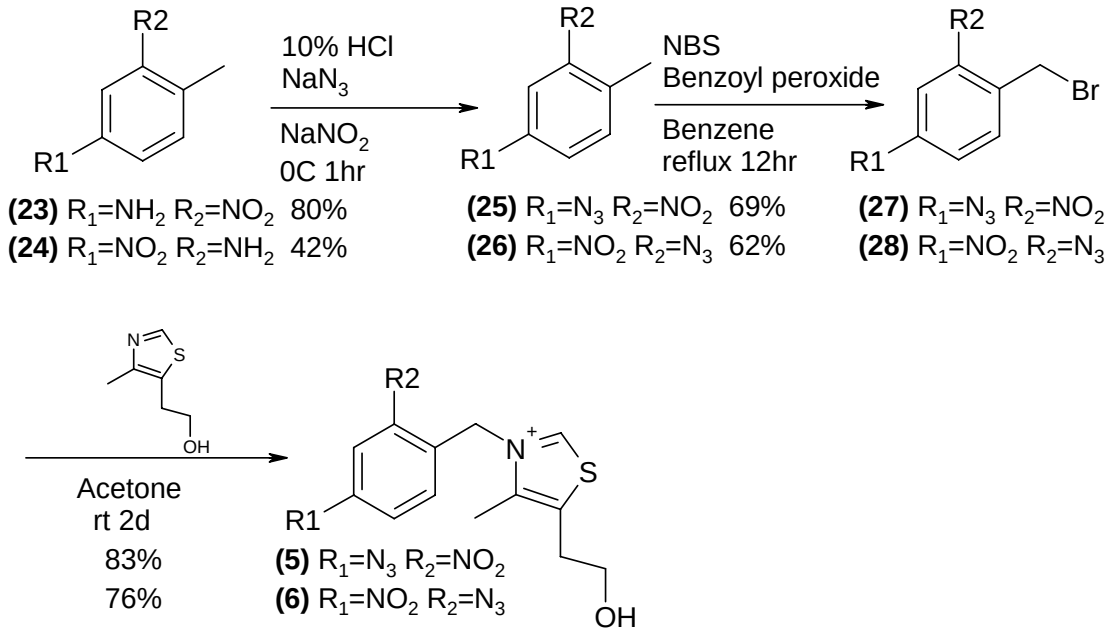

Figure 9.3 Synthesis of 4-azido-2-nitrobenzyl thiamin (5) and 2-azido-4-nitrobenzyl thiamin (6).

The appropriately substituted aniline, (23) or (24), was converted to the azido group by diazotization with nitrous acid followed by displacement of nitrogen (N_2) with sodium azide in 80% and 42% yield respectively. The bromomethyl compound was generated through the radical bromination of (25) and (26) with N-bromosuccinimide and benzoyl peroxide in 69% (27) and 62% (28) yield. Thiamin analogs (5) and (6) were generated by displacement of bromide by the thiazolium ring with yields of 83% and 76%.

Prior to attempting pyrophosphorylation of the molecules, 4-azido-2-nitrobenzyl thiamin (5) was chosen to determine if this generation of probes could label thiamin pyrophosphokinase, as was attempted with the generation 2 probes. The absorbance spectrum of (5) is seen in figure 9.4, clearly showing absorbance above 300 nm.

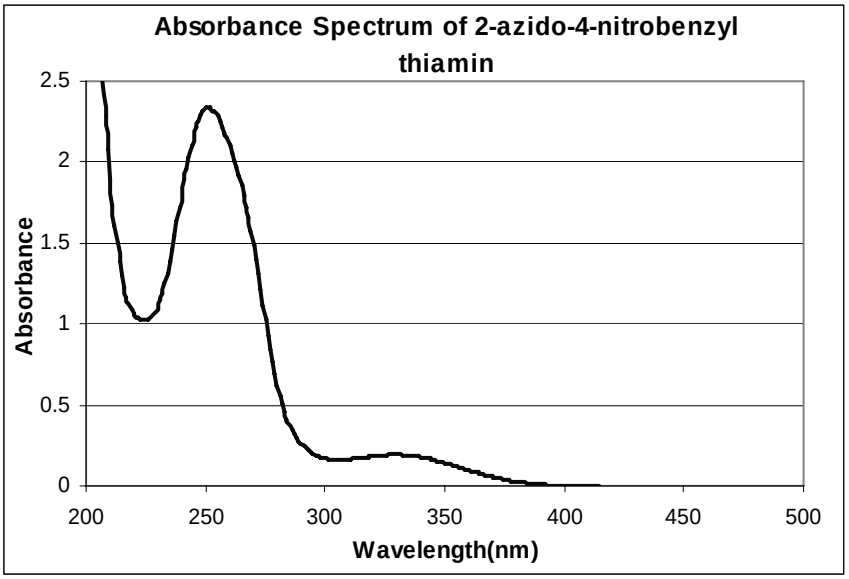

Figure 9.4 Absorbance spectrum of 2-azido-4-nitrobenzylthiamin in water.

Varying concentrations of photoprobe (5) were incubated with thiamin pyrophosphokinase and irradiated with light greater than 300 nm for one hour. The irradiated proteins were run on an SDS-PAGE gel, seen in figure 9.5.

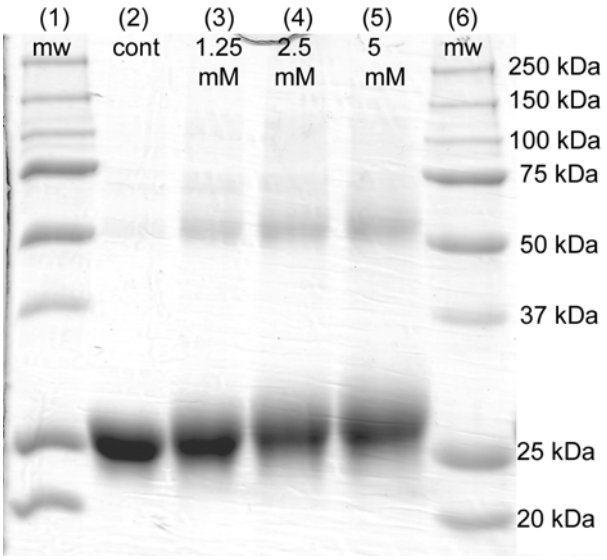

Figure 9.5 SDS PAGE gel of thiamin pyrophosphate kinase (TPK) irradiated with varying concentrations of 4-azido-2-nitrobenzyl thiamin. Lane 1 – molecular weight markers; Lane 2 – TPK + light; Lane 3 – TPK + 1.25 mM 4-azido-2-nitrobenzyl thiamin + light; Lane 4 – TPK + 2.5 mM 4-azido-2-nitrobenzyl thiamin + light; Lane 5 – TPK + 5 mM 4-azido-2-nitrobenzyl thiamin + light; Lane 6 – molecular weight markers (kDa).

The gel clearly shows that the band at ~25 kDa, thiamin pyrophosphokinase, shifted upwards as the concentration of photoprobe used in irradiation was increased. The shift was likely due to decreased mobility of the protein through the gel resulting from increased molecular weight due to covalent attachment of the photoprobe. The large shift suggests that multiple covalent adducts were being formed in a non-specific fashion. An additional band at ~50 kDa was observed that increases in intensity as the amount of photoprobe

increases. Since TPK exists as a dimer in solution, the appearance of this band was not unexpected.

9.3.1 Enzymatic pyrophosphorylation of generation 3 probes

Both 4-azido-2-nitrobenzyl thiamin (5) and 2-azido-4-nitrobenzyl thiamin (6) were very efficiently pyrophosphorylated enzymatically by yeast thiamin pyrophosphokinase, figure 9.6. This was significant because it allowed for a radioactive pyrophosphate group to be added to the photoprobes very cleanly, which was important for detecting if labeling was occurring. This means that the photoaffinity analogs were binding at the enzyme active site of at least this particular enzyme. The pyrophosphorylation reaction of the thiamin analogs was actually more efficient than that of thiamin.

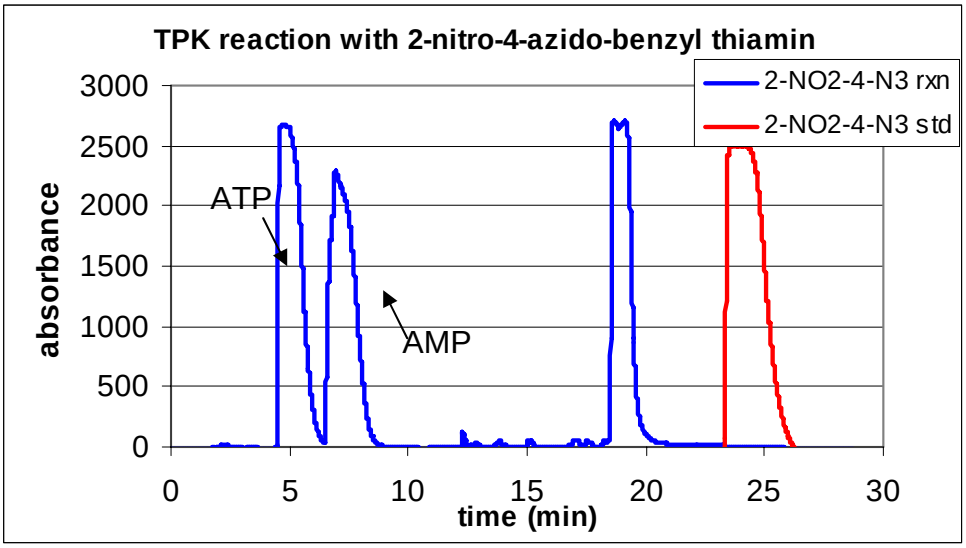

Figure 9.6 Enzymatic pyrophosphorylation of the generation 3 probes by mouse thiamin pyrophosphokinase, ATP, and Mg^{2+}. The pyrophosphorylated species elutes at 19.5 min (blue) and the 4-azido-2-nitrobenzylthiamin elutes at 25 min (red).

9.4 Testing of generation 3 probes

9.4.1 Inhibition of α-ketoglutarate dehydrogenase

Although the generation 3 photoprobes did not exhibit any antibiotic activity (data not shown), this could simply mean that the *E. coli* were not taking up the probes from the media, but that they could still get into the active site of TPP utilizing enzymes and be useful as photoaffinity probes. Thiamin pyrophosphate is usually very tightly bound to the active site of the enzyme that uses it. In order for any of the pyrophosphorylated analogs (5pp or 6pp) to inhibit the proteins, the TPP must be displaced from the enzyme active site (TPP must dissociate and the analog must enter).

To test if either of the generation 3 probes could act as an inhibitor of TPP utilizing enzymes, we looked at inhibition of α-ketoglutarate dehydrogenase. This was the easiest enzyme to assay since it was commercially available and we could monitor its activity spectrophotometrically. When α-ketoglutarate dehydrogenase was incubated with 2-azido-4-nitrobenzyl thiamin pyrophosphate (6pp), no inhibition was seen. Although this analog could be pyrophosphorylated by thiamin pyrophosphokinase, it could not bind to the active site of TPP utilizing enzymes.

When 4-azido-2-nitrobenzyl thiamin pyrophosphate (5pp) was incubated with α-ketoglutarate dehydrogenase, a concentration dependent decrease in the initial reaction rates was seen. As the amount of inhibitor was increased, the reaction rate decreased (figure 9.7). Pre-incubation of the enzyme with 4-azido-2-nitrobenzyl thiamin pyrophosphate (5pp) did not significantly affect the initial rates. 4-azido-2-nitrobenzyl thiamin pyrophosphate (5pp) was able to

bind at the enzyme active site and inhibit the reaction with an IC_{50} of about 200 μM.

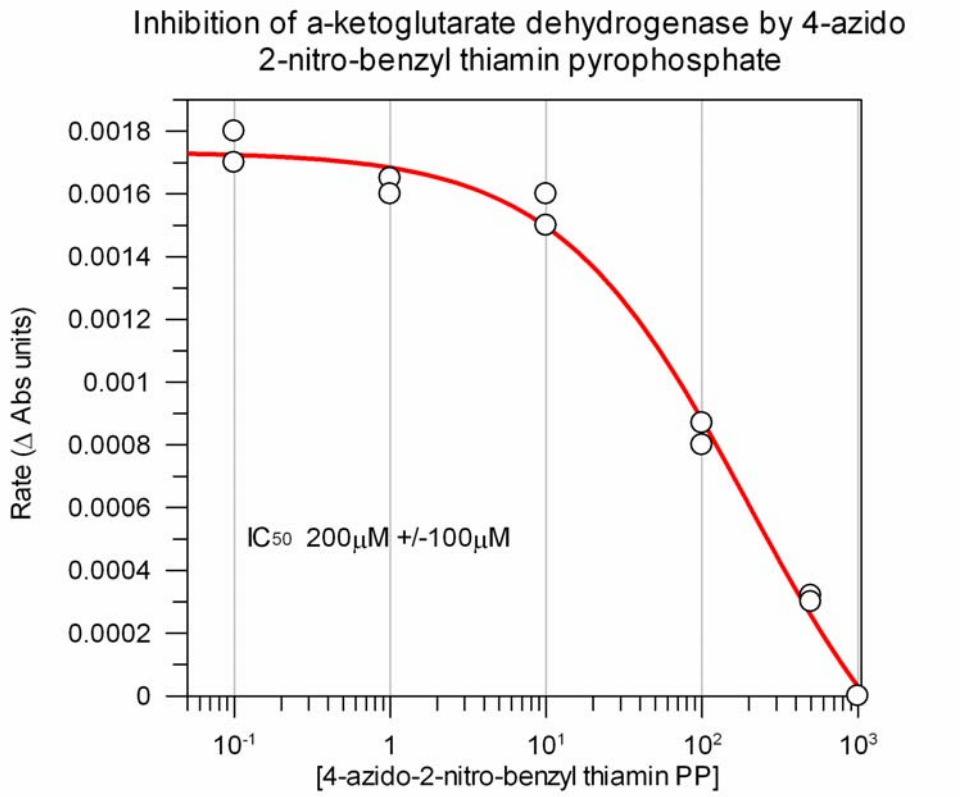

Figure 9.7 Dependence of the initial reaction rate of α-ketoglutarate dehydrogenase on the concentration of 4-azido-2-nitrobenzyl thiamin pyrophosphate (6pp). All data points were determined in duplicate. The IC_{50} was determined to be 200 μM+/-100 μM. The error is high because of the low number of data points obtained.

4-azido-2-nitrobenzylthiamin pyrophosphate was also able to inhibit deoxy-D-xylulose 5 phosphate synthase (not shown). Apparently the perturbations in the pyrimidine moiety of TPP in this probe were not disruptive enough to prevent binding in the enzyme active site. In addition to its ability to inhibit a TPP utilizing enzyme, this probe was also very photo-labile with absorbance at

wavelengths of light greater than 300 nm, making this an ideal candidate for further testing.

9.4.2 Photoaffinity labeling of TPK/DXS with 4-azido-2nitrobenzylthiamin pyrophosphate (5pp)

In order to detect any labeling of a TPP utilizing enzyme, a tag needed to be attached to the photo-labile probe. We choose to enzymatically incorporate a ^{32}P-tag into the pyrophosphate moiety of 4-azido-2-nitrobenzyl thiamin pyrophosphate (5pp). This offered us an extremely sensitive probe, so even low amounts of labeling could be detected.

Initial irradiation attempts with either thiamin pyrophosphokinase (TPK) or DXP synthase (DXS) showed considerable labeling of the protein. Optimal labeling took place after 3-5min of irradiation. However, when a non-TPP utilizing protein was added to the irradiated mixture, it too was labeled. This non-specific labeling was understandable given the photo-lability of the probe and the extremely reactive nature of the nitrene that was generated upon photolysis.

In an attempt to decrease the non-specific labeling of the non-TPP utilizing protein (NifS), a scavenger was added at various concentrations in order to react with any nitrene that was generated outside of the enzyme active site (figure 9.8). Lanes 1 and 2 clearly showed that TPK and its dimer (TPK exists as a dimer in solution) were labeled. Lanes 3 and 4 showed that when NifS was added, it was labeled along with TPK and the TPK dimer. When β-

mercaptoethanol was added to a concentration of 50mM, the labeling of TPK was decreased but it was still observable (lanes 5 and 6).

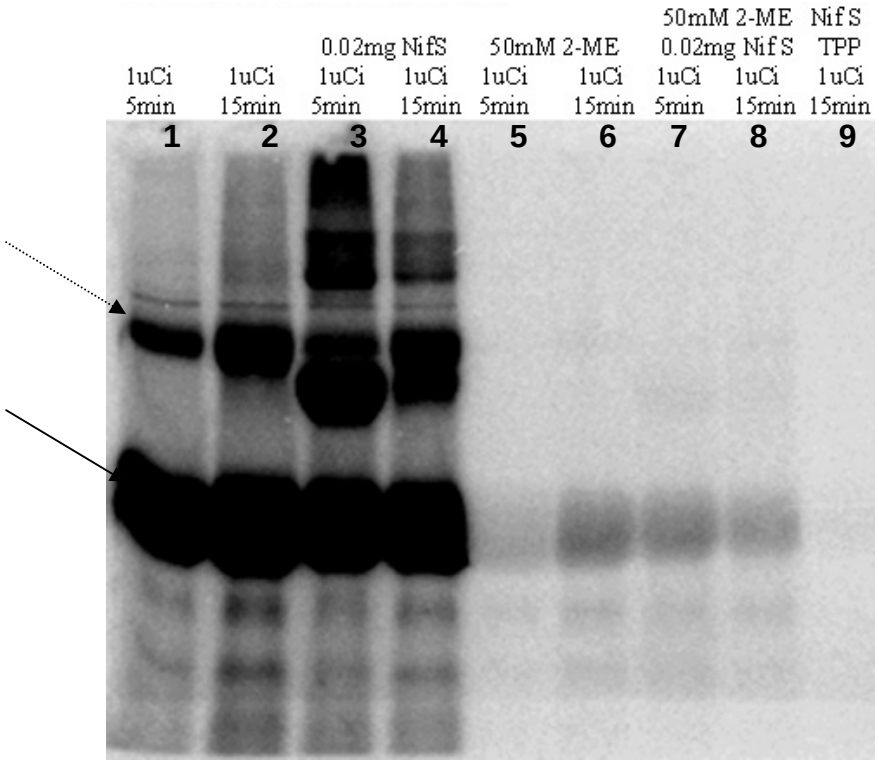

Figure 9.8 Labeling of TPK with ^{32}P-4-azido-2-nitrobenzyl thiamin pyrophosphate, sometimes with NifS or β-ME. The lower band is TPK (solid arrow) and the upper band is the TPK dimer (dotted arrow), the middle band is NifS. All lanes contain 1μCi ^{32}P-4-azido-2-nitrobenzyl thiamin pyrophosphate (5pp) Lane 1: 1 μCi (5pp) + TPK (5 min); Lane 2: 1 μCi (5pp) + TPK (15 min); Lane 3: 1 μCi (5pp) + TPK + NifS (5 min); Lane 4: 1 μCi (5pp) + NifS +TPK (15 min); Lane 5: 1 μCi (5pp) + TPK + 50 mM β-mercaptoethanol (5min); Lane 6: 1 μCi (5pp) + TPK + 50mM β-mercaptoethanol (15min); Lane 7: 1 μCi (5pp) + TPK + NifS + 50 mM β-mercaptoethanol (5min); Lane 8: 1 μCi (5pp) + TPK + NifS + 50 mM β-mercaptoethanol (15 min); Lane 9: 1 μCi (5pp) + TPK + NifS + 50 mM β-mercaptoethanol + TPP (15min).

When both NifS and β-mercaptoethanol were added, lanes 7 and 8, only very faint labeling of NifS was observed with the same amount of labeling of TPK. In lane 9, a competition experiment where TPP was added to and incubated

with the labeling reaction, less labeling of TPK was seen. Because TPP was able to decrease the amount of labeling by the analog, we concluded that the probe was labeling at the enzyme active site.

The same experiment was repeated to test for labeling of DXS with ^{32}P-4-azido-2-nitrobenzyl thiamin pyrophosphate, in the presence of a non-TPP utilizing enzyme (NifS) and with a scavenger (β-mercaptoethanol) (figure 9.9). Overall, the level of labeling was much lower for DXS with a scavenger than for TPK with a scavenger. Clearly in lanes 1 and 2, DXS was labeled as well as some higher molecular weight protein aggregates. Lanes 3 and 4 showed that both DXS and NifS were labeled. When a scavenger, β-mercaptoethanol, was added to a concentration of 50mM, the amount of labeling decreased significantly, but was still observable (lanes 5 and 6). In lanes 7 and 8 where both NifS and β-mercaptoethanol were added, no NifS labeling was observed, and the same level of DXS labeling was seen. In the competition experiment run in lane 9, no labeled DXS was seen when TPP was added.

4-azido-2-nitrobenzyl thiamin pyrophosphate was extremely photo-labile, and unfortunately labels non-TPP utilizing proteins. The addition of a scavenger abolished the non-specific labeling, although drastically decreasing the amount of labeling of the TPP-utilizing protein. The labeling that did occur when a scavenger was added was removed when TPP, the true cofactor or substrate, was added to the irradiation mixture. The TPP out-competes the photoaffinity probe from the active site of either TPK or DXS, implying that the photo-probe was occupying the active site when it was labeling. However, the amount of labeling was not reproducible and also not very high.

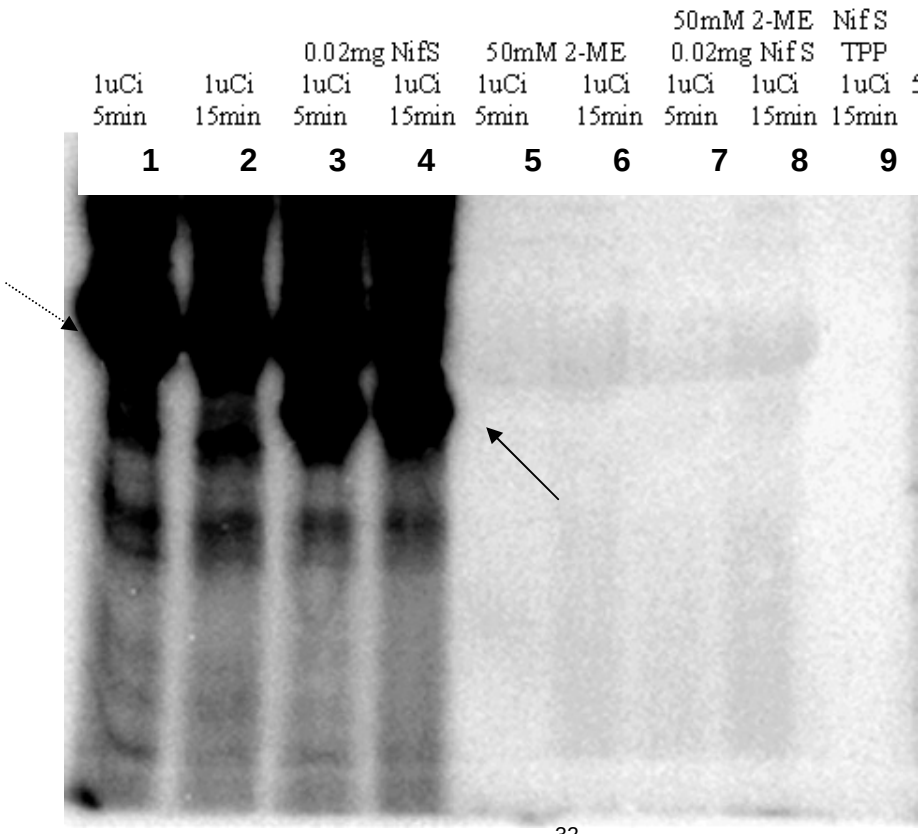

Figure 9.9 Labeling of DXS with ^{32}P-4-azido-2-nitrobenzyl thiamin pyrophosphate, sometimes with NifS or β-ME. The lower band is NifS (solid arrow) and the upper band is the DXS (dotted arrow). All lanes contain 1μCi ^{32}P-4-azido-2-nitrobenzyl thiamin pyrophosphate (5pp) Lane 1: 1 μCi (5pp) + DXS (5 min); Lane 2: 1 μCi (5pp) + DXS (15 min); Lane 3: 1 μCi (5pp) + DXS + NifS (5 min); Lane 4: 1 μCi (5pp) + NifS +DXS (15 min); Lane 5: 1 μCi (5pp) + DXS + 50 mM β-mercaptoethanol (5 min); Lane 6: 1 μCi (5pp) + DXS + 50 mM β-mercaptoethanol (15 min); Lane 7: 1 μCi (5pp) + DXS + NifS + 50 mM β-mercaptoethanol (5 min); Lane 8: 1 μCi (5pp) + DXS + NifS + 50 mM β-mercaptoethanol (15 min); Lane 9: 1 μCi (5pp) + DXS + NifS + 50 mM β-mercaptoethanol + TPP (15 min).

9.5 Conclusions

Generation 3 probes contain the photolabile azido group in the pyrimidine portion of the thiamin analog. To overcome the azido-tetrazole tautomerization, the pyrimidine was replaced with a benzene ring. A nitro group was added to shift the absorbance of the molecule about 300 nm. Both

of the generation 3 probes were extremely photo-labile, and reacted completely within 30 min with 300 nm light.

Both of the generation 3 probes were accepted as substrates by thiamin pyrophosphate kinase, and in both cases they were pyrophosphorylated more efficiently than thiamin itself. However, when their ability to inhibit thiamin pyrophosphate utilizing enzymes like α-ketoglutarate dehydrogenase and DXP synthase was investigated, 2-azido-4-nitrobenzylthiamin pyrophosphate (6pp) was not able to decrease product turnover. 4-azido-2-nitrobenzylthiamin pyrophosphate was found to have an IC_{50} for α-ketoglutarate dehydrogenase of about 200 μM. Though this is not exceptionally low, thiamin pyrophosphate has a K_d of 6.2-8.2 μM, so it does not dissociate from the enzyme very readily.[4] Since some of the binding specificity of the analog has been removed by altering all the major features of the pyrimidine ring, it will not bind with the efficiency of TPP. Regardless, we have shown that 4-azido-2-nitrobenzyl thiamin was both photo-active and that it inhibited TPK and DXS.

When we investigated 4-azido-2-nitrobenzyl thiamin pyrophosphate as a possible proteomics probe, we found that it labeled non-TPP utilizing enzymes in addition to TPP utilizing enzymes. This non-specific labeling was alleviated by the addition of a scavenger, although this drastically decreased the amount of labeling of the TPP-utilizing protein. Because TPP was able to remove the labeling that did occur when a scavenger was added, it implied that the photolabile analog was labeling at the enzyme active site. However, when the non-specific labeling was eliminated, the amount of labeling of the protein target (TPK or DXS) was greatly decreased. Proteomics probes must give a

consistent and reproducible amount of labeling that is well above the limit of detection, and should not have a large amount of background labeling. Unfortunately, though the generation 3 probes were the most promising of the probes, they do not fit all of the criteria.

9.6 Materials and procedures

All materials were obtained from Sigma-Aldrich unless otherwise noted.

9.6.1 Synthesis of 4-azido-2-nitro toluene (25)

Dissolve 350 mg of 4-amino-2-nitro toluene into 10 mL of 10% HCl and cool in an ice bath to 0 ºC. Keeping the reaction at 0 ºC, add 500 mg of sodium azide dissolved in 2 mL water. Very slowly add 500 mg of sodium nitrite dissolved in 2 mL over 20 min. (Bubbling and fizzing occurs). Stir for an additional 1 hr at 0 ºC. The product is extracted into chloroform and purified from starting material via flash chromatography with chloroform as the solvent to give a yellow solid. NMR 300MHz $CDCl_3$ δ(7.657, s, 1H) δ(7.349-7.320, d, 1H) δ(7.179-7.151, s, 1H) δ(2.579, s, 3H) GC/MS m/z=178 Yield: 327 mg (80%)

9.6.2 Synthesis of 4-azido-1-bromomethyl-2-nitro-benzene (27)

This reaction is carried out under reduced light. Into a round bottom flask is weighed 150 mg of 4-azido-2-nitro-toluene, 150 mg of N-bromosuccinimide and 25 mg of benzoyl peroxide. The solids are dissolved in 10 mL of anhydrous benzene under argon. The solution is refluxed overnight. After the solution has cooled to room temperature, it is poured into ether/water and the product is extracted into ether. The combined organic layers are dried with $MgSO_4$ and filtered. The ether is removed and the residue is purified via flash

chromatography with 13:2 hexanes:ethyl acetate to give a yellow solid. NMR 300MHz $CDCl_3$ δ(7.691, s, 1H) δ(7.565-7.537, d, 1H) δ(7.270-7.234, d, 1H) δ(4.794, s, 2H) Yield: 101 mg (69%)

9.6.3 Synthesis of 4-azido-2-nitro(benzyl)thiamin (5)

35 mg of 4-azido-1-bromomethyl-2-nitro-benzene is dissolved in 500 μL of anhydrous acetone. To this is added 25 μL of 4-methyl-5-thiazole ethanol and the solution is stirred in the dark for 2 days. The acetone is then removed *in vacuo* and the residue is dissolved in water. The remaining starting materials are extracted exhaustively with ethyl acetate. The water is lyophilized to yield pure product as a light yellow solid. NMR 300MHz D_2O δ(7.885, s, 1H) δ(7.372-7.336, d, 1H) δ(7.156-7.129, d, 1H) δ(5.759, s, 2H) δ(3.743-3.704, t, 2H) δ(3.045-3.007, t, 2H) δ(2.336, s, 3H) Yield: 45 mg (83%)

9.6.4 Synthesis of 2-azido-4-nitro toluene (26)

Dissolve 1 g of 2-amino-4-nitro toluene into 30 mL of 10% HCl and cool in an ice bath to 0ºC. Keeping the reaction at 0 ºC, add 1.4 g of sodium azide dissolved in 10 mL water. Very slowly add 1.4 g of sodium nitrite dissolved in 20 mL over 20 min. (Note that bubbling and fizzing occurs). Stir for an additional 1 hour at 0 ºC. The product is extracted into chloroform and purified from starting material via flash chromatography with chloroform as the solvent to yield a yellow solid. NMR 300MHz $CDCl_3$ δ(7.960, s, 1H) δ(7.865-7.762, d, 1H) δ(7.500-7.307, s, 1H) δ(4.660, s, 3H) GC/MS m/z=178 Yield: 487 mg (42%)

9.6.5 Synthesis of 2-azido-1-bromomethyl-4-nitro-benzene (28)

This reaction is carried out under reduced light. Into a round bottom flask is weighed 250 mg of 4-azido-2-nitro-toluene, 250 mg of N-bromosuccinimide and 50 mg of benzoyl peroxide. The solids are dissolved in 15 mL of anhydrous benzene under argon, and the solution is refluxed overnight. After the solution has cooled to room temperature, it is poured into ether/water and the product is extracted into ether. The combined organic layers are dried with $MgSO_4$ and filtered. The ether is removed and the residue is purified via flash chromatography with 13:2 hexanes:ethyl acetate to give a yellow solid. NMR 300MHz $CDCl_3$ δ(8.007, s, 1H) δ(7.966-7.931, d, 1H) δ(7.564-7.537, s, 1H) δ(4.460, s, 3H) Yield: 200 mg (62%)

9.6.6 Synthesis of 2-azido-4-nitro(benzyl)thiamin (6)

25 mg of 4-azido-1-bromomethyl-2-nitro-benzene is dissolved in 500 μL of anhydrous acetone. To this is added 20 μL of 4-methyl-5-thiazole ethanol and the solution is stirred in the dark for 2 days. The acetone is then removed *in vacuo* and the residue is dissolved in water. The remaining starting materials are extracted exhaustively with ethyl acetate. The water is lyophilized to yield pure product as a light yellow solid. Yield: 27 mg (76%)

9.6.7 Pyrophosphorylation of 4-azido-2-nitro-benzylthiamin (5) and 2-azido-4-nitro-benzylthiamin (6) and purification by HPLC

4 mg of either of the thiamin analogs is added to the enzymatic reaction solution containing 34.3 mg of ATP, 9.3 mg of KCl, 12.7 mg of $MgCl_2$, 500 μL of TPK (6 mg/mL), 4.24 mL of ddH_2O and 4.25 mL of 100 mM Tris pH 8. The

reaction proceeds at room temperature overnight. The reaction is stopped by removing protein using centricon YM-10 concentrators. The flow-through is collected and the pyrophosphorylated products are purified via HPLC using the following method: time 0 min: 100% 25 mM NH_4OAc; time 6min: 100% 25 mM NH_4OAc; time 7 min: 90% 25 mM NH_4OAc 10% MeOH; time 20 min: 30% water, 40% 25 mM NH_4OAc, 30% MeOH; time 22 min: 100% NH_4OAc. 4-azido-2-nitro-benzylthiaminPP was collected from 16.8 min to 22.2 min. 2-azido-4-nitrobenzylthiaminPP was collected from 15.2 min to 20.0 min.

9.6.8 General procedure for enzymatic pyrophosphorylation of thiamin analogs with γ-^{32}P-ATP

The enzymatic reaction solution consists of 1 mM thiamin analog, 2.5 mM cold ATP, 10 mM KCl, 5 mM $MgCl_2$, and 100 mM tris pH 8. To this cold solution is added 125 μCi of γ-^{32}P-ATP*, and the reaction is initiated by the addition of 20 μL of thiamin pyrophosphokinase (6 mg/mL). This produced about 50 μCi of ^{32}P-thiamin analog assuming that the reaction goes to completion. The reaction is allowed to continue at room temperature overnight. The TPK is then filtered from the hot reaction mixture using microcon YM-10 concentrators for 60 min at 10000 rpm. The flowthrough is collected and stored in the freezer for further use.

9.6.9 Irradiation of proteins with ^{32}P-4-azido-2-nitro-benzylthiamin pyrophosphate (5pp)

Into UV-transparent cuvettes was placed TPK (20 μL @ 6 mg/mL) and/or DXP synthase (100 μL @ 0.5 mg/mL) and 100 mM tris pH 7.6. In addition, some reactions contained β-mercaptoethanol (to act as a scavenger) or other non-

TPP utilizing enzymes (NifS – 16 μL @ 5 mg/mL). If a competition experiment was being carried out, exogenous TPP was added to the reaction. Into the enzyme containing solutions was pippetted ^{32}P-4-azido-2-nitro-benzylthiamin pyrophosphate (5pp). In general, different amounts of γ-^{32}P-ATP are used: 0 μCi (Control), 0.5 μCi, 2.0 μCi, or 4.0 μCi. ^{32}P-4-azido-2-nitro-benzylthiamin pyrophosphate (5pp) was allowed to incubate with the enzymes for 1hr at room temperature. Irradiation with >300 nm light was carried out for various times. The samples were then concentrated to ~30 μL using microcon YM-10 concentrators (25-30 min @10000 rpm). To the protein was added 30 μL of 2x SDS sample buffer, and the samples were heated at 95 ºC for 5 min. The samples were loaded onto the gel and run at 120 V. Gels were then stained and destained so the major protein bands could be identified, and then they were dried. Radioactive bands were identified by exposure to a phosphorimaging screen (Molecular dynamics) and analysis by a Storm 860 Phosphorimager (Amersham Biosciences).

9.7 References

1. Nishimura, H., et al., *Photoaffinity labeling of thiamin-binding component in yeast plasma membrane with [3H]4-azido-2-nitrobenzoylthiamin.* FEBS, 1989. **255**(1): p. 154-158.

2. *Vitamins and Coenzymes Part I*. Methods in Enzymology, ed. D.B. McCormick, J.W. Suttie, and C. Wagner. Vol. 279. 1997, San Diego: Academic Press.

3. Jordan, F., et al., *Dual Catalytic Apparatus of the Thiamin Diphosphate Coenzyme: Acid-Base via the 1',4'-Iminopyrimidine Tautomer along with Its Electrophilic Role.* Journal of the American Chemical Society, 2003. **125**(42): p. 12732-12738.

4. Walsh, D.A., et al., *The elementary reactions of the pig heart pyruvate dehydrogenase complex. A study of the inhibition by phosphorylation.* Biochemical Journal, 1976. **157**(1): p. 41-67.